Aus dem Institut für Humangenetik
Theoretische Medizin und Biowissenschaften
der Medizinischen Fakultät
der Universität des Saarlandes, Homburg/Saar

Differential loading of the Argonaute complex in Epstein-Barr Virus (EBV)-infected cell lines derived from diffuse large B-cell lymphoma (DLBCL)

Dissertation zur Erlangung des Grades eines Doktors der
Naturwissenschaften der Medizinischen Fakultät
der UNIVERSITÄT DES SAARLANDES
2018

Vorgelegt von: Mohammad Hiresh Ayoubian
geb. am. 4.07.1980 in Tehran, Iran

Declaration

I hereby declare that the Ph.D. thesis entitled "Differential loading of the Argonaute complex in Epstein-Barr Virus (EBV)-infected cell lines derived from diffuse large B-cell lymphoma (DLBCL)" is a presentation of my original research work. Where other sources of information have been used, they have been acknowledged. No portion of work contained in this thesis has been submitted in support of any application for any other degree or qualification.

Homburg,
12.12.2017
Hiresh Ayoubian

To My dearests:

My parents Rashid and Poran

& My siblings Hana and Rashed

Zusammenfassung

MicroRNAs sind essentielle post-transkriptionelle Regulatoren der Genexpression die an unterschiedlichen Prozessen wie Entwicklung, Signaltransduktion oder Wachstumskontrolle durch Bindung und Inhibition der Translation ihrer mRNA Ziel mRNAs beteiligt sind. Obwohl angenommen wird, dass ihre relative Expression in der Zelle das Ausmaß ihrer biologischen Funktion bestimmt, zeigt die Beladung der „Argonaute" (Ago)-mRNA Komplexe mit miRNAs deren Relevanz besser an.

In der vorliegenden Arbeit wurde die miRNA Beladung der Ago-Komplexe mit den miRNA Profilen der Gesamt-RNA zweier diffus-großzelliger B-Zell Lymphome (DLBCL) Linien nach Epstein-Barr Virus (EBV) -Infektion, verglichen. DLBCL ist ein hochmaligner Tumor, welcher in Aktivierte B-Zell (ABC-) und Germinal Center B-Zell (GCB-) DLBCL unterschieden wird. Etwa 10% aller DLBCLs sind mit dem onkogenen EBV, welches selbst 44 reife miRNAs exprimiert, infiziert.

Die miRNA Profile aus Gesamtzellextrakten und des Ago2-Profils zweier DLBCL Linen wurden durch Hochdurchsatzsequenzierung (RNA-Seq) analysiert. In den Gesamt-Profilen konnten zwischen 713-851 humane miRNAs identifiziert werden, während die Ago2-Profile 1102-1372 humane miRNAs ergaben. Bei Anwendung eines 0.1% „cut-offs" verringerte sich die Zahl der funktionellen miRNAs auf 56-62., welche jedoch immer noch 92-95% aller miRNAs-reads ausmachten. In Abhängigkeit von Latenztyp repräsentierten die viralen miRNAs 1.6% - 28% aller „reads". In beiden Zelllinien hatte die EBV-Infektion den Verlust von miRNAs im Ago2-Komplex zur Folge. Die erhobenen Daten konnten für ausgewählte miRNAs durch RT-qPCR und im Northern Blot bestätigt werden. Auch die Analyse der Ago2-Komplexe der einzelnen Zellen ergab eine auffällige Umverteilung miRNAs zwischen Gesamt- und Ago2-assoziierten miRNAs. Zum Beispiel war die miRNA miR-423 in allen Zellen 6-8-fach im Ago2-Komplex angereichert, während die miR-142 im Ago2-Komplex depletiert vorliegt , was auf einen Funktionsverlust hinweist. Die hier erhobenen Daten werden zum weiteren Verständnis des Beitrags von miRNAs bei der Entstehung und Aufrechterhaltung von DLBCLs leisten.

Summary

MicroRNAs are important post-transcriptional regulators of gene expression in all eukaryotic cells and play essential roles, i.e. in development, signal transduction or growth control by binding to and inhibiting the translation of their mRNA targets. While it is widely assumed that their overall level in a cell reflects their functional relevance, the loading and transfer of miRNAs to the "Argonaute" (Ago)-mRNA complex appears to give a more accurate indication of their activity in a cell.

In this thesis, the miRNA loading of the Ago complex was compared with the total cellular miRNA profile of two cell lines derived from diffuse large B-cell lymphoma (DLBCL) in comparison with their Epstein-Barr Virus infected counterparts. DLBCL is a highly malignant tumor subdivided into Activated B-cell (ABC-) and Germinal Center B-cell (GCB-) subtypes. About 10% of DLBCL are infected with the oncogenic Epstein-Barr virus which itself encodes 44 mature miRNAs.

The cellular and Ago2-bound miRNAs in two DLBCL lines were subjected to ultra-deep sequencing (RNA-seq). In the total profiles, 713-851 human miRNAs were detected while the Ago2-immunoprecipitation (Ago2-IP) resulted in 1102-1372 different miRNAs. When a 0.1% cut-off was applied which is considered to yield the functionally relevant miRNAs, only between 56-62 miRNAs were left. These, however, represented 92-95% of all reads. In the two EBV-infected counterparts, EBV-miRNAs represented between 1.6% - 28% of all reads depending on the viral latency type. In the case where EBV miRNAs accounted for 28 % of total reads cellular miRNAs were replaced from the Ago2-complex. The results could be confirmed for selected miRNAs by RT-qPCR and Northern blotting. Also within each cell line, various miRNAs were enriched or depleted from the Ago2 complex. For instance, mir-423-5p and mir-423-3p were highly enriched, by over 6-8-fold in Ago2-IP, compared to total cellular profile in all cell lines while miR142 was strongly depleted from the Ago2-complex indicating a functional loss in DLBCL. The data obtained will help to further understand the contribution of cell and viral miRNAs in induction and maintenance of DLBCL.

CONTENTS

1 Introduction

1.1 Lymphoma

Lymphoma is a tumor of lymphocytes, representing almost 5% of all new cancer cases worldwide (MUGNAINI, GHOSH, 2016). Lymphomas are classified into two main groups: Hodgkin´s lymphoma (HL), representing about 10% of lymphoma, and non-Hodgkin´s lymphoma (NHL), accounting for the remaining 90%. The incidence of NHL is increasing with age and most of the patients are above 65 years old. NHL is categorized into B-cell, T-cell and natural killer (NK) cell types (MUGNAINI, GHOSH, 2016; SHANKLAND et al., 2012).

1.2 Genetics of Diffuse large B-cell lymphoma

Diffuse large B-cell lymphoma (DLBCL) is the most common aggressive subtype of NHL, as it accounts for about one third of all malignant lymphoma cases in adults (MIYAZAKI, 2016). DLBCL is characterized by expressing specific cell surface markers like CD19, CD20, CD22, and CD79a on B-cells Even though there are different markers for characterizing DLBCL, it is a heterogeneous disease with distinct clinical and biological features. Based on microarray gene expression profiling (GEP), the World Health Organization (WHO) classified DLBCL into three major clusters: (1) Germinal Center B-cell like (GCB), (2) Activated B-cell like (ABC) and cases, which could not be assigned to either group and were therefore, termed unclassifiable (ALIZADEH et al., 2000; CAMPO et al., 2011; ROSENWALD et al., 2002; SWERDLOW et al., 2016). In addition to GEP for classifying DLBCL, next-generation sequencing (NGS), including whole genome and exome sequencing also allows to differentiate the genetic alteration patterns of ABC and GCB (ZHANG et al., 2013). Germinal centers (GCs) are the sites in secondary lymphoid tissue where B cells proliferate, differentiate and undergo immunoglobulin somatic hypermutation (SHM), class switch recombination (CSR), and affinity selection, to produce high affinity antibodies (VICTORA, NUSSENZWEIG, 2012). Due to the high rate of B cell proliferation and differentiation, germinal center cells can undergo genetic aberration, resulting in lymphomagenesis (BASSO, DALLA-FAVERA, 2015). GCB-DLBCL

originates from germinal center centroblasts, is more common among young people and GEP shows the characteristics of tonic B-cell receptor (BCR) signaling (COPIE-BERGMAN et al., 2002; CUMMIN, JOHNSON, 2016). ABC-DLBCL (often also termed non-GCB), is derived from post germinal center cells. It has been shown that MYC/BCL2 double translocations, amplification of the oncogenic mir-17–92 microRNA cluster, mutations in genes such as BCL2 , the proto-oncogene MYC (gain of function), histone methyl-transferase EZH2 (gain of function), S1PR2, GNA13 (loss of function), occur more often in GCB-DLBCL (INTLEKOFER, YOUNES, 2014; ROSCHEWSKI et al., 2014; SWERDLOW et al., 2016). In comparison to GCB-DLBCL, ABC-DLBCL is often characterized by mutations affecting in B-cell receptor signaling, especially the NF-κB-pathway (COPIE-BERGMAN et al., 2002; CUMMIN, JOHNSON, 2016). ABC-DLBCL is preferentially associated with mutations in genes, such as CD79A, MYD88, CARD11 and TNFAIP3, which activate the B-cell receptor, the Toll-like receptor and also the NF-kB pathways (BASSO, DALLA-FAVERA, 2015; LENZ et al., 2008; SWERDLOW et al., 2016; ZHANG et al., 2013).

This molecular genetic difference in gene expression profile and signaling pathways, can lead to the conclusion that there is a unique pathogenicity mechanism, differentiating GCB- from ABC-DLBCL, resulting in a different strategy for treatment.

1.3 Clinical genetic diagnosis of DLBCL

A diagnosis of DLBCL is obtained from a tissue biopsy of the enlarged lymph node and assessment of lymph node architecture. Since GEP is not routinely available as the clinical diagnostic test for differentiation of GCB- and ABC-DLBCL, the "Hans algorithm" (Figure 1) has been used frequently with an accuracy of about 90%, and recommended for routine diagnosis. This algorithm is based on immunohistochemistry (IHC) staining, and evaluating the expression patterns of cluster of differentiation (CD10), B-cell lymphoma 6 (BCL6), and interferon regulatory factor-4/multiple myeloma-1 (IRF4/MUM1) expression (HANS et al., 2004; SWERDLOW et al., 2016). Novel methods, such as gene panel (Lymph2Cx assay) from Formalin-fixed paraffin-embedded (FFPE) tissues (SCOTT et al., 2014), NGS,

flow cytometry, cytogenetic analysis using fluorescence in situ hybridization (FISH) or polymerase chain reaction (PCR), for chromosomal translocations or rearrangements of genes, can be considered as alternative medical genetic diagnostic methods, to differentiate various types of lymphoma.
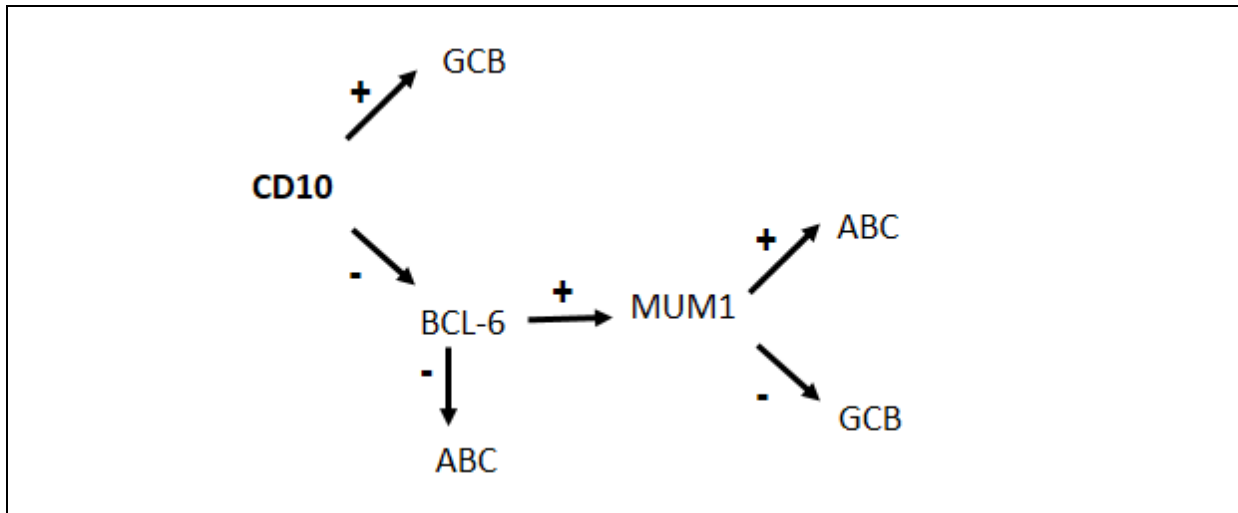
Figure 1: Hans algorithm for differentiation of diffuse large B-cell lymphoma (DLBCL).
Immunohistochemical staining (IHC) to differentiate GCB-DLBCL from non-GCB-DLBCL (ABC-DLBCL). Adapted and modified from (HANS et al., 2004).

1.4 Medical Treatment of DLBCL; future perspective

Diffuse large B-cell lymphoma (DLBCL) is a human malignancy with a very poor prognosis. About 15% of all DLBCLs are EBV positive by virtue of the presence of EBER-transcripts in the tumor cells (DELECLUSE et al., 2007; IMIG et al., 2011). The standard treatment for patients with ABC or GCB-DLBCL is R-CHOP therapy. CHOP is a combination of rituximab, anti-CD20 monoclonal antibody, cyclophosphamide, doxorubicin, vincristine, and prednisone (TOMITA et al., 2013; YU, LI, 2015). As DLBCL constitutes a distinct molecular disease and therefore has a different clinical and prognostic features, it is promising to use novel strategies, based on molecular insights of affected signaling pathway and targeting genes, which are characteristic of GCB- or ABC-DLBCL. For example, targeting BCL-6 to prevent cell proliferation, using an HDAC inhibitor (PAREKH et al., 2008), etoposide to inhibit topoisomerase II (DUNLEAVY et al., 2013; KUROSU et al., 2003) or targeting of *EZH2*, which is

mutated in GCB-DLBCL (BÉGUELIN et al., 2013). In the case of ABC-DLBCL, which has the worst prognosis among DLBCLs, targeting the NF-κB-pathway to prevent constitutive activation and overexpression of NF-κB, could have a potential therapeutic effect, such as using ibrutinib, which inhibits BTK in the NF-κB-pathway (WILSON et al., 2015).

1.5 Molecular genetics of Micro RNA

MicroRNAs (miRNAs) are conserved, short single stranded noncoding RNA molecules of 19-25 nucleotides in length, which are processed from longer hairpin-structured transcripts (Figure 2) (AMBROS et al., 2003; CULLEN, 2004). The main function of miRNAs in the cell is to fine-regulate gene expression. The first miRNA was discovered in Victor Ambros' lab in 1994, where it was shown that the interaction of *Lin 4* with the *Lin14* mRNA in the worm Caenorhabditis elegans (C. elegans) causes reduction in the amount of LIN-14 protein, resulting in a distinct phenotype. This interaction is important in the timing of the development and transition from the first to the second larval stage (BARTEL, 2004; KIM, 2005; LEE et al., 1993). A few years later, the Ruvkun group found the second small RNA, termed let-7, controlling the *Lin41* mRNA. They also demonstrated that this interaction is essential for the transition from larval stage 4 to the adult (REINHART et al., 2000). Most importantly, they also found that a let-7 homolog exists which is expressed in humans and other species (PASQUINELLI et al., 2000). This important discovery opened a new era in molecular biology to understand the functional importance of miRNAs (AMBROS, 2004; BARTEL, 2004).

1.6 Biogenesis of miRNAs

About 1% of the genes encode for miRNA, and it is estimated that about one third of all human genes might be targeted by miRNAs. MiRNAs are transcribed from either intronic (coding and non-coding), or exonic regions of the genome. The primary transcription is typically several kilobases long, with (a) hairpin structure(s) that contain(s) either one miRNA or a cluster of miRNA hairpin structures, as shown in Figure 2 (BARTEL, 2004; HA, KIM, 2014; KIM et al., 2009).

The key proteins for biosynthesis of miRNAs are two RNase III type endonucleases, Drosha and Dicer, and the "Argonaute" proteins. The region of the genome encoding a miRNA is first transcribed by RNA polymerase II (Pol II), leading to a primary miRNA transcript (pri-miRNA). Subsequently pri-miRNA is recognized and cleaved in the nucleus by the RNase-III endonuclease Drosha, together with the cofactor DGCR8/Pasha. This cleavage creates a hairpin structure about 70-bp length with 2-nucleotide long 3′ overhangs at the cleavage site, which is termed precursor miRNA (pre-miRNA) hairpin. Then the pre-miRNA is translocated to the cytoplasm by exportin 5, which is a Ran guanosine triphosphate-dependent (Ran-GTP) dsRNA-binding protein (BOHNSACK et al., 2004; LUND et al., 2004). In the cytoplasm, the pre-miRNA is further processed by the RNase III endonuclease "Dicer", which results in the formation of ~22-nucleotide mature duplex miRNAs (BARTEL, 2004; HA, KIM, 2014; KRICHEVSKY, GABRIELY, 2009).
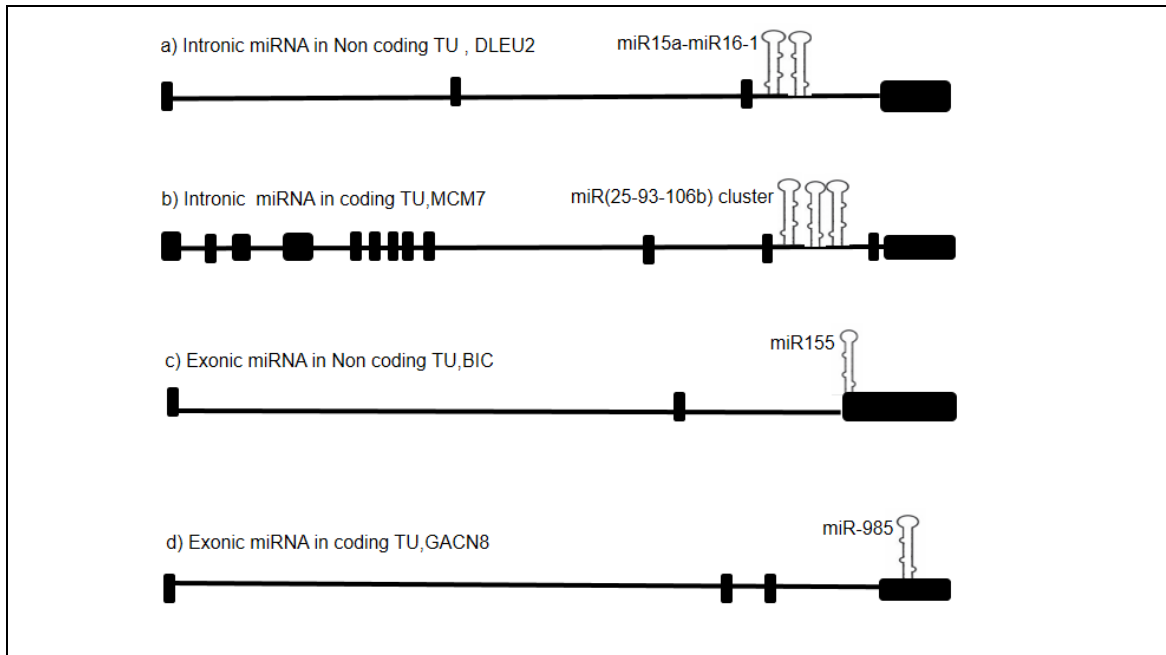
Figure 2: Genomic organization of miRNAs.
MiRNAs can be classified into different groups based on their location in the genome. a) MiRNA located in the noncoding region of TU like the miR-15a and miR-16-1 cluster in DLEU2 (non-coding RNA gene). b) MiRNA located in the intron of coding TU for protein such as miR-25, miR-93 and miR-106b cluster in MCM7 transcript. c) MiRNA located in the exon of noncoding TU such as miR-155 in the BIC1 Gene .d) miRNA located in the exon of protein coding regions such as miR-985 in coding region of CACNG8. MiRNA can be transcribed as a polycistronic TU (a and b) or single TU (c and d). TU, transcription unit. Adapted and modified from (KIM et al., 2009).

1.7 RNA-induced silencing complex (RISC) formation

The mature miRNA duplexes are then incorporated into the Argonaute/EIF2C complex. The one strand with less thermodynamic base pairing stability, for instance a GU base pair, as compared to a GC base pair at the 5´ end, remains in the Ago complex and forms a functional mature miRNA, termed guide miRNA while the other miRNA strand named passenger miRNA (miRNA*) is released from the Ago-complex and degraded. However, in other cases, like miR-142, both miR-142-3p and miR142-5p, are incorporated into the RISC complex (KWANHIAN et al., 2012). Dicer1 is also believed to associate with Ago2 in this process. Finally, Ago2, Dicer and TRBP (TAR RNA-binding protein or TARBP2 form the miRNA Induced Silencing Complex (RISC),

to silence their mRNA target (Figure 3) (BARTEL, 2004; KIM et al., 2009; LIN, GREGORY, 2015).
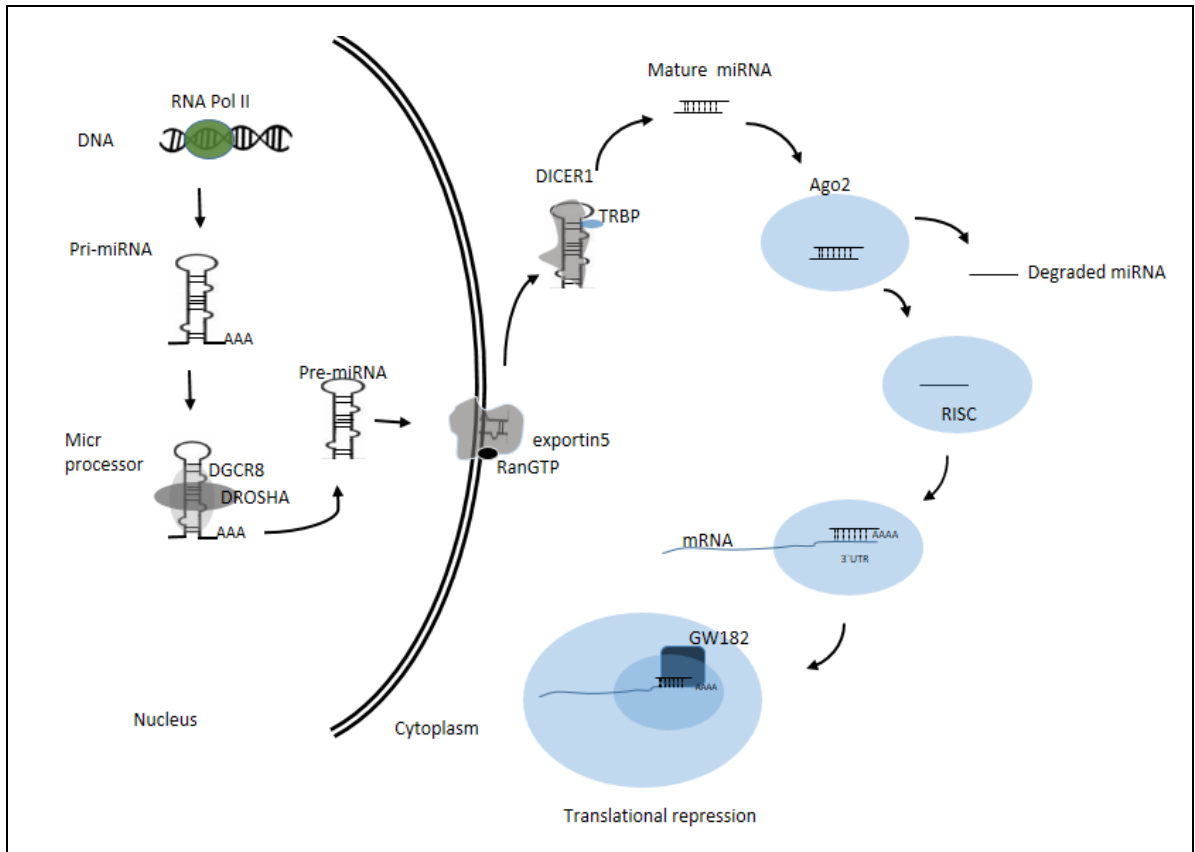
Figure 3: miRNA biogenesis.
MiRNA genes are transcribed by RNA pol II into pri-miRNA and then processed by Drosha–DGCR8 to generate the pre-miRNAs. The pre-miRNAs (about 65-70 nucleotides) are recognized by the exportin5 / Ran GTP complex and transferred to the cytoplasm. In the cytoplasm, Dicer (RNase III) further processes the pre-miRNA to generate the mature miRNA duplex. The mature miRNA is loaded into the AGO-GW182 protein complex and forms the RISC complex. Finally the miRNA directs the "Argonaute"-complex to the mRNA gene target to perform the silencing effect. Adapted and modified from (LIN, GREGORY, 2015).

1.8 Mechanism of miRNA-directed regulation

Once the "Argonaute"-complex has been recruited to the 3´UTR of its mRNA target, it interacts with the N terminal domain of the GW182 protein (Drosophila) or the TNRC6A (mammalian) protein. GW182 possesses at the N-terminus glycine-tryptophan (GW) amino acid repeats and a crystallographic study showed that two tryptophan residues are important for AGO binding (SCHIRLE, MACRAE, 2012). At the C-terminus, GW182 through a RNA recognition motif (RRM) and a poly(A)-binding protein-interacting motif 2 (PAM2) motif, directly interacts with the PABPC (poly(A)-binding protein C) on the poly(A) tail of the mRNA. GW182 also interacts directly with NOT1 which is a part of CCR4–NOT deadenylation machinery. Recruiting the CCR4–NOT complex to the 3´ UTR results in removing and shortening of the poly(A) tail, and also leads to cap removal from mRNA and calling the XRN1 exonuclease and finally degrading the mRNA (MEISTER, 2013).

1.9 The Argonaute proteins

Argonaute (Ago) are the key proteins in the RISC complex. The AGO families are divided into three subclades: PIWI, AGO and WAGO (Worm-specific Argonaute). The PIWI subclade, which has a homology to Drosophila melanogaster PIWI, is mainly expressed in the germ line and associated with PIWI-interacting RNAs (piRNAs). The AGO subclade, which is similar to Arabidopsis thaliana AGO, is involved in the miRNA or the siRNA pathway (MEISTER, 2013). In humans, four types of the AGO subfamily have been identified, namely **1)** hAGO, EIF2C1 **2)** hAGO2, EIF2C2 **3)** hAGO3, EIF2C3 **4)** hAGO4, EIF2C4. The Ago family is highly conserved, ubiquitously expressed in numerous tissues, and have a molecular weight of approximately 100 kDa (SASAKI et al., 2003; ZHAI et al., 2016). Among the human AGO subfamily, Ago2 is the only protein which possesses the catalytic RNAse activity, and has an important role in RNA guided silencing processes. Recently the crystal structures of AGO2 were resolved and it revealed four main domains: an N-terminal domain, a PAZ (Piwi-Argonaute-Zwille), a MID (middle) and a Piwi domain (Figure 4) (ELKAYAM et al., 2012; SCHIRLE, MACRAE, 2012). As shown in Figure 4, these domains form a bi-lobal shape, one lobe with N-terminal domain and PAZ domain and the other lobe with

MID and PIWI domains. These lobes are connected, by Linker 1 (L1) and Linker 2 (L2), in order to form a hinge, connect the two lobes and bond them together. The N-terminal domain is important for loading the RNA duplex and unwinding of miRNA. The PAZ domain binds to the 2-nucleotide of 3´ overhang of miRNA. The MID domain provides a binding pocket for the 5´ overhang of the guide RNAs, with preferential binding to U or A nucleotides. The PIWI Domain has a homology to RNase H and possesses endonucleolytic activity to slice mRNAs, between nucleotide positions 10 and 11, from the 5´ end of the small guide miRNA. Therefore, binding of the small guide RNA at 5´end, to PAZ and MID domain in one hand, and the 3´overhang to PIWI domain on the other hand, cause the small guide miRNA to accommodate in an A-form helix conformation, between two lobes. It also causes exposure of nucleotide 2 to 7 of guide miRNA, termed a seed sequence, and the finding of a complementary sequence of the mRNA target. All human AGO proteins subclades were able to induce translational suppression, degradation of mRNA targets through the formation of the RISC complex. Ago2 is the only Argonaute protein that has the capability to slice perfectly matched mRNA (HA, KIM, 2014; LIU et al., 2004; MEISTER, 2013; PARKER et al., 2005; YE et al., 2015; ZHAI et al., 2016). Ago2 knockdown, using siRNA results in increased expression of other Ago proteins, especially Ago1 and vice versa (MATSUI et al., 2015).
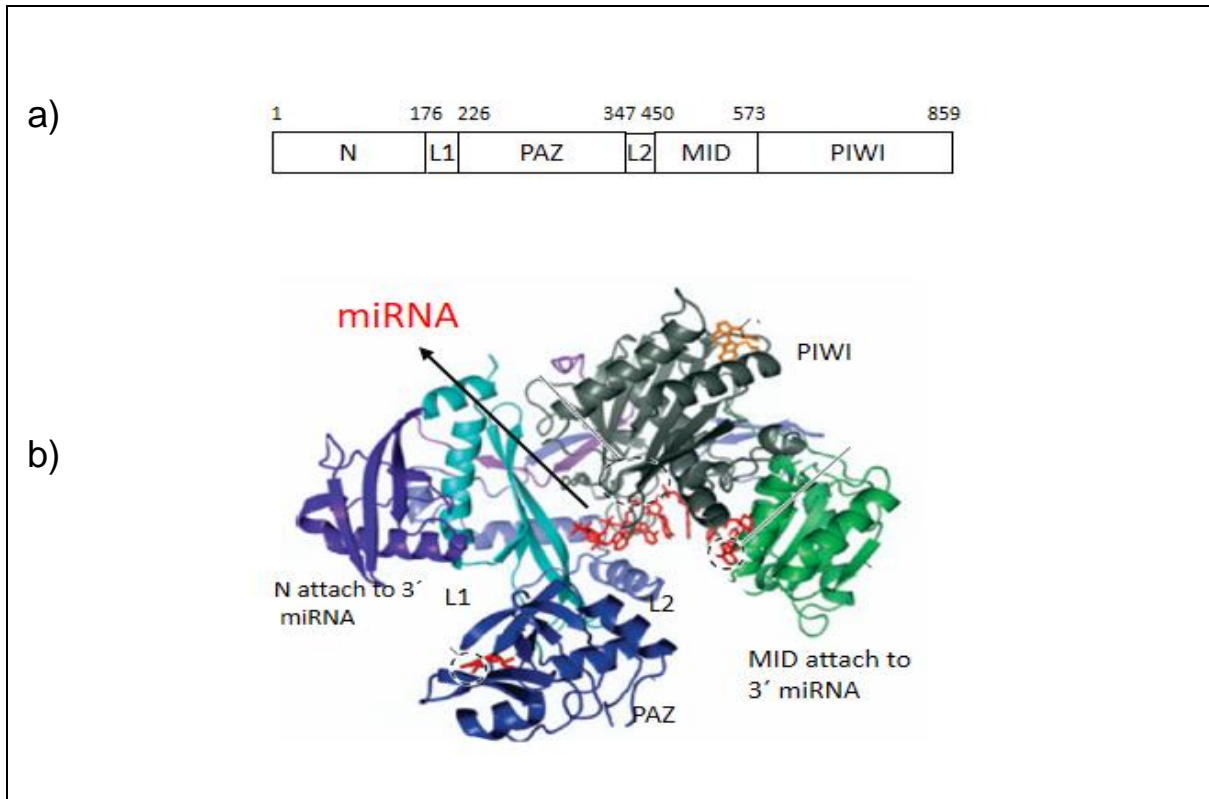
Figure 4: Schematic depiction of the Ago2 protein.
a) Ago2 consists of an N terminal domain, a PAZ domain (binds to 3´ guide miRNA), the MID (middle) and the PIWI domain (binds to the 5´ monophosphate of the guide miRNA). The numbers indicate location of each domains in Ago2. b) 3D structure of human AGO2 with guide miRNA in red color. Adapted and modified from (ELKAYAM et al., 2012; HA, KIM, 2014)

1.10 MicroRNAs in cancer

Since the discovery of miRNAs by Victor Ambros in developmental timing in C. elegans, the function of miRNA was extended to their contribution to cancer. We now know that miRNAs can act as oncogenes (oncomiRs), by inducing different mechanisms such as cell proliferation, migration and invasion, tumor growth and metastasis, or act as a tumor suppressor by inhibiting cell proliferation, migration and invasion (LEE et al., 2016). The most common molecular genetic changes in miRNA expression levels are as follows:

1) Downregulation of miRNA processing enzymes, such as a) Drosha by inducing expression of the oncogenic transcription factor c-MYC or RNA-specific deaminase

ADARB1, which results in the reduction of pri-miRNA processing and downregulation of the tumor suppressor microRNAs MiR-15/-16 (ALLEGRA et al., 2014). b) Dicer downregulation by different mechanisms, such as downregulation or loss of function of transcription factor TAp63 (binds to the promoter of Dicer), or by miRNA-mediated downregulation such as let-7 (TOKUMARU et al., 2008), miR-103/107 (MARTELLO et al., 2010), and miR-630 (RUPAIMOOLE et al., 2016). c) Induced ago2 phosphorylation at Tyr$_{393}$, by the epidermal growth factor receptor (EGFR), which affects binding of Ago2 to Dicer, during hypoxia leading to reduced miRNA processing (SHEN et al., 2013). d) Mutation in the exportin 5 encoding gene, leading to decreased transport of miRNA from the nucleus to the cytoplasm, which induces expression of the *EZH2* and the *MYC* oncogene (MELO et al., 2010; RUPAIMOOLE, SLACK, 2017). 2) Downregulation of tumor-suppressor miRNAs such as a) the miR-34 family including miR-34a, miR-34b and miR-34c. b) the let-7 family (consisting of ten isoforms), involved in targeting many oncogenic mRNAs, like *KRAS* in the RAS signaling pathway, c) the miR-200 family such as miR-200a/b/429 and miR-200c/141, involved in epithelial–mesenchymal transition (EMT), which is important for metastasis and invasiveness of cancer cells (DE CRAENE, BERX, 2013), d) miR-15/16 located on chromosome 13q14 ,which is lost in B-cell chronic lymphocytic leukemia (CLL) and targets BCL-2 expression (PEKARSKY, CROCE, 2015), e) miR-506 inducing senescence by targeting CDK4 and CDK6 proteins (LIU et al., 2014) and targeting *RAD51*, a double-strand DNA damage repair gene, in ovarian cancer (LIU et al., 2015a), f) miR-520 (RUPAIMOOLE, SLACK, 2017).
3) Molecular genetic alterations such as a) chromosomal deletion, for example, deletion(s) in the 13q14 chromosome, which is normally lost in B cell chronic lymphocytic leukemia (B-CLL), containing tumor suppressor miR-15 and miR-16 (CALIN et al., 2002). b) Chromosomal amplifications such as amplification of the 17q23.2 chromosomal region, which contains the oncogenic mir-21, deregulated in many types of cancer (breast, lung, gastric, ovarian and prostate cancers) (KRICHEVSKY, GABRIELY, 2009) or amplification of the miR-17-92 cluster family on chromosome 13q 31.1, which is amplified in B cell lymphoma (MENDELL, 2008; RUPAIMOOLE, SLACK, 2017).

1.11 Epstein - Barr Virus (EBV)

The Epstein–Barr virus (EBV), a human tumor virus, was discovered in 1964 by Antony Michael Epstein, Bert Achong and Yvonne Barr, using biopsy material of Burkitt's lymphoma (BL) patients (EPSTEIN et al., 1964). It is estimated that more than 95% of the adult human population are seropositive for EBV infection. In the infected individual, EBV persists probably without any gene expression in CD19^{+} memory B-cells, where it is occasionally reactivated, and shed through the oropharynx into the saliva (THORLEY-LAWSON, 2001). Although the viral infection usually occurs without symptoms in the infected individual, EBV can induce tumors under certain conditions. EBV is responsible for approximately 1.8% of cancer deaths worldwide (DE MARTEL et al., 2012; KHAN, HASHIM, 2014; YOUNG et al., 2016).

1.12 EBV latent genes and transformation

EBV is a γ-herpesvirus with a double-stranded DNA genome of approximately 172 kilobase pairs in length, encoding about 90 genes (KIEFF , RICKINSON 2007; SAMPLE et al., 1990; TASHIRO, BRENNER, 2017). The oncogenic potential of EBV is readily observed *in vitro* by transformation of resting B-cells into permanently growing lymphoblastoid cell lines (LCLs). These LCLs are correlated in vitro with the so-called "Post-Transplant Lymphoprolifertive Disease" (PTLD), observed under immunosuppression (DELECLUSE et al., 2007). EBV growth-transforms infected B cells by expressing a set of viral proteins, termed latent proteins including six EBV nuclear antigens (EBNA1, -2, -3A, -3B, -3C and –LP), and three membrane proteins (LMP1, 2A and 2B), (Table1). In addition to these nine proteins, EBV expresses two non-coding RNAs (EBER1 and EBER2), and 44 viral miRNAs (Figure 5) (GRUNDHOFF et al., 2006; PFEFFER et al., 2004). During latency, the EBV lytic cycle replication is usually repressed by different mechanisms, such as upregulation of important transcription factors like STAT3 (Signal transducer and activator of transcription 3) in BL or LCL cells. STAT 3 upregulation can affect several Zn-finger repressors, such as ZNF253, ZNF257, SNF589 and SETDB1. Koganti *et al.* have shown a decline in B cells proliferation, when B cells from patients with hypomorphic

mutations in STAT3, are infected with EBV (KOGANTI et al., 2014; LIEBERMAN, 2015). However, lytic cycle reactivation more likely occurs when the EBV-CD19$^+$ memory in B-cells is recalled (LAICHALK, THORLEY-LAWSON, 2005; MIYASHITA et al., 1995). It has been shown that EBV lytic cycle can be induced, by activation of transcription factor BZLF1 or other proteins such as X-Box-binding protein 1 (XBP-1) and protein kinase D (PKD), which has an important role in switching from latency to lytic cycle, during EBV infection (BHENDE et al., 2007; COUNTRYMAN, MILLER, 1985; YOUNG et al., 2016) .

Table 1: Different stages of EBV latency. Different EBV latency stages are associated with different tumors. Adapted and modified from (HEALY, DAVE, 2015).		
Latency Stages	Expressed EBV protein	Associated Tumors
I	LMP2A, EBNA1	Burkitt lymphoma DLBCL NOS T cell-rich DLBCL
II	Protein in latency I + LMP1,LMP2B	Classic Hodgkin's lymphoma Angioimmunoblastic T cell lymphoma NK/T cell lymphoma, N Nasopharyngeal carcinoma Gastric carcinoma
III	Protein in latency II + LP,EBNA2,EBNA3A, EBNA3B,EBNA3C	Primary EBV infection Post-transplant lymphoproliferative disease AIDS-related lymphomas (plasmablastic DLBCL, primary CNS lymphoma, primary effusion lymphoma) EBV + DLBCL of the elderly

1.13 EBV miRNAs

EBV was the first human DNA virus identified to encode miRNAs (PFEFFER et al., 2004). EBV miRNAs are encoded in two clusters, the so-called BHRF1-cluster (Bam HI fragment H rightward open reading frame 1), which encodes 3 miRNAs and the BART-cluster (Bam HI-A region rightward transcript), encoding 41 miRNA (YOUNG et al., 2016). It has been shown that EBV miRNAs are important for keeping EBV in latency by targeting EBV proteins, such as BART(1-5p,16,17-5p), downregulating the LMP1 protein (LO et al., 2007), BART-2, downregulating the DNA polymerase BALF5 expression (BARTH et al., 2008) and BART22, downregulating LMP2A (LUNG et al., 2009). EBV miRNAs also have been shown by many research groups to target cell mRNAs and downregulating their protein expression. For instance, BART1 targets the tumor suppressor phosphatase and tensin homolog (PTEN) (CAI et al., 2015), BART3 and BART16 target IPO7 and TOMM22, respectively (DÖLKEN et al., 2010), BART9 targets E-Cadherin (HSU et al., 2014) and BART6 targets Dicer (IIZASA et al., 2010; KANDA et al., 2015).
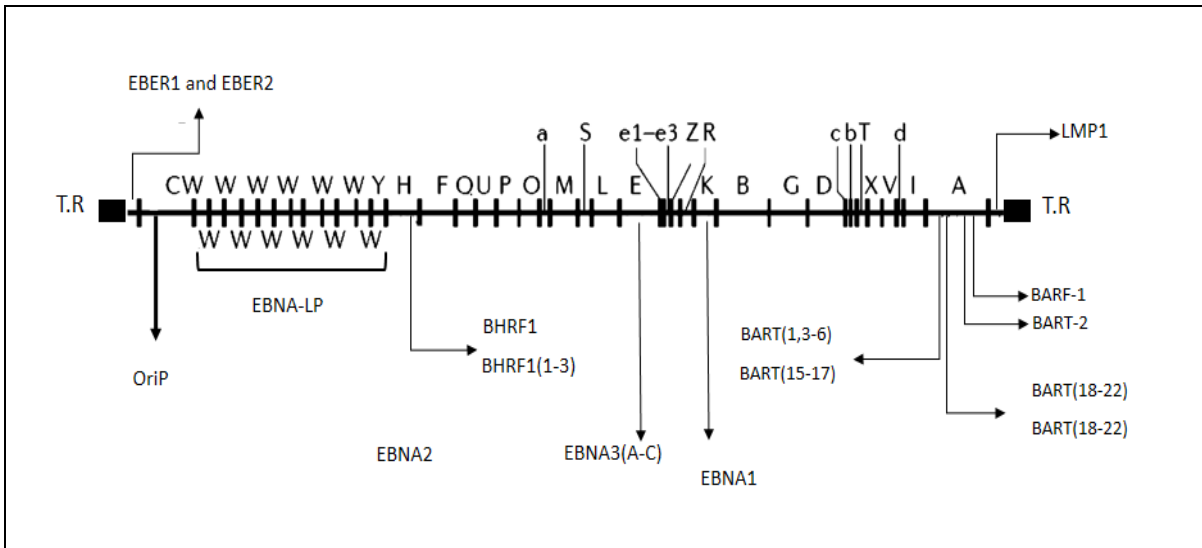
Figure 5: EBV BamHI restriction map.
BamHI restriction maps for the EBV B95-8 strain and locations of latent cycle proteins and the EBV encoded miRNAs. The BamHI fragments are shown according to size using alphabetical letters, a capital letter A for the largest and small letter for the smaller fragment in descending order.TR, terminal repeats are shown as black blocks. BART, BamHI-A rightward transcript,(BHRF1) BamHI fragment H rightward open reading frame, (BARF1) BamHI-A fragment rightward reading frame, (LMP) latent membrane proteins, EBNA (Epstein–Barr nuclear antigens). Adapted and modified from (YOUNG et al., 2016).

1.14 Aim of the study

A very promising approach to understand the involvement of a certain miRNA in the process of a disease such as cancer, is to assess the miRNA expression profile of cancer patients. The comparison with their normal counterpart is a very promising approach for understanding the involvement of (a) certain miRNA(s) in a disease of interest. This may lead to the discovery of a novel prognostic or diagnostic biomarker. Although it is believed that the miRNA profile from extracted total cellular RNA is an actual indicator of RISC complex-associated miRNA, due to quick degradation of non-guide miRNA, this hypothesis was challenged by the Cullen group, when they compared the miRNA profile of the total cellular miRNAs with the RISC associated miRNAs (Ago-IP) pool. Intriguingly, they have found that the total cellular miRNA profile differs from the Ago-bound profile, and therefore they challenged the idea that the total cellular miRNA profile is accurately reflecting the Ago RISC-associated miRNAs (FLORES et al., 2014).

The effect of EBV infection and dysregulation of the total cellular miRNA profile in DLBCL was reported by many researchers, as already discussed above. To the best of our knowledge, this is the first time that Ago2 immunoprecipitation was performed, followed by sequencing (Ago2-IP-seq) in two different DLBLC cell lines and their EBV infected counterparts, in order to profile the miRNAs according to their functional level. The U2932 and SUDHL5 cells and their EBV infected counterparts were used as a model for ABC-DLBCL and GCB-DLBCL, respectively.

The questions addressed in this project were as follows:

1. Determination of differentially expressed miRNA in DLBCLs cell lines, in comparison with their EBV infected counterparts.
2. Assessment of various expressed miRNA, in Ago2-IP in DLBCLs cell lines in comparison to EBV infected counterparts.
3. Evaluation of enriched or depleted miRNA in the Ago2-IP, compared to the total cellar miRNA profile in each cell line by RNA-seq.

2 Materials and Methods

2.1 Material
2.1.1 Laboratory equipment's.

Adjustable pipettes	Gilson,Peqlab
Agilent 2100 Bioanalyzer	Agilent (Santa Clara, USA)
Centrifuge	Megafuge 1.0 R (Heraeus)
Centrifuge	202 MK (Sigma)
Centrifuge 1-16K	Sigma
Chemidoc XRS system	Bio-Rad
CO2 incubator	HeracellTM 150i (Thermo Scientific)
Electrophoresis power supply	Consort EV-231 (Consort bvba)
Electrophoresis power supply	Phero Stab 300 (Biotec Fisher)
Heat block	Thermomixer Compact (Eppendorf)
Oven for hybridization	UM 400B Hyp (Bachhofer)
Phosphoimager	PhosphoimagerTM-Typhoon with plates and cassettes for exponation (Molecular Dynamics, Amersham)
Photometer	NanoDropTM 2000c (Peqlab)
Plates (MicroAmp® Fast Optical 96-Well Reaction	(Carlsbad, USA)
Real-Time PCR System (StepOnePlus™); 96-Well	Applied Biosystems/Life Technologies
Semi-Dry Blotter	2117 Multiphor (LKB Bromma)
Shaker	Thermomixer Compact (Eppendorf)
Shaker	POLYMAX 1040 (Heidolph)
Shaker	REAX 2000 (Heidolph)
Shaker	Edmund buehler
Tank-Blotting chamber	2005 Transphor Electro Blotting Unit (LKB Bromma)
Vortex	Heidolph
Weighing balance	Sartorius

2.1.2 Reagents and chemicals

3-Mercapto-1,2-propandiol	Sigma
Ammonium persulfate (APS)	Serva
Bisacrylamide 2%	Roth
Blocking reagent	Boehringer
Blue protein standard	Biolabs
Bovines Serumalbumin (BSA)	Serva
Bradford-Reagent Roti®-Quant	Carl Roth
Bromophenol blue	Serva
´´Complete Mini ``Protease Inhibitor Cocktail	Roche Diagnostics
Coomassie Brilliant Blue R 250	Roch
Denhardt's solution 50x	Sigma
Diethylpyrocarbonate (DEPC)	Sigma
EDC-Hydrochlorid	Sigma
Ethanol	Roth
Ethylendiamintetraacetat (EDTA)	Serva
Fetal calf serum (FCS)	Gibco
G 418 (Geneticin)	Invitrogen
Gamma P-32 UTP	Hartmann Analytics
Glycin	Sigma
H_2O_2 30%	Merck
HybondTM-N membrane	GE healthcare life science Amersham
IGAPEL CA 630	Sigma
KCL	Merck
Klenow Fragment (DNA Polymerase I)	Klenow Fragment (EP0051)
Luminol(3-Aminophthalhydrazide)	Sigma
Magnesium chloride hexahydrate	Roth
Methanol	Roth

Methylimidazole	Peqlab
TEMED	Serva
NaCl	Merck
Nitrocellulose membrane protran 0.2 µM	GE healthcare life science Amersham
Neubauer chamber	C-Chip Neubauer Improved , Digital Bio
Nucleotides (dNTPs)	Peqlab
Nucleotides (NTPs)	Invitrogen
P-coumaric acid	Sigma
pH meter Hydrus 300	Fisherbrand Hydrus 300
PonceauS TM	Sigma
Real-Time PCR System (StepOnePlus™); 96-Well	Applied Biosystems/Life Technologies
Sepharose 4 Fast Flow Protein G	GE Healthcare, Freiburg, Germany
Skim milk powder	Töpfer
Sodium azide	Merck
Sodiumdodecylsulfate (SDS)	Serva
Tris base Trizma	Sigma

2.1.3 Miscellaneous materials

mirVANA TM kit	Ambion
miScript II RT Kit	Qiagen (Hilden, Deutschland)
miScript II RT Kit	Qiagen (Hilden, Deutschland)
miScript SYBR® Green PCR Kit	Qiagen (Hilden, Deutschland)
Primers for qRT-PCR	Qiagen
Primers for NB	Eurofins MWG operon
RPMI -1640	Sigma
SequaGel - UreaGel System	National Diagnostics USA

2.1.4 Antibodies

Antibody	Source and Isotype	Dilutions used	Reference
Ago2(11A9)	Rat monoclonal IgG2a	1:50	a kind gift from Prof. Gunter Meister, University of Regensburg
Sec 23b	Rat monoclonal IgG2a	1:50	Prof.Kremmer, Dr.Szczyrba
EBNA1(1H4)	Rat monoclonal	1:10	Prof.Kremmer, Prof.Grässer
LMP(S12)	Mouse Monoclonal	1:10	a kind gift of Prof.Martin Rowe, University of Birmingham
EBNA2 (R3)	Rat monoclonal	1:50	Prof.Kremmer,Prof. Grässer
α-GAPDH(14C10)	Rabbit	1:5000	Cell signaling
Peroxidase AffiniPure Goat Anti-Rat IgG + IgM (H+L)		1:8000	Jackson ImmunoResearch Laboratories
Anti-Mouse IgG (whole molecule)– Peroxidase antibody produced in rabbit		1:8000	Sigma aldrich
Anti-Rabbit IgG (whole molecule)– Peroxidase antibody produced in goat		1:8000	Sigma aldrich

2.1.5 Buffers and Solutions

Ammonium persulfate (APS)	APS in dd H_2O 10%
Blocking reagent	5% skim milk powder in PBS
Crosslinking reagent for NB	Methylimidazole 245 µL EDC-hydrochloride 0.75 g ddH_2O up to 24 mL
Coomassie-Brilliant blue stain (C.B.B)	300 mL Isopropanol 780 mL dd H_2O 120 mL acetic acid 0.3 g Coomassie Brilliant Blue R 250
dNTPs	dATP, dCTP , dGTP , dTTP each one 10 mM
ECL-Solution A	Luminol 1 gr DMSO 22.6 mL Up to 50 mL with dH2O
ECL-Solution B	P-coumaric acid 0.5 gr DMSO 33.8 mL Up to 45 mL with ddH_2O
ECL-Solution C	1 M Tris HCl pH 8.5
ECL working solution	Solution A 2.5 mL Solution B 1.113 mL Solution C 25 mL up to 250 mL with ddH2O for WB: 1 µl H_2O_2 added to 1mL ECL before use

Hybridization buffer	20x SSC	7.5 mL
	1 M Na_2HPO_4	0.6 mL
	10% SDS	21 mL
	50x Denhardt's Solution	0.6 mL
	blocking reagent	a pinch
lysis buffer	Tris/HCl pH 7.4	25 mM
	KCl	150 mM
	EDTA	2 mM
	NaF	1 mM
	IGEPAL	0.5%
	Working solution:	
	1 tablet complete mini protease inhibitor in 10 mL Lysis buffer before use	
MSE 5X	MOPS	1M
	NAAc	0.3M
	EDTA	0.3M
	H2O	
PBS	Solution A(10X)	
	NaCl	80g
	KCl	2g
	$MgCl_2.6H2O$	1g
	$CaCl_2.2H2O$	1.32g
	Make the volume with dH_2O to one liter	
	Solution B(10X)	
	$Na_2Hpo_4.12H2O$	28.98g
	KH_2PO_4	2g
	Make the volume with dH_2O to one liter	
	working dilution : 1X from A+B	

Polyacrylamide gel 12.5% (Separating gel)	Separating Stock buffer	4 mL
	30% Acrylamide	6.7 mL
	2% Biscrylamide	2.68 mL
	ddH$_2$O	2.62 mL
	10% APS	140 µL
	TEMED	14 µL
	Total	16.15 mL
Polyacrylamide gel 10% (Separating gel)	Separating Stock buffer	4 mL
	30% Acrylamide	5.3 mL
	2% Biscrylamide	2.12 mL
	ddH$_2$O	4.58 mL
	10% APS	140 µL
	TEMED	14 µL
	Total	16.15 mL
Polyacrylamide gel 4% (stacking gel)	Stacking Stock buffer	1.25 mL
	30% Acrylamide	750 µL
	2% Biscrylamide	300 µL
	ddH$_2$O	2.7 mL
	10% APS	100 µL
	TEMED	10 µL
	Total	5 mL
Ponceau S-stain	Trichloroaceticacid	30 g
	Ponceau S	5 g
	Make up to 1 liter with dd H$_2$O	

"Low Molecular Weight" marker	Protein	kDa	Concentration µg/µL
	Phosphorylase b	94	0.5
	BSA	67	0.7
	Ovalbumin	43	1.0
	Carboanhydrase	30	0.5
	Trypsin inhibitor	20.1	1.0
	Lactalbumin	14.4	0.5

RNA loading buffer		
	Formamide	750 µL
	5x MSE	150 µL
	formaldehyde	240 µL
	50% glycerol	200 µL
	dH$_2$O	160 µL
	bromphenol blue	a pinch
	xylene cyanol FF	a pinch

SDS-loading buffer 2x		
	Tris/HCl pH 6.8	130 mM
	SDS	6%
	ß-Mercapto-1,2-propandiol	10%
	glycerol	10%

SDS-loading buffer 4x		
	SDS	1,6 g
	β-Mercaptoethanol	4 mL
	Glycerol	2 mL
	Tris pH 7 (1M)	2 mL
	Bromo phenol blue	4 mg
	ddH$_2$O	2 mL

SDS Running Buffer for SDS-PAGE		
	glycine	72 g
	Tris	15 g
	SDS (20%)	25 mL

Separating Stock buffer	Tris	1.5 M
	SDS	0.4%
	pH	8.8
Stacking Stock buffer	Tris	0.5 M
	SDS	0.4%
	pH	6.8
Stripping buffer for NB	0.5% SDS	
SSC 20X	NaCl	3 M
	trinatriumcitrat dihydrate	0.3 M
Tranfer Buffer for WB	glycine	72 g
	Tris	15 g
	SDS (20%)	12.5 mL
	Methanol	1 liter
	Make up to 5 liters with dd H_2O	
TBE buffer 10X	Tris	0.89 M
	Boric acid	0.89 M
	EDTA	20 mM
TE buffer (pH=8)	Tris	10 mM
	EDTA	1 m
Washing buffer for IP	Tris/HCl pH 7,4	50 mM
	KCl	300 mM
	$MgCl_2$	1 mM
	IGEPAL	0.5%
Washing buffer I (for NB)	SSC	5x
	SDS	1%
Washing buffer II (for NB)	SSC 1X	
	SDS 1%	

2.1.6 Cell lines

The following cell lines have been used in this study:

U2932: a B-cell line, derived from a patient with HL followed by the NHL, and it has a characteristic of post-GC derived origin (ABC-DLBCL) of the tumor cells (AMINI et al., 2002).

U2932 EBV positive clone A: a U2932 cell line, infected with EBV-GFP, not expressing EBNA2 (BOCCELLATO et al., 2007).

SUDHL5: a B-cell line, derived from a lymph node of a 17-year-old woman with B-cell non-Hodgkin lymphoma (B-NHL) and has characteristic of GCB-DLBCL.

SUDHL5 EBV positive: SUDHL5 cell line, infected with EBV-GFP, obtained from Prof. Pankaj Trivedi, University of Rome.

2.1.7 Primers for real time PCR

The following Primer sequences were ordered from Qiagen for RT-qPCR analyses:

Primer	Sequences	Cat. No.
let-7c-5p	UGAGGUAGUAGGUUGUAUGGUU	MS00003129
miR-10a-5p	UACCCUGUAGAUCCGAAUUUGUG	MS00031262
miR-146a-5p	UGAGAACUGAAUUCCAUGGGUU	MS00003535
miR-155-5p	'UUAAUGCUAAUCGUGAUAGGGGU	MS00031486
miR-15a-5p	UAGCAGCACAUAAUGGUUUGUG	MS00003178
miR-221-3p	AGCUACAUUGUCUGCUGGGUUUC	MS00003857
miR-28-3p	CACUAGAUUGUGAGCUCCUGGA	MS00009254
miR-363-3p	AAUUGCACGGUAUCCAUCUGUA	MS00009576
miR-423-3p	AGCUCGGUCUGAGGCCCCUCAGU	MS00004179
miR-423-5p	UGAGGGGCAGAGAGCGAGACUUU	MS00009681
miR-486-5p	UCCUGUACUGAGCUGCCCCGAG	MS00004284
miR-92a-3p	UAUUGCACUUGUCCCGGCCUGU	MS00006594

2.1.8 Probes used for Northern Blots (NB) and Ago2-IP NB.

The following oligo DNA probes were obtained from Eurofins Genomics for generating miRNA probes for Northern Blots.

Oligo probe	Sequences
let-7c-5p	TGAGGTAGTA GGTTGTATGG TTcctgtctc
miR-101-3p	TACAGTACTG TGATAACTGA Acctgtctc
miR-142-3p	TGTAGTGTTT CCTACTTTAT GGAcctgtctc
miR-142-5p	CATAAAGTAG AAAGCACTAC Tcctgtctc
miR-21-5p	TAGCTTATCAGACTGATGTTGAcctgtctc
miR-221-3p	AGCTACATTG TCTGCTGGGT TTCcctgtctc
miR-222-3p	AGCTACATCT GGCTACTGGGTcctgtctc
miR-363-3p	AATTGCACGG TATCCATCTG TAcctgtctc
miR-423-5p	TGAGGGGCAGAGAGCGAGACTTTcctgtctc
miR-4485-3p	TAACGGCCGCGGTACCCTAAcctgtctc
miR-4792-5p	CGGTGAGCGCTCGCTGGCcctgtctc

2.2 Methods

2.2.1 Cell culture

The U2932, SUDHL5, U2932 (EBV positive), SUDHL5 (EBV positive) cell lines were maintained in RPMI 1640 medium at 37 ℃ in a 5% humidified CO_2 incubator. RPMI 1640 was supplemented with10% fetal calf serum, antibiotic mix (40 IU/mL penicillin, 50 µg/mL streptomycin, 1 IU/mL Neomycin-sulfate, 90 IU/mL Nystatin). An additional 200 mg/mL G418 (Geneticin) was used for EBV positive cell lines.

2.2.2 Cell counting (Hemocytometer)

The Neubauer Improved C-Chip was used to count the number of cells. Depending on the cell density, a 1:5 or 1:50 dilution was made in PBS and 2 to 4 outer big squares were counted.

Cell density (cells/mL)

$$= ((No. \text{ of counted cells}): (No. \text{ of large Squares})) \times 10^4 \times \text{Dilution factor}.$$

2.2.3 RNA related techniques

2.2.3.1 RNA isolation

Suspension cells (5 to 10 mL) were harvested by centrifugation at 500 x g for 5 minutes at room temperature (RT). 700 µL of Qiazol (Qiagen) was added to the pellet and incubated for 5 min at RT. Afterwards, 125 µL of chloroform was added to the sample and vortexed for 15 sec, and subsequently again incubated for 10 min at RT. the sample was then centrifuged at 12000 xg for 15 min at 4 ℃ and the upper phase was transferred to a new 1.5 mL microcentrifuge tubes and 500 µL of isopropanol was added to the tube and incubated on ice for 15 min, followed by centrifugation at 12000 xg for 30 min in 4 ℃ . After that, the pellet was air dried at RT for 15 min and dissolved in 50 µl of RNase free H_2O and the RNA was dissolved by incubation at 55 ℃ for 15 min.

RNA isolation for sequencing, qRT –PCR and Ago2-IP for NB was performed using the miRNeasy Mini kit (Qiagen) according to manufacturer's instructions. Briefly, 700 µl of QIAzol was added to 100 µl of cell lysate or directly to the beads, after the last washing step with PBS (Ago2-IP and control-IP).Then the mixture was vortexed and incubated at room temperature for 5 min. Centrifugation was performed at 12000 xg for 15 min at 4°C. Then the upper aqueous phase transferred to a new collection tube. Subsequently, 1.5 volumes of 100% ethanol were added and mixed by pipetting up and down few times, and the mixture was loaded on the spin column in a 2 mL collection tube. Next, the samples were centrifuged at 12000 xg for 1 min the supernatant discarded and this step was repeated, until all the solutions were loaded on the column. The column was washed once with 700 µl RWT buffer and twice with 500 µl RPE buffer. All centrifugations were performed at 12000 xg for 1 min, and finally the column was transferred to a new collection tube. The RNA was eluted in 30 µl of RNase-free water by centrifuging at 12000 xg for 2 min. Tumor specimens from DLBCL patients were extracted from snap-frozen tissues using TriZol instead of Qiazol, as described above. The concentrations of all extracted RNAs, were measured by NanoDrop, and samples were stored at -70 ℃.

2.2.3.2 MiRNA microarray and data analysis

MiRNA expression profiling of 1205 human miRNAs and 44 EBV miRNAs was performed in triplicate using the Agilent human miRNA microarray (release 16.0, Agilent, Cat. No, G4870A). Briefly, 100 ng of isolated RNA from total lysates or immunoprecipitates from U2932 or U2932-EBV cell line was dephosphorylated, labelled with pCp-Cy3 and hybridized to the microarray according to the manufacturer's instructions.

Microarray data analysis was performed as described (LUDWIG et al., 2015). In brief microarrays were scanned using the Agilent Microarray Scanner and expression values were extracted with the Agilent Feature extraction software. Raw data of cellular input and immunoprecipitate arrays was quantil normalized separately using R software. Unpaired two-sided t-tests were performed. For identification of significantly differentially expressed miRNAs between U2932E-EBV vs. U2932 cell lines for total lysates and immunoprecipitates, two-fold changes and P-values of <0.05 were considered statistically significant.

2.2.3.3 MiRNA sequencing and processing of data

Sequencing was performed by next generation sequencing(IKMB, University of Kiel) using total cellular lysate and purified RNA from U2932, SUDHL5 and the EBV positive counterpart using TruSeq small RNA Library Type on the HiSeq 2500 system from Illumina. The analysis of sequencing data was performed by Tobias Fehlmann under the guidance of Prof.Dr. Andreas Keller (Chair for Clinical Bioinformatics, Saarland University). Briefly, the miRMaster tools was used to remove the trimmed adaptors and to quality filter the reads (FEHLMANN et al., 2017). Then the Bowtie sequence alignment software was used to map with Genome Reference Consortium GRCh38 (hg38) with one mismatch pairing allowed (LANGMEAD et al., 2009). Those reads which mapped with hg38 were used for human miRNA quantifications and those which are not mapped to human genome were used for EBV miRNA. miRBase (v21) (KOZOMARA, GRIFFITHS-JONES, 2014) and the miRMaster tools were used for mapping of miRNA for human and EBV miRNA.

2.2.4 qRT-PCR

Quantitative Real Time-PCR (qRT-PCR) was performed to validate the NGS data using the miScript II RT Kit and the miScript SYBR Green PCR Kit on the StepOnePlus™ Real-Time PCR System.

2.2.4.1 Reverse Transcription to generate cDNA for qRT-PCR

The extracted RNA was converted to cDNA in the following reaction:

Components	Volume
5x miScript HiSpec Buffer	4 µL
10x miScript Nucleic Mix	2 µL
RNase free water	11µL
miScript Reverse Transcriptase Mix	2 µL
Template RNA	200 ng for total cellular and 20 ng for Ago2 IP RNA extract (1 µL)

The reaction mixture was incubated for 60 min at 37ºC, followed by 5 min at 95ºC to inactivate miScript Reverse Transcriptase. The reaction was diluted 1 to 10 in RNase-free H2O, and the samples were stored at -20 ºC until further use. qRT-PCR reaction was performed in duplicate and miR-30d was used as an endogenous control as our NGS data showed no expression difference of human miR-30d between U2932 and SUDHL5 cell lines and the EBV positive counterparts in total cell lysates or Ago2-IP miRNA profile. Fold change in EBV negative versus EBV infected DLBC cell lines was calculated by the following formula for cellular input and Ago2-IP:

Fold change diffrence = $2^{\wedge((\text{miR-XEBVneg} - \text{miR-30dEBVneg}) - (\text{miR-XEBVpos} - \text{miR-30dEBVpos}))}$.

To define if a miRNA was deregulated two criteria applied to our data:

1) At least 2-fold expression difference between EBV negative and positive counterpart.

2) qRT-PCR result in the same direction as in the sequencing results.

The following cycling program was used for StepOne instrument:

Components	Volume
cDNA-Template (1:10 diluted)	2 µL
2x QuantiTect SYBR® Green PCR Master Mix	5 µL
10x miScript Universal Primer	1 µL
10x miScript Primer Assay	1 µL
H20 RNase-free	1 µL

PCR Initial activation step	95 °C	15 min
3-step cycling:		
	94 °C	15 s
	55 °C	30 s
	70 °C	30 s

2.2.4.2 Northern blot for the Analysis of the miRNA

Northern blot is a technique used to detect a specific RNA in a sample. This technique was performed to compare and validate significantly deregulated miRNA from NGS and qRT-PCR data in total cellular lysate and Ago2-IP data.

Equal amounts of extracted RNA from total cellular (15 -20 µg) or Ago2-IP and isotype control (200 ng of purified RNA), were mixed with 5 µl RNA loading buffer, and loaded on a 12% urea polyacrylamide gel. The gel was run at 20W for 3 to 4 hours in 1X TBE buffer. To check the loading control and the quality of RNA, the gel was stained with ethidium bromide (10 µg in 100 mL 1X TBE) for 5 min and the RNAs were visualized at 254nm. The ethidium bromide picture was documented, using ChemiDoc XRS (Bio-Rad). An equal amount of 1.5 µg RNA, from DLBCL and lymph nodes of patient samples was loaded for Northern blot.

Composition of 12% of a Urea polyacrylamide gel

Components	Volume
UreaGel 29:1 Concentrate	24 mL
UreaGel Diluent	21 mL
UreaGel Buffer	5 mL
TEMED	20 µl
APS 10%	400 µl

2.2.4.3 Transfer of RNA to a Membrane

To transfer the RNA to a nylon membrane (Hybond N; Amersham), an electroblot transfer sandwich was set up as follows: five pre-wet Whatman papers with dH_2O, nylon membrane, gel, five more pre-wet Whatman paper. Transfer was carried out at 15V for 30 minutes, using a semi-dry chamber with transfer from anode to cathode. Following the transfer the membrane, on top of three Whatman papers, soaked in freshly prepared EDC crosslinking regent and then the NB membrane was wrapped in Saran-Wrap and incubated at 60 ℃ for 1 to 2 hours. Following crosslinking, the membrane was transferred to a glass tube and incubated with 30 mL pre-hybridization buffer with continued rotation at 50 °C for 30 min. Then the [32] P-labeled miRNA probe

(see below) was added to the hybridization buffer, and incubated overnight with a continued rotation at 50 ℃, in an oven. The next day the membrane was washed two times with 5XSSC and two times with 1XSSC (each time about 20 min). The membrane was wrapped with Saran-Wrap and exposed to Phosphorimager, and the next day scanned with the Phosphorimager TM Typhoon.

2.2.4.4 Generating radiolabelled ^{32}P RNA probe

To generate radiolabelled ^{32}P RNA probes a two-step procedure was used. First a double strand DNA template from a single stranded oligonucleotide which has a CCTGTCTC AT at 3´ end (complementary to T7 promoter sequence) was generated using the mirVANA TM kit. In second step the 32p RNA probe was generated from the double stranded template.

Double strand DNA (dsDNA) template synthesis;

a) The following components were incubated at 70 ℃ for 5 min and then at RT for 5 min.

Components	Volume
H2O	6µL
T7-Promoter Primer (100µM)	2µL
Oligonucleotide Template (100 µM)	2µL

b) To complete the reaction, the following components were added and this mixture was incubated at 37 ℃ for 30 min. The prepared double strand DNA template for miRNA of interest was stored at -20 ℃ until use.

Components	Volume
Nuclease-free H2O	4 µl
10 x Klenow buffer	2 µl
10 x dNTPs	2 µl
Exo-Klenow	2 µl

2. Generation of ^{32}P RNA probe at radioactive lab

Components	Volume
Nuclease free H2O	7 µl
dsDNA template	2 µl
NTPs(without U)	3 µl
10 x RNA polymerase buffer	2 µl
T7-RNA polymerase	2 µl
32P -labeled UTP (radioactive)	5 µl

After adding the above components, the mixture was put on continuous shaker (700RPM) for 10 min at 37 ℃ and then 1 µl of DNase I was added and again put on continuous shaker (700 RPM) for 10 min at 37 ℃, and finally as discussed the prepared probe was added to the glass tube containing hybridization buffer and cross-linked NB membrane.

2.2.4.5 NB stripping

To re-probe the NB membrane with a different ^{32}p-labelled probe, the previous signal was removed using stripping buffer. The membrane was put into a glass tube and incubated with warmed stripping buffer, for one hour at 70°C in the oven under continuous rotation. After removing the stripping buffer, the membrane was wrapped with a Saran-Wrap and exposed to the phosphor imager overnight (Phosphorimager TM Typhoon) to ensure that the previous signal was erased.

2.2.5 Protein related techniques

2.2.5.1 Immunoprecipitation and immunoblotting of Ago2 – IP

To perform the RISC associated miRNA profiling, the Ago2 Immunoprecipitation was carried out as described previously (DEMBLA et al., 2014; DOLKEN et al., 2010). The cell lines, either U2932 or SUDHL5 or the EBV positive counterparts were cultured, in large scale (400 to 500 mL) in RPMI1640, supplemented with 10% FCS and antibiotics (see material and methods). After counting the cells, about 3.5×10^8 cells were used for each IP (3). Antibody coupling was performed one day before performing IP. For coupling, about 200 µL of Sepharose Protein G beads were washed 3 times with cold PBS buffer (at 500 xg for 3 min), and then at the last step the supernatant was removed and the pellet divided into two tubes. In each tube, about 100 µL of Sepharose Protein G beads was incubated overnight with 1.6 mL monoclonal antibody, Ago2 antibody 11A9 (rat IgG2a) or with isotype control (rat IgG2a) antibody, on vertical rotator at 4°C. The next day the beads were washed three times with PBS, and once with lysis buffer before incubating with lysate. For Ago2-IP, about 3.5×10^8 cells from U2932, SUDHL5 and their EBV positive counterparts, were pelleted and washed three times with PBS (at 500 xg for 3 min). Then, 1.5 mL of lysis buffer were added to the pellet in 1.5 mL reaction tube, and incubated for 30 min on the vertical rotator at 4°C. Subsequently, the tube was centrifuged at 20,000 xg for 30 min at 4°C. Afterwards, to decrease the non-specific binding, the lysate was precleared with 100 µL of protein G-Sepharose beads (washed 3 times in PBS) alone for 60 min at 4°C, using a vertical rotator. Next, samples were centrifuged at 20,000 xg for 5 min at 4°C. 100 µL of the cleared lysate was removed for preparing total RNA, and 50 µL as a protein input. The remaining lysate was divided in two equal volumes for the Ago2-IP and the isotype control-IP experiment and the volumes were adjusted to 1 ml with lysis buffer. The coupled beads were incubated with the lysis buffer overnight on a vertical rotator at 4 °C.

The next day, the beads were pellet down at 500 xg for 3 min at 4 ℃, and washed three times with wash buffer (50 mM Tris HCl, pH 7.4, 300 mM KCl, 1mM $MgCl_2$, 0.5% IGEPAL) and once with PBS. 25 µL of each immunoprecipitated fraction was removed

and this sample was used to check the efficiency of Ago2 IP, by Western blot (GROSS et al., 2010) and the remaining beads was incubated with 700 µL Qiazol regent (Qiazol, Hilden, Germany), followed by RNA extraction, using the miRNA easy kit.

2.2.5.2 SDS-PAGE

Sodium dodecyl sulfate-polyacrylamide gel electrophoresis (SDS-PAGE), is used to separate proteins according to the molecular mass, under denaturing conditions. SDS-PAGE was performed as described by Laemmli, 1970; Sambrook et al., 1989. Before loading the samples, either the lysate or immunoprecipitated fractions from different cell lines were diluted in 4X SDS loading buffer and heated for 6 min at 94℃. Three µl of molecular mass marker proteins were also separated on the gel. SDS-PAGE was carried out at 80V (stacking gel) and 125 V (separating gel), for about 3.5 hours.

2.2.5.3 Western Blot

Following SDS-PAGE, the proteins were transferred to a nitrocellulose membrane by electrophoresis, at 400 mA for 3 hours at 4℃. After blotting, the membrane was stained with Ponceau S, to ensure that the transfer was carried out properly. The membrane was destained with PBS for 15 min under agitation and then blocked with 5% nonfat dry milk in PBS for 75 min under agitation at room temperature. Subsequently, the membrane was incubated with the indicated primary antibody, overnight at 4 °C. The membrane was washed 3 times with PBS, for about one hour, and then incubated with appropriate secondary antibody(conjugated with horseradish peroxidase), in blocking reagent (5% milk in PBS) for 2 hour under agitation at 4 °C. The membrane was washed 3 times with PBS for about one hour at room temperature. Finally, the membrane was developed using ECL (see Material and Methods part) and documented with the Bio-Rad Gel-Doc apparatus, using the Quantity One (Bio-Rad) software.

3 Results

Here we tested (i) the miRNA profiles of the DLBCL cell lines U2932 and SUDHL5 and their EBV-converted counterparts U2932-EBV and SUDHL5-EBV , (ii) the miRNA profiles of the Ago2-complex of four cell lines, and(iii) whether the EBV-infection would alter the loading of the Ago2-complex. Previous work had shown that the overall miRNA profiling of a cell line did not necessarily reflect the function of a given miRNA as the Ago-loading might be very different from its overall content in the cell (FLORES et al., 2014).

In the following, we refer to the sequencing of cellular miRNA as "Total" and to the miRNA obtained from the Argonaute 2 immunoprecipitation as "Ago2-IP".

3.1 Characterizations of cell lines

The type of EBV latency was determined by Western blot with antibodies against EBNA1, LMP and EBNA2, using U2932-EBV and SUDHL5-EBV cellular extracts. As shown in Figure 6, SUDHL5-EBV has the characteristics of type III EBV-latency as it expresses EBNA1, LMP and high amounts of EBNA2. In contrast, U2932-EBV clone A has the characteristics of type II latency, as it express EBNA1 and LMP1 but low amounts of EBNA2.

Figure 6: EBV latency in U2932-EBV and SUDHL5-EBV cells.
Extract of the U2932-EBV and SUDHL5-EBV cell lines was assayed by immunoblotting using antibodies against EBNA1, LMP and EBNA2 .The EBNA2 blot was restained with GAPDH antibody as a loading control.
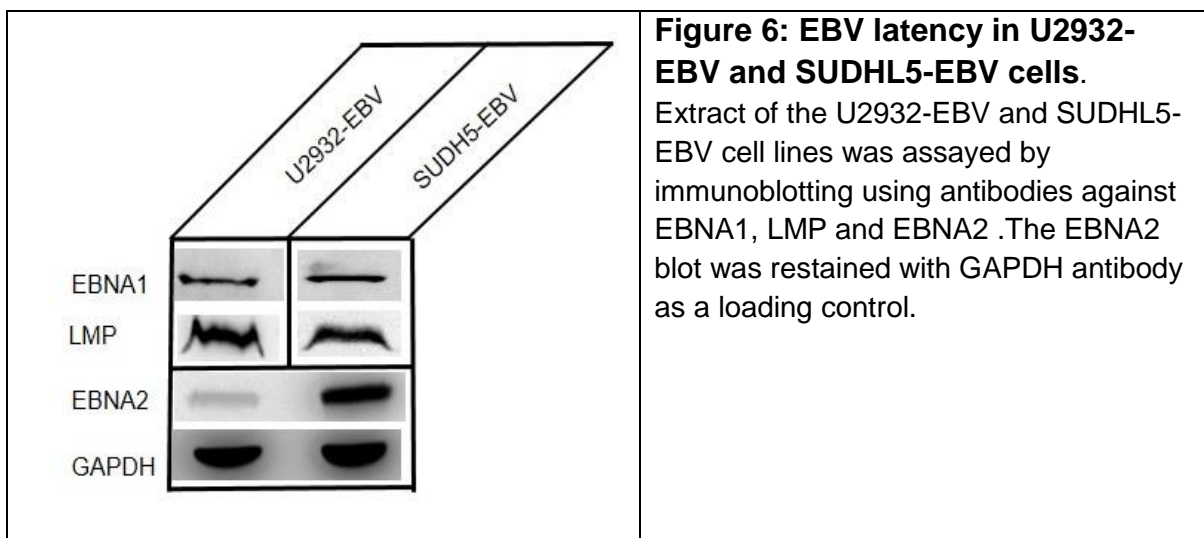
3.2 Microarray results

The isolated RNA from the Ago2-IP in U2932 and U2932-EBV, was analyzed by microarray. In addition, the RNA was isolated from the total cellular lysate to determine the miRNA profile prior to precipitation. Two replicates of the total cellular fraction failed the array quality control and were therefore excluded (marked as None Applicable (NA) from the study. the summary of the microarray data is shown in Table 2. We detected 206 miRNAs in U2932-EBV, and 170 miRNAs in the U2932 cell line. Of the total cellular miRNAs, detectable in both cell lines, nine were significantly upregulated (≥2) and 14 were significantly downregulated (≤2), in U2932-EBV compared to the U2932, respectively. Data are presented in Table 3 with the expression level taken into account. In the Ago2-IP, 386 miRNAs were detected in the U2932-EBV, and 395 in the U2932 cell line. In comparison with the Ago2-IP profile of U2932-EBV vs. U2932, 15 miRNAs were upregulated, while 169 miRNAs were downregulated. A complete list of up and downregulated miRNAs is shown in the appendix (Table A9).

Table 2: Summary of miRNAs detected by microarray, in "Total" and "Ago2-IP" profile in U2932-EBV and U2932.							
No. of miRNAs	Replicate1	Replicate 2	Replicate 3	Replicate 4	Mean	St dev.	Summary
Total cellular profile U2932-EBV	219	219	208	NA	215.33	6.35	206
Total cellular profile U293	182	190	163	NA	178.33	13.87	170
Ago2_IP U2932-EBV	413	408	388	392	400.25	12.12	386
Ago2_IP U2932	417	409	397	408	407.75	8.22	395

Table 3: Top 10 up regulated miRNAs and top 14 down regulated miRNAs in U2932-EBV vs. U2932 measured by microarray.

Total cellular miRNAs profile		Ago2-IP miRNAs profile	
miR-551b	7.08	miR-551b	8.85
miR-630	2.77	miR-137	6.89
miR-363	2.58	miR-363	6.53
miR-130a	2.45	miR-494	6.37
miR-15a	2.24	miR-449a	5.08
miR-574-5p	2.23	miR-130a	4.77
miR-1268	2.21	miR-630	3.48
miR-222	2.14	miR-3651	2.87
miR-335	2.06	miR-10a	2.75
		miR-718	2.67
miR-140-5p	-2.02	miR-148a*	-5.69
miR-25	-2.05	miR-199b-5p	-5.85
miR-374a	-2.10	miR-1180	-6.19
miR-3174	-2.12	miR-193a-3p	-6.25
miR-193b	-2.14	miR-126	-6.44
miR-134	-2.22	miR-624*	-6.45
miR-24	-2.30	miR-345	-6.48
miR-148a	-2.35	miR-1260	-7.17
miR-21*	-2.38	miR-1260b	-7.32
miR-125a-3p	-2.45	miR-1274b	-8.48
miR-3656	-2.47	miR-720	-10.62
miR-342-3p	-2.58	miR-340*	-12.56
miR-642b	-2.68	miR-1274a	-12.75
miR-4327	-2.79	miR-340	-75.41

3.3 Sequencing results

In order to investigate the miRNAs that were differentially associated with Ago2-complex, in comparison to the total cellular miRNA profile, and to determine whether EBV infection changes the loading of miRNA in the RISC complex, we performed Ago2 immunoprecipitation (Ago2-IP), in extracts from the uninfected DLBCL cell lines (U2932, SUDHL5) and their EBV infected counterparts (U2932-EBV, SUDHL5-EBV). The RNAs from the Ago2-IPs and from the total cellular extracts were subjected to next generation sequencing (NGS).

The specificity of the Ago2-IPs was determined from an aliquot of the precipitate, before the RNA was subjected to sequencing. As shown in Figure 7, the Western blot of the Ago2-IP demonstrated that the Ago2 protein was successfully precipitated from all four cell lines, and that the controls did not contain Ago2-protein
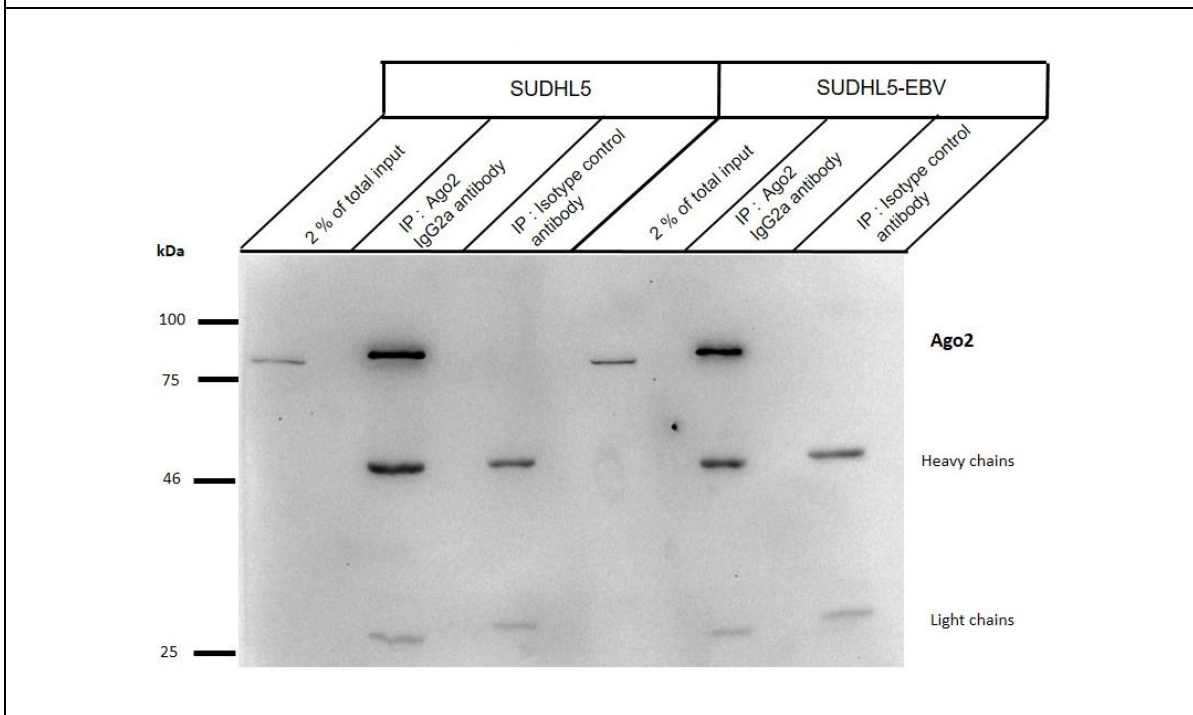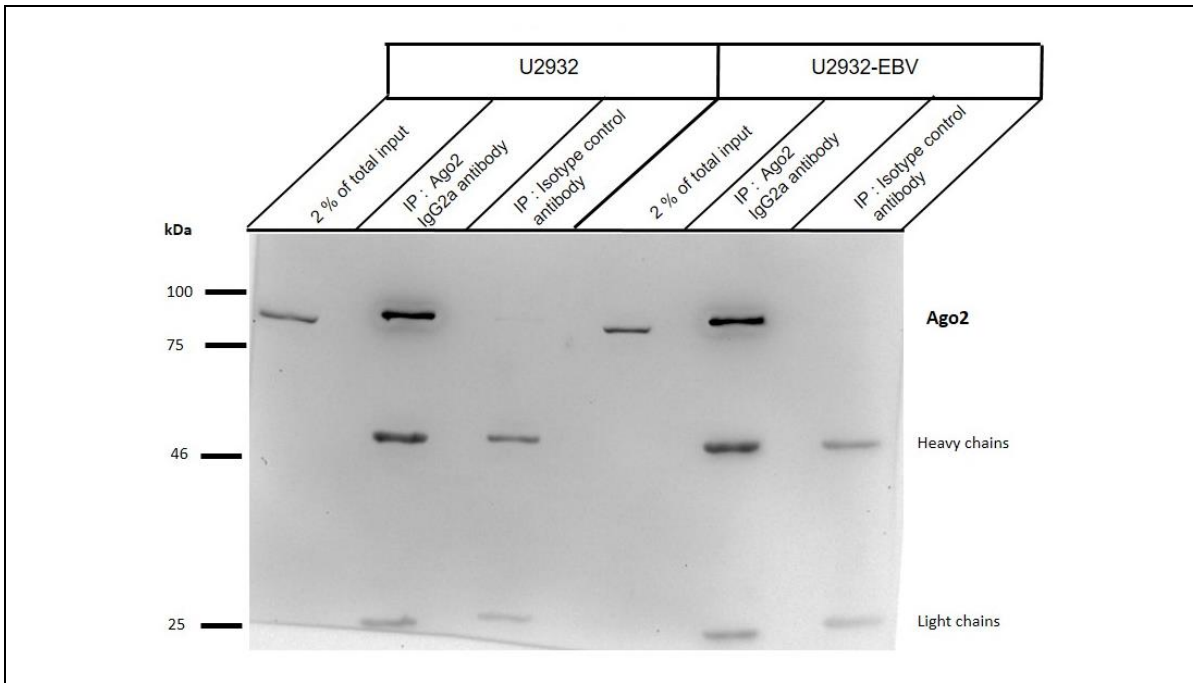
Figure 7: Immunoprecipitation of Ago2 from U2932, SUDHL5 and their EBV positive counterparts.

Extract of the indicated cell lines was precipitated with Ago2 specific antibody (11A9) and an appropriate isotype control antibody. The membrane was first stained with Ago2 and then with mouse-anti rat IgG coupled to horseradish peroxidase as a secondary antibody. The precipitated Ago2-protein was visualized by the ECL method. The molecular mass marker proteins (in kDa) and the position of Ago2 are indicated by bars to the left side of the blot.

The overall results from the total cellular profiling and the Ago2-IP are shown in Table 4. We obtained about 8.7-15.3 x10^6 reads, corresponding to 12 to 23% of total reads that matched to miRBase. The total cellular miRNA profiling yielded 700-850 annotated miRNAs from the four cell lines. The Ago2-IP sequencing resulted in about 28-55 x10^6 reads, corresponding to 78.82-68.25% of all reads. The Ago2-IP miRNA profiling, yielded 1102 to 1372 miRNAs, annotated in miRBase. Thus, the total number of reads for known human miRNA reads, increased about 10 times, as compared to the total cellular profile, indicating that the Ago2-IP strongly enriched the miRNAs, proving the specificity of the procedure.

	Cell line	Total reads	Total reads match with miRBase	% of match reads	Detected miRNA
Total	U2932-EBV	10423487	1,815,328	17.42	851
	U2932	8752305	2,076,239	23.72	758
	SUDHL5-EBV	11470056	2,019,181	17.60	763
	SUDHL5	15322853	1,944,300	12.69	713
Ago2_IP	U2932 -EBV +	55928169	38,168,544	68.25	1372
	U2932	42384180	26,494,508	62.51	1185
	SUDHL5-EBV	34811526	27,005,099	77.58	1141
	SUDHL5	28245506	22,264,473	78.82	1102

Table 4: Overview of sequencing reads in "Total" and "Ago2-IP" obtained from U2932 and SUDHL5 and their EBV positive counterparts.

It has been suggested that only miRNAs which represent more than 0.1% of the total reads are functional (FLORES et al., 2014; MULLOKANDOV et al., 2012). For this reason, a 0.1% cut-off was applied for further analysis in all cell lines for selection of functionally relevant miRNAs. This means that in our analysis, only a miRNA with at least an expression of 0.1% of the total reads in one of the cell line was taken into account.

At the 0.1% cut-off level, only 61 to 62 of human miRNA remained in the total cellular miRNA profile of U2932 and U2932-EBV cells; however, these corresponded to 96.4% to 94.4% of total annotated miRNA reads, respectively. In SUDHL5 and SUDHL5-EBV, 59 to 58 of human miRNA were detected in the total cellular lysate, representing

73.3% and 97.0% of detected miRNAs, respectively. At the 0.1% cut-off level in the Ago2-profile 51 to 66 of human miRNA were detected in U2932-EBV and U2932, corresponding to 94.8% to 97.0% of the total miRNAs, respectively. In SUDHL5-EBV and SUDHL5, 50 to 54 human miRNA were detected in the Ago2-IP, representing 68.6% and 97.2% of miRNA reads, respectively.

The presence of EBV miRNA was also analyzed in the total cellular and the Ago2-IP miRNA profile. In U2932-EBV cells, six EBV-miRNAs (1.3% of all reads), and in SUDHL5-EBV cells, 26 EBV-miRNAs (23.4% of total reads), remained above 0.1% cut-off level, whereas in the Ago2-IP profiling of U2932-EBV cell line, 6 EBV (1.6% of total miRNA reads) and the SUDHL5-EBV cell line, 23 EBV miRNAs (28.2% of total reads) were present above the 0.1% cut-off level (Table 5).

Table 5: MiRNA reads in "Total" and "Ago2-IP" at 0.1% cut-off.					
	Cell line	Human miRNA	EBV miRNA	% of Human miRNA	% of EBV miRNA
Total	U2932 -EBV	62	6	94.4%	1.3%
	U2932	61	-	96.4%	-
	SUDHL5-EBV	58	26	73.3%	23.4%
	SUDHL5	59	-	97.0%	
Ago2_IP	U2932-EBV	51	6	94.8%	1.6%
	U2932	57	-	97.0%	-
	SUDHL5-EBV	50	23	68.6%	28.2%
	SUDHL5	54	-	97.2%	-

3.4 Highly expressed miRNAs in U2932 and SUDHL5 and their EBV-positive counterparts

There is an inverse relation between the expression level of a miRNA and its inhibitory potential for a specific mRNA target, and a crucial role for Ago2 protein in the RISC silencing complex (LEUNG et al., 2011; LIU et al., 2016). Therefore, we analyzed the expression of the most abundant miRNAs in the total cellular and Ago2-IP miRNA profiles in each cell line, separately, at the 0.1% cut-off level. The top 20 miRNAs in the total cellular and the Ago2-IP profile are listed in descending order in Table 6 and Table 7. These miRNAs comprised about 74 to 85% of all identified miRNA reads in the four DLBCL cell lines. For instance, in the total cellular profiles, miR-92a-3p and miR-191-5p were among the most abundant miRNAs in the U2932 cell lines and miR-21-5p and miR-142-5p were, among the most highly expressed miRNA in the SUDHL5 cell lines.

Table 6 : Top 20 miRNAs in U2932 and SUDHL5 and their EBV positive counterparts in "Total" profile at 0.1% cut-off. EBV miRNAs are underlined.							
% of relative expression of total miRNA pool							
U2932				**SUDHL5**			
miRNA	**EBV +**	**miRNA**	**EBV -**	**miRNA**	**EBV +**	**miRNA**	**EBV -**
miR-92a-3p	16.783	miR-92a-3p	17.205	miR-21-5p	14.164	miR-142-5p	28.391
miR-191-5p	9.169	miR-191-5p	11.556	miR-142-5p	6.891	miR-21-5p	10.992
miR-181a-5p	7.785	miR-148a-3p	8.417	miR-BHRF1-1	5.971	miR-181a-5p	5.613
miR-146a-5p	5.849	miR-181a-5p	7.073	miR-148a-3p	5.807	miR-26a-5p	5.057
miR-148a-3p	5.704	let-7a-5p	4.559	miR-191-5p	4.947	miR-191-5p	4.122
miR-142-5p	5.213	miR-26a-5p	4.159	miR-181a-5p	3.619	miR-16-5p	3.588
miR-16-5p	3.929	miR-142-5p	3.854	miR-16-5p	3.321	miR-30d-5p	3.031
let-7f-5p	3.555	let-7f-5p	3.787	miR-BART10-3p	3.254	miR-92a-3p	3.013
let-7a-5p	3.472	miR-146a-5p	3.380	miR-22-3p	3.158	let-7a-5p	2.848
miR-30d-5p	3.379	miR-16-5p	3.123	miR-30d-5p	3.060	miR-22-3p	2.781
miR-26a-5p	2.887	miR-30d-5p	2.736	miR-BART8-5p	2.975	let-7f-5p	2.746
miR-21-5p	2.551	miR-182-5p	2.566	let-7a-5p	2.587	miR-148a-3p	2.681
miR-27b-3p	1.753	miR-30e-5p	1.728	let-7f-5p	2.587	miR-142-3p	2.657
miR-19b-3p	1.744	miR-20a-5p	1.666	miR-26a-5p	2.549	miR-30e-5p	1.960
miR-182-5p	1.609	miR-27b-3p	1.625	miR-92a-3p	2.364	miR-28-3p	1.466
miR-155-5p	1.339	miR-192-5p	1.623	miR-30e-5p	1.862	miR-4792	1.349
miR-192-5p	1.300	miR-21-5p	1.331	miR-182-5p	1.550	miR-21-3p	1.106
miR-20a-5p	1.157	let-7g-5p	1.322	miR-BART7-5p	1.367	miR-192-5p	0.881
miR-30e-5p	1.139	miR-186-5p	1.048	miR-BART19-5p	1.267	let-7g-5p	0.776
miR-186-5p	0.879	miR-22-3p	0.860	miR-146b-5p	1.188	miR-4485-3p	0.709
Total sum in percent	81.196		83.618		74.488		85.767

In the Ago2-IP-profiles, miR-92a-3p, miR-181a-5p, miR-146a-5p, and miR-148a-3 had the highest abundance in the U2932 cell lines and miR-21-5p, miR-142-5p, miR-92a-3p and miR-181a-5p were the most abundant human miRNAs in the SUDHL5 lines.

Table 7: Top 20 miRNAs in U2932 and SUDHL5 and their EBV positive counterparts in "Ago2-IP" profile at 0.1% cut-off. EBV miRNAs are underlined.							
% of relative expression of Ago2-IP miRNA pool							
U2932				SUDHL5			
miRNA	EBV +	miRNA	EBV -	miRNA	EBV +	miRNA	EBV -
miR-92a-3p	26.551	miR-92a-3p	23.235	miR-21-5p	16.151	miR-21-5p	14.373
miR-181a-5p	10.446	miR-181a-5p	9.224	miR-BHRF1-1	7.030	miR-142-5p	13.376
miR-146a-5p	10.051	miR-148a-3p	7.232	miR-92a-3p	4.881	miR-181a-5p	8.794
miR-191-5p	5.372	miR-146a-5p	7.106	miR-148a-3p	4.216	miR-92a-3p	7.077
miR-16-5p	4.615	miR-191-5p	6.580	miR-BART8-5p	4.154	miR-26a-5p	6.298
miR-148a-3p	4.096	miR-26a-5p	4.317	miR-181a-5p	4.149	miR-16-5p	5.130
miR-30d-5p	3.184	miR-16-5p	3.565	miR-22-3p	3.862	miR-22-3p	4.762
miR-26a-5p	3.124	miR-182-5p	3.089	miR-142-5p	3.435	miR-191-5p	3.399
let-7f-5p	2.665	miR-30d-5p	3.074	miR-16-5p	3.231	let-7f-5p	3.294
miR-21-5p	2.581	let-7f-5p	2.949	miR-BART6-3p	3.143	miR-28-3p	3.260
miR-142-5p	2.074	let-7a-5p	2.257	miR-191-5p	2.883	miR-30d-5p	3.027
miR-182-5p	1.966	miR-21-5p	1.956	miR-30d-5p	2.617	miR-148a-3p	2.644
miR-27b-3p	1.916	miR-142-5p	1.939	let-7f-5p	2.566	miR-423-5p	1.639
miR-155-5p	1.311	miR-27b-3p	1.707	miR-BART10-3p	2.498	miR-30e-5p	1.612
let-7a-5p	1.153	miR-30e-5p	1.502	miR-26a-5p	2.210	miR-142-3p	1.501
miR-192-5p	1.080	miR-192-5p	1.470	miR-BART11-3p	1.950	let-7a-5p	1.437
miR-186-5p	0.865	miR-22-3p	1.289	miR-BART19-5p	1.889	miR-146a-5p	1.258
miR-30e-5p	0.804	miR-186-5p	1.275	miR-182-5p	1.827	miR-192-5p	1.018
miR-378a-3p	0.790	miR-378a-3p	0.852	miR-28-3p	1.728	miR-186-5p	0.944
miR-22-3p	0.756	miR-19b-3p	0.750	miR-BART7-5p	1.677	miR-27b-3p	0.892
Total sum in percent	85.400		85.368		76.097		85.735

55

3.5 Comparative analysis of up and down regulated miRNAs in EBV infected cell line to EBV negative DLBCL cell lines in total cellular and Ago2-IP

EBV encodes 44 mature miRNAs, and the EBV-infection might change the total cellular miRNA profile. Therefore it could also influence the loading of the Ago2-complex with human miRNAs. Accordingly, the fold changes of human miRNAs were analyzed and compared, between EBV-infected and their non-infected counterparts. For the sake of this comparison, we again considered only miRNAs above the 0.1% cut-off level, for functionally relevant miRNAs. The top 10 induced and reduced miRNAs, due to EBV infection in total cellular profile are shown in Table 8, and the complete lists can be found in the appendix (Tabel A5).

Table 8: Comparison of miRNA profiles in EBV+ vs. EBV- in "Total" profile in U2932 and SUDHL5 at 0.1% cut-off.

U293. Total				SUDHL5 Total			
miRNA	EBV +	EBV -	Ratio EBV +/ -	miRNA	EBV +	EBV -	Ratio EBV +/ -
miR-4485-3p	**0.276**	**0.062**	**4.432**	**miR-182-5p**	**1.55**	**0.419**	**3.699**
miR-221-3p	**0.21**	**0.056**	**3.767**	**miR-146b-5p**	**1.188**	**0.367**	**3.235**
miR-222-3p	0.122	0.037	3.332	miR-10a-5p	0.155	0.061	2.561
miR-193b-3p	0.104	0.034	3.087	miR-148a-3p	5.807	2.681	2.166
miR-18a-5p	0.103	0.035	2.985	miR-148a-5p	0.184	0.103	1.793
miR-1246	0.151	0.051	2.976	miR-146a-5p	0.799	0.477	1.674
miR-15a-5p	0.255	0.091	2.787	miR-27a-3p	0.153	0.097	1.579
miR-155-5p	1.339	0.503	2.663	miR-155-5p	0.219	0.163	1.341
miR-19b-3p	1.744	0.664	2.626	miR-486-5p	0.403	0.302	1.335
miR-19a-3p	0.276	0.113	2.454	miR-21-5p	14.164	10.992	1.289
miR-22-3p	0.49	0.86	0.57	miR-28-3p	0.877	1.466	0.598
miR-210-3p	0.058	0.108	0.537	miR-181b-5p	0.102	0.172	0.592
miR-30c-5p	0.224	0.422	0.53	miR-181a-3p	0.108	0.197	0.547
miR-1260b	0.062	0.127	0.488	miR-26a-5p	2.549	5.057	0.504
miR-1260a	0.061	0.126	0.486	miR-28-5p	0.137	0.277	0.494
miR-339-3p	0.064	0.142	0.454	miR-4532	0.054	0.138	0.392
miR-146b-5p	0.073	0.163	0.448	miR-142-5p	6.891	28.391	0.243
miR-92b-3p	0.049	0.125	0.389	miR-1246	0.069	0.339	0.205
miR-27a-3p	**0.032**	**0.177**	**0.179**	**miR-142-3p**	**0.468**	**2.657**	**0.176**
let-7c-5p	**0.024**	**0.245**	**0.097**	**miR-4792**	**0.095**	**1.349**	**0.07**

In the total cellular profile of U2932-EBV, miR-4485-3p, -221-3p and -222-3p were found to be the most strongly induced, while miR-182-5p,-146-5p and -10a-5p had the highest induction in SUDHL5-EBV. In contrast, let-7c-5p and miR-27a-3p were most strongly reduced in U2932-EBV, and miR-4792 and miR142-3p had the strongest reduction in the total cellular miRNA profile in SUDHL5-EBV.

A comparison of the Ago2-IP in EBV positive versus EBV negative cells are shown in Table 9, for the top 10 induced and reduced miRNA, and the complete lists can be found in the appendix (Tabel A6). MiRNAs such as miR-15a-5p, -221-3p and- 155-5p had the strongest relative presence in the Ago2-complex of 2932-EBV, compared to U2932. MiR-363-3p,-182-5p had the strongest induction in SUDHL5-EBV, compared to SUDHL5 while miR-let-7c-5p and -27a-3p showed the strongest reduction in U2932-EBV as compared to U2932 . MiR-142-3p and -5p were the most strongly depleted from the Ago2-complex in SUDHL5-EBV compared to SUDHL5.

Table 9: Comparison of "Ago2-IP"profile in EBV-positive vs. non-infected cell lines vs. "Total" profile at 0.1% cut-off.							
U2932 Ago2-IP				**SUDHL5 Ago2-IP**			
miRNA	EBV +	EBV -	Ratio EBV +/-	miRNA	EBV +	EBV -	Ratio EBV +/ -
miR-15a-5p	0.276	0.109	2.539	**miR-363-3p**	0.105	0.017	6.046
miR-221-3p	0.114	0.045	2.538	**miR-182-5p**	1.827	0.667	2.739
miR-155-5p	1.311	0.730	1.795	miR-146b-5p	0.988	0.472	2.095
miR-130b-3p	0.145	0.082	1.759	miR-10a-5p	0.189	0.097	1.956
miR-423-5p	0.738	0.442	1.671	miR-148a-3p	4.216	2.644	1.595
miR-9-5p	0.286	0.200	1.430	miR-148a-5p	0.126	0.085	1.476
miR-146a-5p	10.051	7.106	1.414	miR-27a-3p	0.130	0.097	1.336
miR-181b-5p	0.504	0.368	1.369	miR-21-5p	16.151	14.373	1.124
miR-21-5p	2.581	1.956	1.320	miR-146a-5p	1.381	1.258	1.098
miR-16-5p	4.615	3.565	1.294	miR-155-5p	0.338	0.310	1.091
miR-25-3p	0.373	0.678	0.550	miR-15a-5p	0.093	0.187	0.501
miR-183-5p	0.117	0.214	0.547	miR-181b-5p	0.191	0.383	0.498
let-7b-5p	0.064	0.119	0.542	miR-151a-5p	0.304	0.625	0.486
miR-339-3p	0.080	0.149	0.536	miR-181a-5p	4.149	8.794	0.472
miR-30e-5p	0.804	1.502	0.535	miR-186-5p	0.443	0.944	0.469
let-7a-5p	1.153	2.257	0.511	miR-28-5p	0.189	0.515	0.366
miR-30c-5p	0.139	0.291	0.480	miR-26a-5p	2.210	6.298	0.351
miR-146b-5p	0.090	0.191	0.468	miR-486-5p	0.036	0.124	0.292
miR-27a-3p	0.031	0.143	0.215	**miR-142-5p**	3.435	13.376	0.257
let-7c-5p	0.013	0.115	0.116	**miR-142-3p**	0.219	1.501	0.146

3.6 Differential RISC associated of human and EBV miRNAs in comparison to cellular miRNA profile

As mentioned, the Cullen group challenged the notion that the total cellular miRNA profile is a realistic functional indicator of the association of a miRNA with the RISC complex. They found a discrepancy in various miRNAs in the Ago2-IP profiling as compared to the total cellular profile (FLORES et al., 2014). Accordingly, we also analyzed the relative enrichment or depletion of human Ago-bound miRNAs, versus the total cellular miRNA profile at 0.1% cut-off for each of the four DLBCL cell lines, separately. The top 10 enriched or depleted human miRNAs in Ago2-complex are

shown in Table 10, for U2932 and its EBV positive counterpart, and in Table 11 for SUDHL5 and its EBV positive counterpart. For instance, miR-423-5p and -5p were enriched 2.5-8 fold in Ago2-IP in comparison to the total cellular miRNA profile in the four cell lines.

Table 10:List of miRNAs enriched or depleted from the "Ago2-IP"as compared to the "Total" profile in U2932-EBV and U2932 at 0.1% cut-off.							
U2932-EBV				**U2932**			
miRNA	% of total miRNA pool	% of RISC assoc. pool	RISC enriched	miRNA	% of total miRNA pool	% of RISC assoc. pool	RISC enriched
miR-423-5p	0.217	0.738	3.407	miR-320a	0.064	0.151	2.345
miR-423-3p	0.233	0.516	2.22	miR-423-5p	0.195	0.442	2.267
miR-146a-5p	5.849	10.051	1.718	miR-146a-5p	3.38	7.106	2.103
miR-92a-3p	16.783	26.551	1.582	miR-425-5p	0.333	0.544	1.635
miR-22-3p	0.49	0.756	1.542	miR-22-3p	0.86	1.289	1.498
miR-181b-5p	0.334	0.504	1.512	miR-21-5p	1.331	1.956	1.469
miR-425-5p	0.338	0.484	1.434	miR-155-5p	0.503	0.73	1.452
miR-181a-5p	7.785	10.446	1.342	let-7i-5p	0.34	0.478	1.407
miR-28-3p	0.338	0.454	1.342	miR-423-3p	0.313	0.429	1.369
miR-182-5p	1.609	1.966	1.222	miR-28-3p	0.508	0.695	1.367
miR-30b-5p	0.377	0.129	0.343	miR-142-5p	3.854	1.939	0.503
miR-18a-5p	0.103	0.035	0.342	let-7a-5p	4.559	2.257	0.495
miR-98-5p	0.399	0.134	0.336	let-7c-5p	0.245	0.115	0.47
let-7a-5p	3.472	1.153	0.332	let-7g-5p	1.322	0.595	0.45
miR-20a-5p	1.157	0.355	0.307	miR-98-5p	0.566	0.231	0.408
miR-19b-3p	1.744	0.505	0.29	miR-20a-5p	1.666	0.54	0.324
miR-486-5p	0.425	0.033	0.077	miR-486-5p	0.199	0.03	0.15
miR-4485-3p	0.276	0.004	0.013	miR-4792	0.384	0.003	0.008
miR-1246	0.151	0.001	0.003	miR-1260b	0.127	0.0005	0.004
miR-4792	0.287	0.001	0.003	miR-1260a	0.126	0.0004	0.003

MiR-4792, -1246 and -4485-3p in U2932-EBV and miR-1260a ,-1260b and -4792 in U2932 were identified to be strongly depleted more than 69 fold in the RISC complex, as compared to the total cellular miRNA profile.

In SUDHL5-EBV, miR-486-5p, -260a, -260b,-and -4485-3p were the most strongly depleted miRNAs from Ago2-complex, whereas miR-4532, -1260a and -4792 were depleted about 78 to 3000 fold, from the Ago2-complex in SUDHL5.

Table 11: List of miRNAs enriched or depleted in the "Ago2-IP"as compared to the "Total" profile in SUDHL5–EBV and SUDHL5 at 0.1 % cut –off.

SUDHL5-EBV				SUDHL5			
miRNA	% of total miRNA pool	% of RISC assoc. pool	RISC enriched	miRNA	% of total miRNA pool	% of RISC assoc. pool	RISC enriched
miR-423-5p	0.134	0.936	6.989	miR-423-5p	0.188	1.639	8.721
miR-423-3p	0.175	0.496	2.834	miR-423-3p	0.254	0.785	3.087
miR-92a-3p	2.364	4.881	2.064	miR-146a-5p	0.477	1.258	2.636
miR-28-3p	0.877	1.728	1.972	miR-92a-3p	3.013	7.077	2.349
let-7i-5p	0.2	0.377	1.886	let-7i-5p	0.283	0.662	2.337
miR-181b-5p	0.102	0.191	1.873	miR-181b-5p	0.172	0.383	2.225
miR-146a-5p	0.799	1.381	1.729	miR-28-3p	1.466	3.26	2.224
miR-155-5p	0.219	0.338	1.547	miR-106b-3p	0.082	0.159	1.932
miR-28-5p	0.137	0.189	1.381	miR-155-5p	0.163	0.31	1.901
miR-425-5p	0.108	0.143	1.323	miR-425-5p	0.095	0.179	1.879
miR-142-5p	6.891	3.435	0.498	miR-486-5p	0.302	0.124	0.409
miR-142-3p	0.468	0.219	0.468	miR-30b-5p	0.378	0.153	0.405
let-7a-5p	2.587	1.06	0.41	miR-20a-5p	0.334	0.118	0.352
miR-30b-5p	0.332	0.133	0.4	miR-98-5p	0.229	0.081	0.351
miR-98-5p	0.26	0.077	0.295	miR-4485-3p	0.709	0.009	0.013
miR-20a-5p	0.302	0.084	0.278	miR-1246	0.339	0.001	0.002
miR-486-5p	0.403	0.036	0.089	miR-1260b	0.117	0.00012	0.001
miR-4485-3p	0.517	0.004	0.009	miR-4792	1.349	0.001	0.001
miR-1260b	0.107	0.0003	0.003	miR-1260a	0.117	0.00009	0.001
miR-1260a	0.107	0.0002	0.002	miR-4532	0.138	0.00004	0.0003

3.7 Presence of EBV miRNAs in the Ago2-containing RISC complex.

We analyzed the presence and abundance of EBV miRNAs in the total cellular fraction and the Ago2-miRNA profile in the EBV-infected cell lines. As shown in Table 12, the overall amount and the presence of virus-encoded miRNAs varied between the two cell lines. As already pointed out, the virus contributed only about 1.3% to the total amount of miRNAs in U2932-EBV, while 23.4% of the total miRNA reads were derived from the virus in SUDHL5-EBV. In U2932-EBV, EBV-miR-BART10-3p constituted only 0.43%, and BART8-5p, 0.29% of the total counts. In SUDHL5-EBV, the viral miRNAs EBV-miR-BHRF1-1, -BART10-3p and -BART8-5p contributed to 5.97%, 3.25% and 2.97% of the total miRNA reads, respectively.

In the Ago2-profiling of the U2932-EBV cell line, EBV-miR-BART8-5p, -BART11-3p and -BART6-3p were the most abundant viral miRNAs, with 0.42%, 0.33% and 0.31% abundance, respectively. In the SUDHL5-EBV, BHRF1-1, BART8-5p and BART6-3p were the most abundant EBV miRNAs in total cellular profile, with 7.02%, 4.15% and 3.14% abundance, respectively. The most abundant EBV miRNAs in total cellular profile were found to be same in the Ago2-complex, while BHRF1-1, BART10-3p and BART8-5p were the most abundant miRNA in total cellular profile in SUDHL5 (see below).

Table 12: EBV miRNAs in the "Total" and the "Ago2-IP" profile in U2932-EBV and SUDHL5-EBV.

U2932				SUDHL5			
miRNA	Total	miRNA	Ago	miRNA	Total	miRNA	Ago2
	rel. expr. %		rel. expr. %		rel. expr. %		rel. expr. %
BART10-3p	0.4365	BART8-5p	0.42474	BHRF1-1	5.971	BHRF1-1	7.0296
BART8-5p	0.2964	BART11-3p	0.33851	BART10-3p	3.2542	BART8-5p	4.1537
BART6-3p	0.1967	BART6-3p	0.31849	BART8-5p	2.9754	BART6-3p	3.1426
BART11-3p	0.1582	BART10-3p	0.24271	BART7-5p	1.3665	BART10-3p	2.4979
BART22	0.1281	BART19-5p	0.18918	BART19-5p	1.2667	BART11-3p	1.9503
BART7-5p	0.1138	BART7-5p	0.13593	BART11-3p	1.1298	BART19-5p	1.889
				BART6-3p	1.0978	BART7-5p	1.6766

The enrichment of EBV miRNAs in the Ago2-complex, in comparison to the total cellular profile, was determined. As shown in Table 13, miR-BART11-3p and miR-BART19-5p were enriched more than 2- fold in U2932-EBV, while miR-BART10-3p was depleted from the Ago2-complex by 1.8-fold, as compared to the total cellular profile. In SUDHL5-EBV, miR-BART6-3p and miR-BART11-3p were strongly enriched, by 2.8 and 1.7 fold, respectively, while EBV-miR-BART5-5p and -BART1-3p were depleted, below the 0.1% cut-off.

Table 13: List of EBV-miRNA enriched or depleted in the "Ago2-IP"compared to "Total" profile in U2932-EBV positive and SUDHL5-EBV at 0.1 % cut-off.

U2932-EBV				SUDHL5-EBV			
EBV miRNA	% Total miRNA pool	% RISC assoc. pool	RISC enriched fold change	EBV miRNA	% Total miRNA pool	% RISC assoc. pool	RISC enriched fold change
miR-BART11-3p	0.158	0.339	2.140	miR-BART6-3p	1.098	3.143	2.863
miR-BART19-5p	0.092	0.189	2.053	miR-BART11-3p	1.130	1.950	1.726
miR-BART6-3p	0.197	0.318	1.619	miR-BART17-5p	0.511	0.844	1.653
miR-BART8-5p	0.296	0.425	1.433	miR-BART19-5p	1.267	1.889	1.491
miR-BART7-5p	0.114	0.136	1.194	miR-BART16	0.125	0.185	1.476
				miR-BART8-3p	0.287	0.221	0.769
				miR-BART10-3p	3.254	2.498	0.768
				miR-BART9-5p	0.300	0.201	0.669
				miR-BART7-3p	0.323	0.201	0.623
				miR-BART1-5p	0.131	0.075	0.572
				miR-BART19-3p	0.354	0.175	0.494
				miR-BART17-3p	0.274	0.115	0.418
miR-BART22	0.128	0.098	0.767	miR-BART1-3p	0.137	0.044	0.320
miR-BART10-3p	0.436	0.243	0.556	miR-BART5-5p	0.120	0.034	0.281

3.8 Validations of sequencing results by RT-qPCR

In order to validate the NGS sequencing results, 12 miRNAs with different expression levels, either up- or down-regulated, were selected for reverse transcription quantitative PCR (RT-qPCR), based on their presence above the 0.1% cut-off level. The RT-qPCR was carried out in duplicate on independent biological replicates for both cell lines and their EBV-infected counterparts, in the total cellular RNA and the RNA isolated from the Ago2-IP.

The RT-qPCR results of 8 out of 12 selected miRNAs gave results corresponding to the NGS results of total cellular RNA from U2932-EBV, compared to U2932. As shown in Figure 8, we validated the relative upregulation of four miRNAs, including miR-10a-5p, -146a-5p, -221-3p and -363-3p and the relative downregulation of four miRNA, including let7c-5p, miR-283p, miR-423-3p and miR-92a-3p.
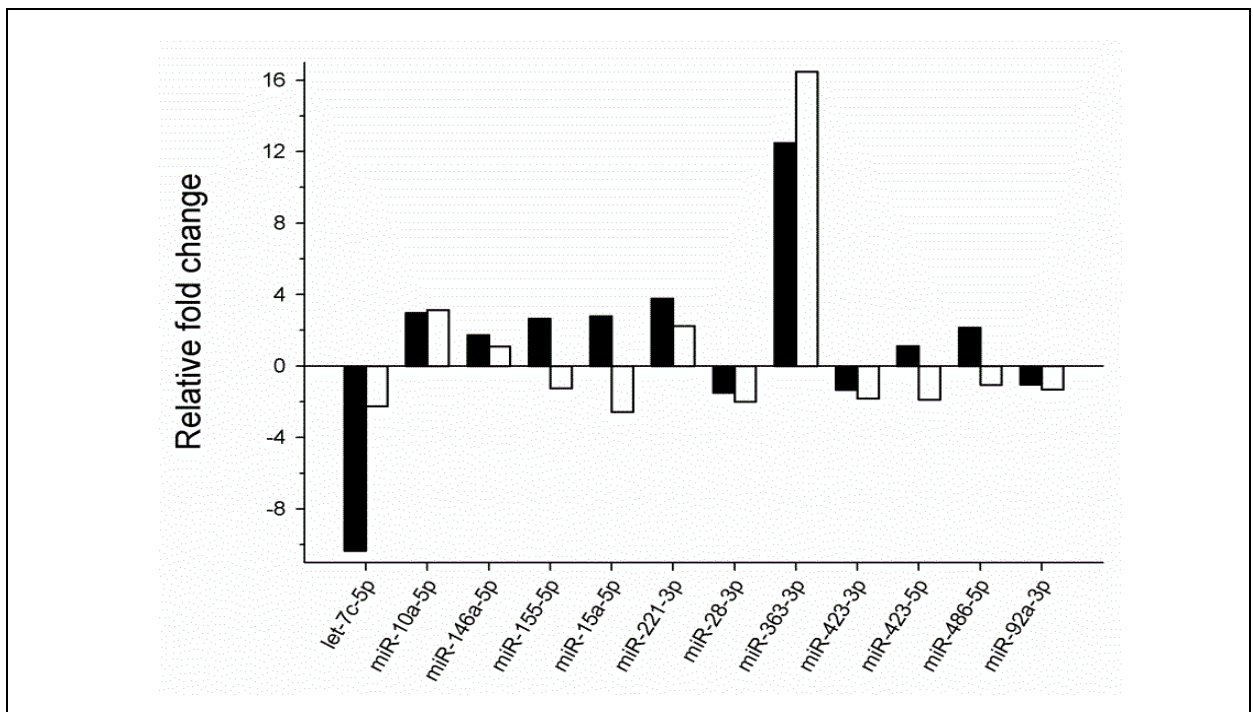

Figure 8:RT-qPCR validation for U2932-EBV vs. U2932 in "Total"

Black bars represent NGS data and white bars represent RT-qPCR results.

Furthermore, using RNA extracted from the Ago2-IP of U2932-EBV and U2932, the relative upregulation of miR-10a-5p, miR-146a-5p, miR-155-5p, and miR-15a-5p, miR-221-3p, miR-363-3p, mi -486-5p, miR-92a-3p and relative downregulation of let-7c and miR-28-3p were confirmed. These data are presented in Figure 9.
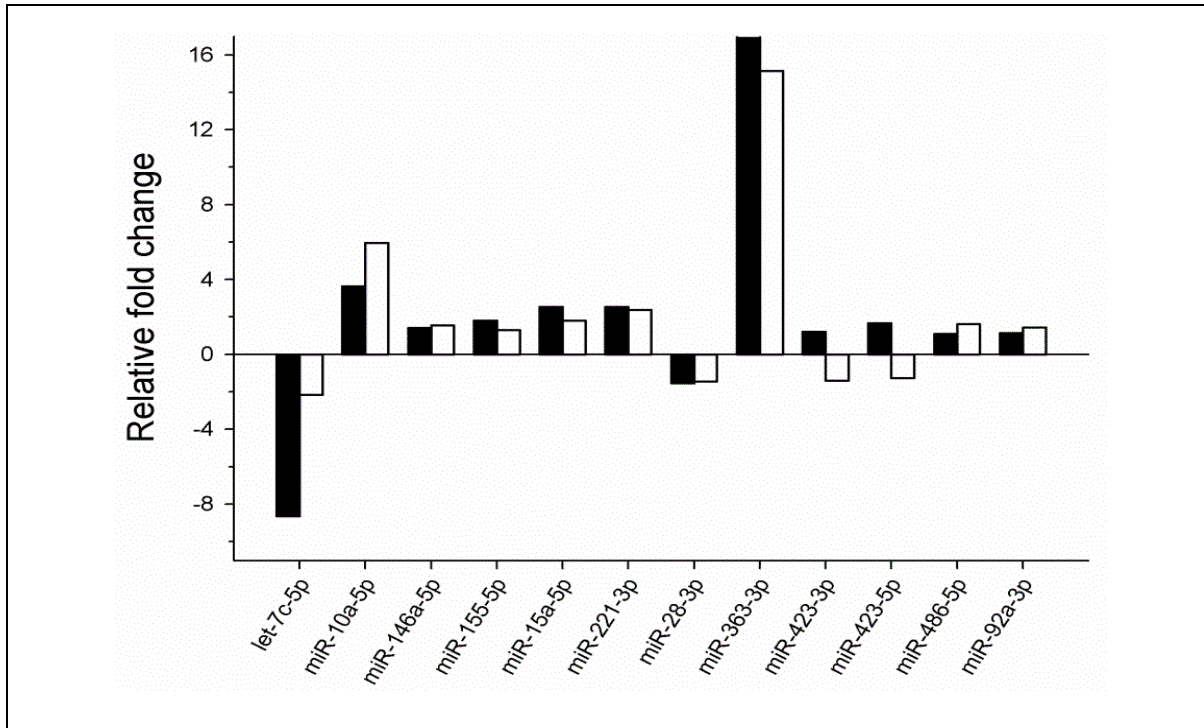

Figure 9:RT-qPCR validation of U2932-EBV vs. U2932 for "Ago2-IP"

Black bar represent NGS data and open bars represent RT-qPCR results.

The analogous experiments, employing RNA obtained from whole cells or the Ago2-IPs were carried out, for comparing SUDHL5-EBV vs. SUDHL5. Here, 10 out of 12 selected miRNA yielded consistent results for the sequencing of total cellular miRNA profile. As shown in Figure 10, we confirmed the relative up-regulation of five miRNAs, including miR-10a-5p, -146a-5p, -155-5p, -221-3 and -363-3p and a relative downregulation of five miRNAs, including miR-15a-5p, -28-3p, -423-3p, -423-5p and -92a-3p.
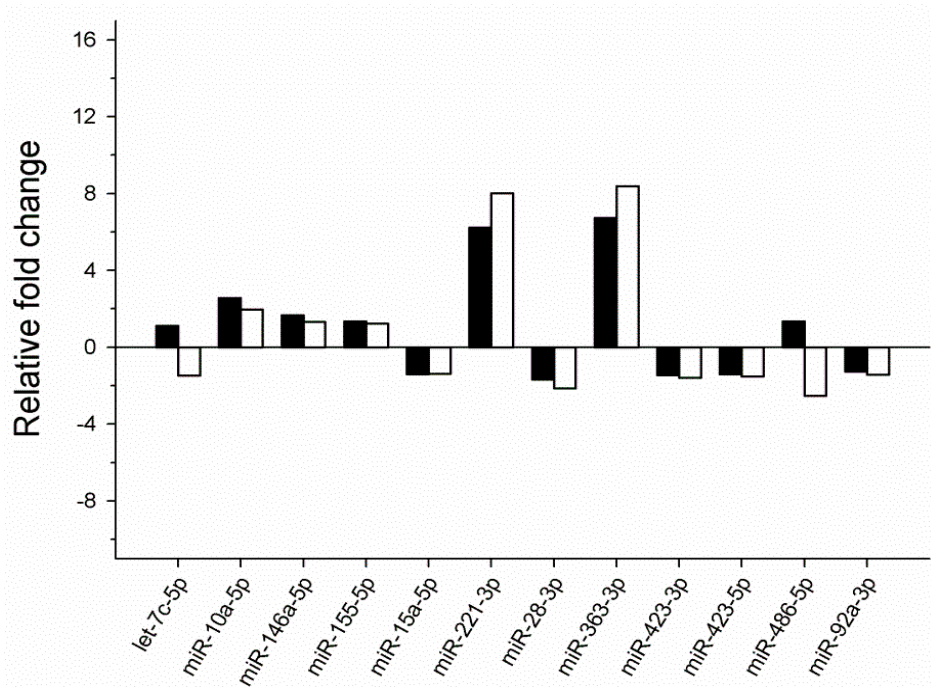
Figure 10:RT-qPCR validation for SUDHL5-EBV vs. SUDHL5 for "Total"

 Black bars represent NGS data and open bars represent RT-qPCR results.

Using RNA extracted from Ago2-IP for comparing by RT-qPCR SUDHL5-EBV vs. SUDHL5, we confirmed the relative up- and downregulation of selected miRNAs as shown in Figure 11. In particular, the relative upregulation of miR-10a-5p, -146a-5p, -155-5p, -221-3p and -363-3p and the relative downregulation of miR-let-7c,-15a-5p, -28-3p, -423-3p, -423-5p, -486-5p and -92a-3p were validated.
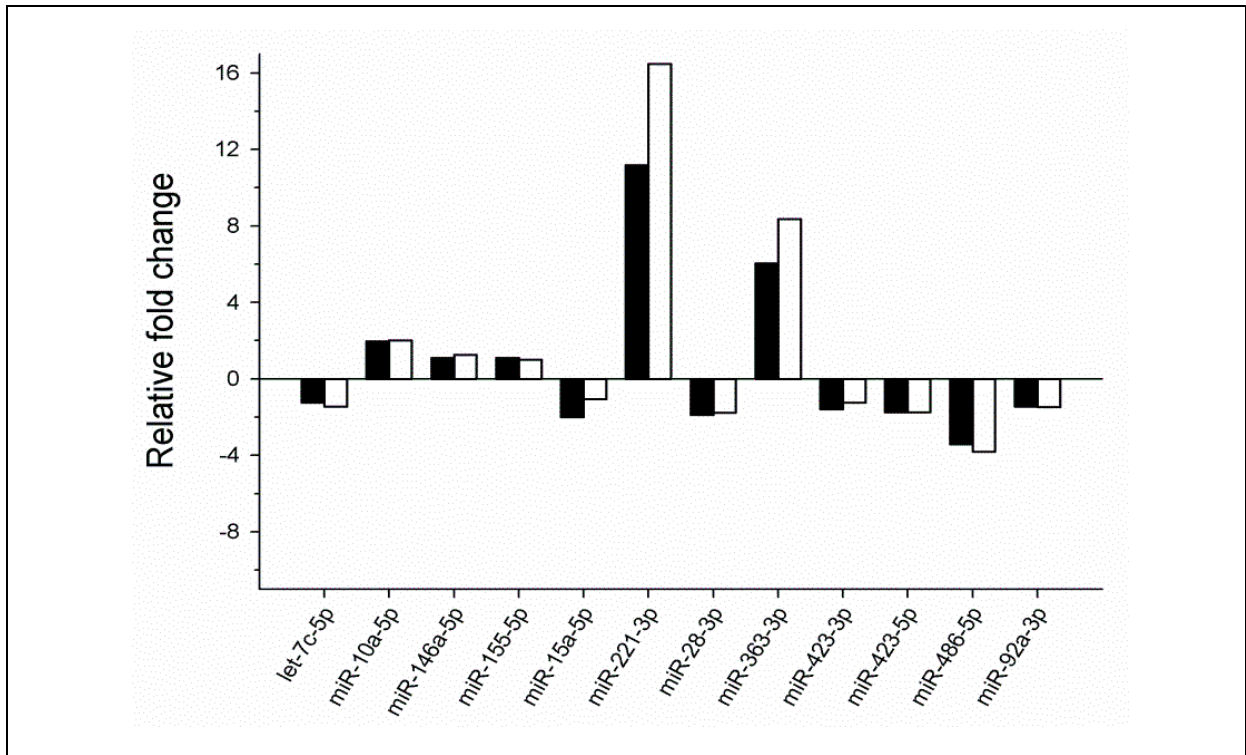
Figure 11: RT-qPCR validation for SUDHL5-EBV vs. SUDHL5 for "Ago2-IP".

 Black bar represent NGS data and open bars represent RT-qPCR results.

3.9 Verification of sequencing by Northern blotting

3.9.1 Analysis of total cellular miRNAs

Northern blotting (NB) is considered the gold standard for validation of miRNA expression, as it avoids the false positive results that may arise from the enzymatic manipulation and amplifications that are necessary for biochemical reactions during the NGS or RT-qPCR procedures. Second, it unambiguously detects differences in expression in given cellular settings, like the ones analyzed in this work. For this reason, we performed NB as a powerful second validation method for some miRNAs that were found to be up- or downregulated by NGS and RT-qPCR.

The results of NB from total extracted RNA from U2932, SUDHL5 and their EBV-positive counterparts, are shown in Figures 12, 13, and 14. In comparison of U2932-EBV with U2932, we confirmed the upregulation of miR-222-3p, -551b-3p,-142-3p, -155-5p and -142-5p and the downregulation of hsa-let-7c-5p. In SUDHL5-EBV, we also verified the upregulation of miR-363, -21-5p and downregulation of miR-142-5p, compared to SUDHL5.

NGS data from Ago2-IP indicated that miR-4485-3p and 4792-5p were highly depleted from the Ago2-IP profile (Table 10 and Table 11), while miR-4485-3p and -4792-5p were above 0.1% cut-off level of total known miRNA reads, in the total cellular miRNA expression profile. MiR-4485-3p and miR-4792-5p were not present at the 0.1% cut off in U2932 and SUDHL5-EBV, respectively. We could not detect a signal either for miR-4485-3p or 4792-5p by northern blot (Figure 15).

Figure 12: Validation of NGS results by northern blotting.
Total RNA isolated from U2932, SUDHL5 and their EBV positive counterparts (20µg/lane) was assayed using probes for the indicated miRNAs. The EtBr loading control is shown beneath each blot.

Figure 13: Validation of NGS results by northern blotting.
Total RNA isolated from U2932 and SUDHL5 and their EBV positive counterparts (20µg/lane) was assayed using probes for the indicated miRNAs probes. The EtBr loading control is shown beneath each blot.

Figure 14: Validation of NGS results by northern blotting.

Total RNA isolated from U2932 and SUDHL5 and their EBV positive counterparts (20µg/lane) and human tissue from a DLBCL patient were assayed by the probes for the indicated miRNAs. The EtBr loading control is shown beneath each blot.
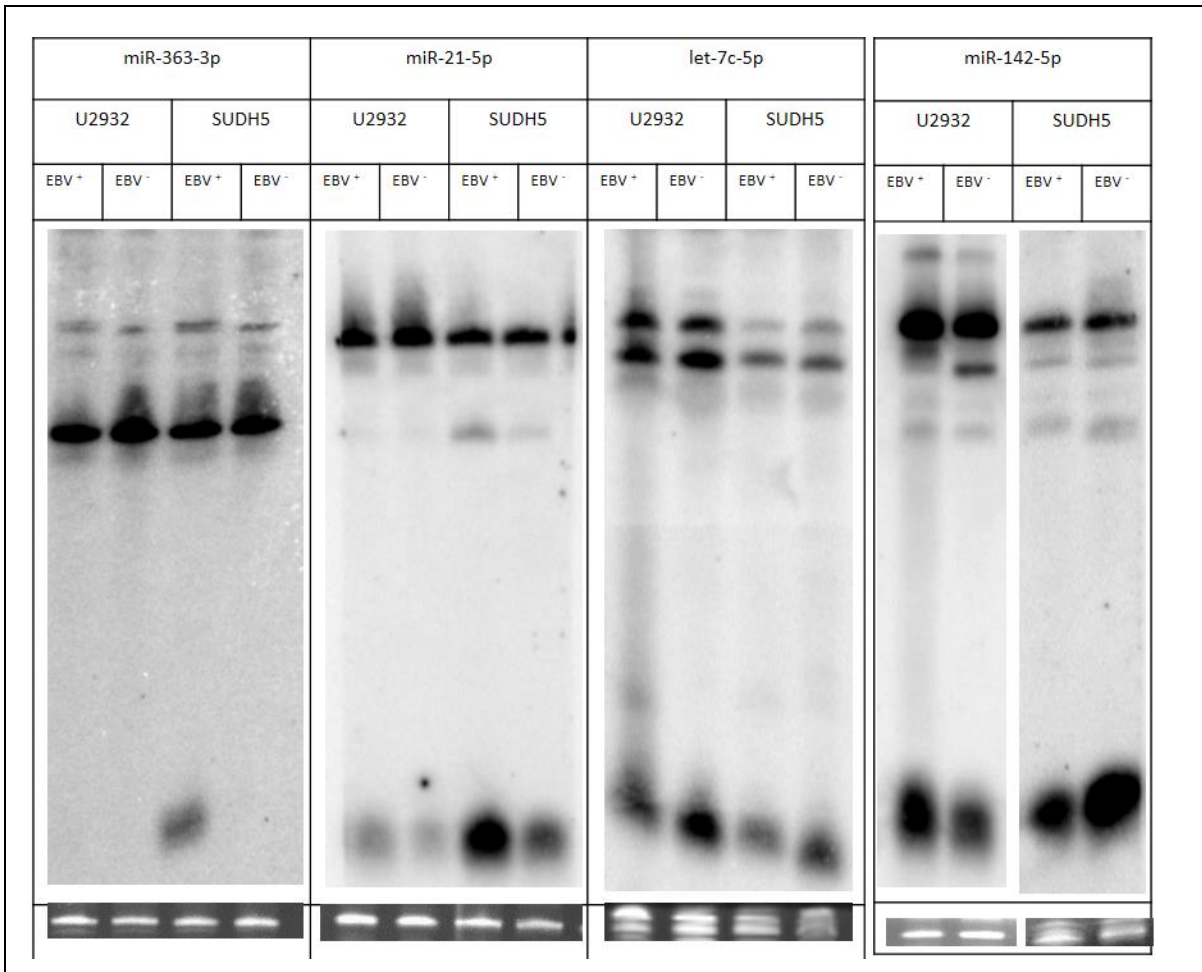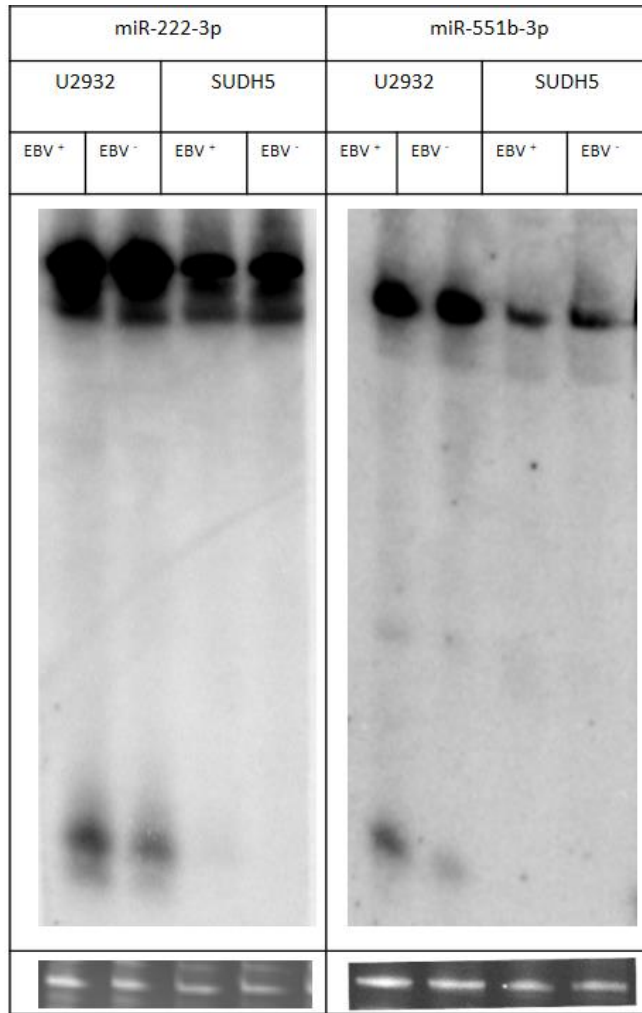
Figure 15: Validation of NGS results by northern blotting.
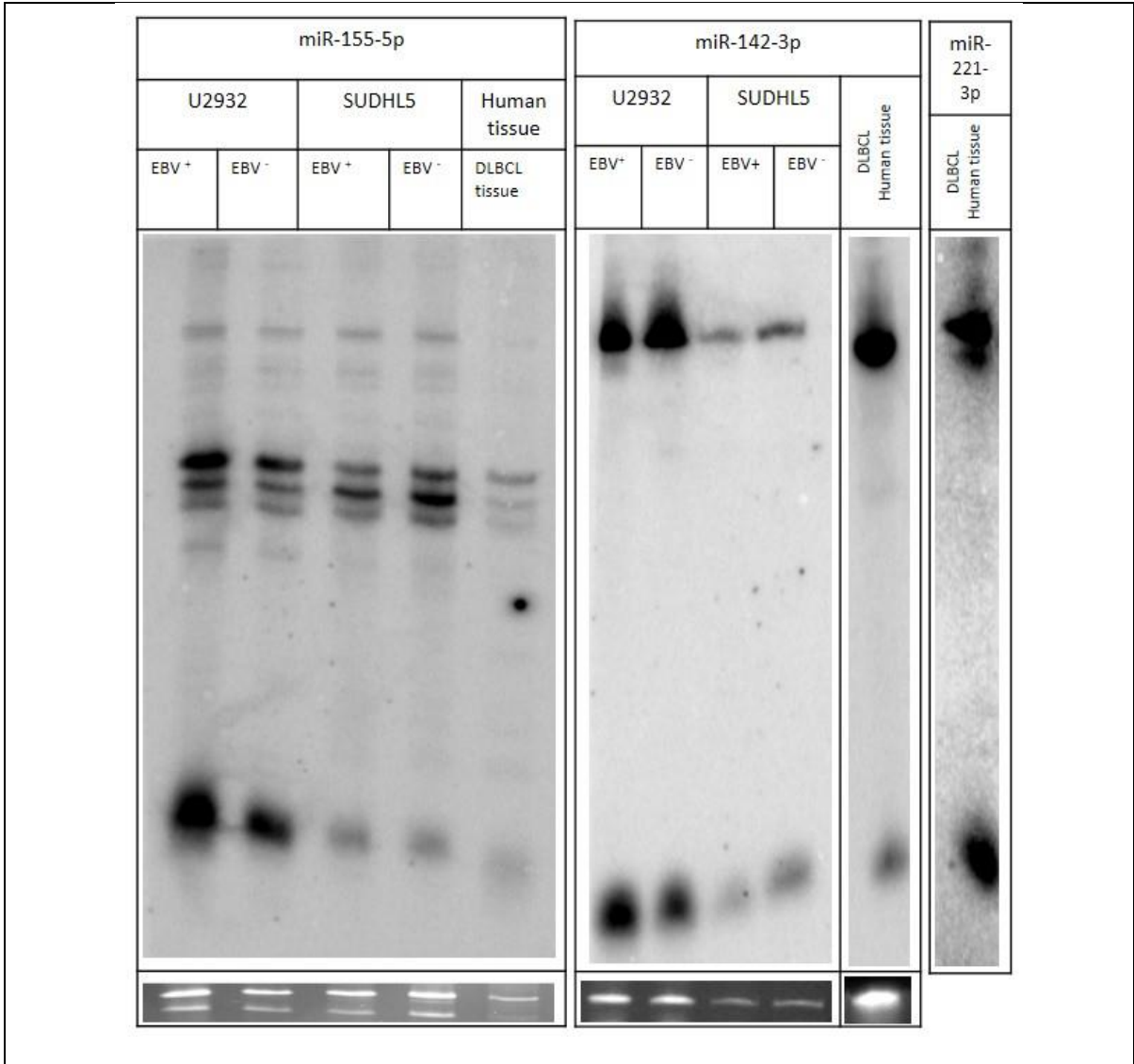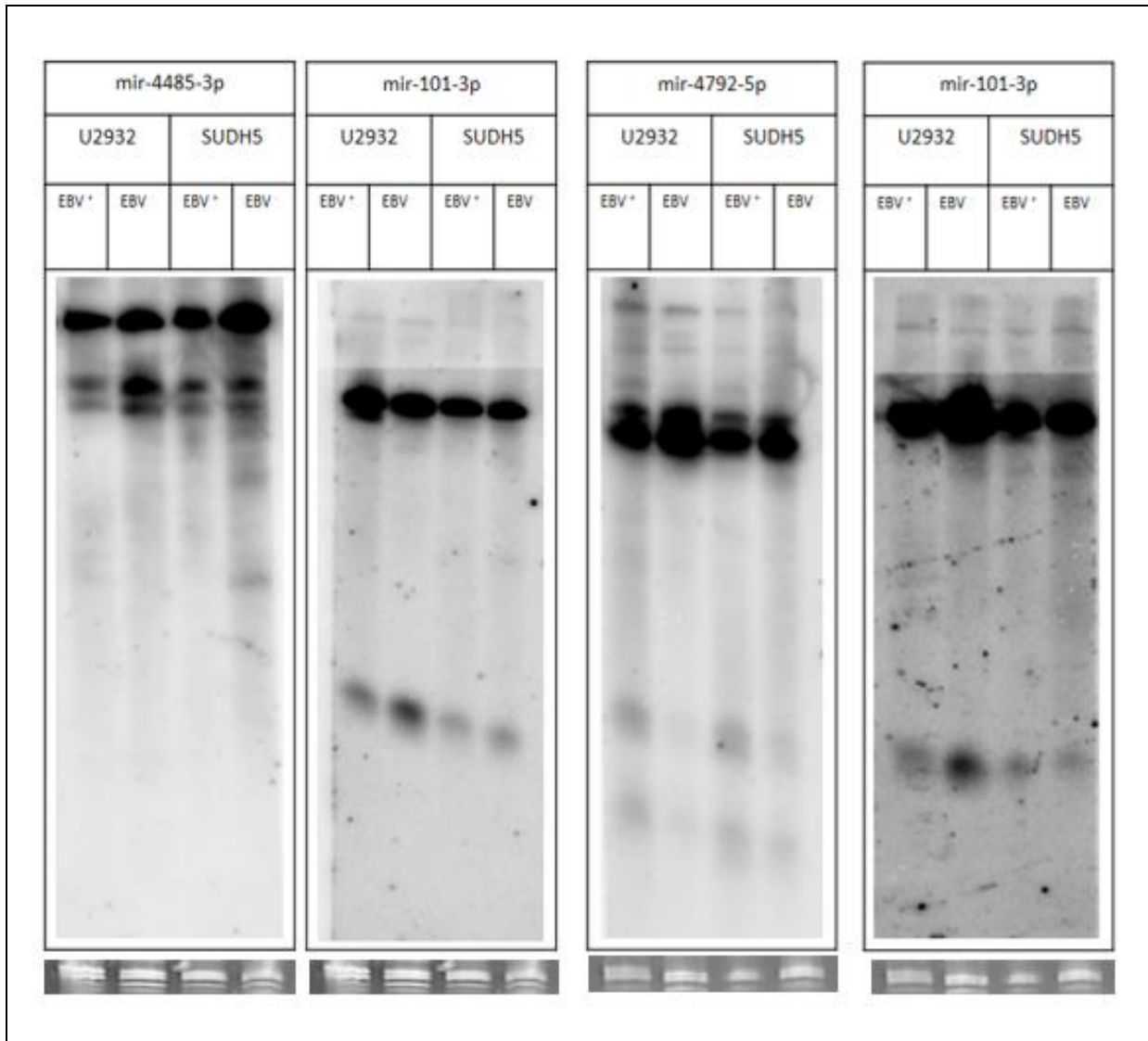
Total RNA isolated from U2932 and SUDHL5 and their EBV positive counterpart (20μg/lane) were assayed by NB using probes for miR-4485-3p and miR-4792-5p as indicated. No proper signal detected for miR-4485-3p and 4792-5p) while reprobing of the same membrane after stripping gave a detectable signal for mir101-3p. The EtBr loading control is shown beneath each blot.

3.9.2 Analysis of Ago2-IP miRNAs by northern blotting.

From our NGS results and their validation using RT-qPCR, we found that by comparing Ago2-IP in U2932-EBV versus U2932 cell lines, miR-221-3p was strongly upregulated (0.114% versus 0.045%) by 2.5-fold and hsa-let-7c-5p was strongly downregulated (0.013% vs. 0.115%) by 8-fold. We then speculated if we could detect the difference by NB, using RNA extracted from the Ago2-IP- fraction. We were able to isolate RNA from the Ago2-IP and, to a lesser extent, from the control IP. The amounts isolated were sufficient to run several Northern blots. We loaded equal amounts (200 ng) of RNA extracted from the Ago2-IP and the control-IP of U2932, as shown in Figure 16. As expected, miR-221-3p was enriched in both Ago2-IP fraction and total cellular lysate in U2932-EBV, in comparison to U2932. By stripping the membrane to remove the previous signal (miR-221-3p), and probing with hsa-let7c-5p, which was downregulated in U2932-EBV cell lines, from Ago2-IP NGS data, we observed the depletion of let-7c-5p in U2932-EBV in total cellular lysate and in the Ago2-IP. These results were in line with our NGS and RT-qPCR data for miR-221-3p and hsa-let7c-5p.

From our NGS results for SUDHL5-EBV versus SUDHL5, we found that miR363-3p (0.105 vs. 0.017) in Ago2-IP has the strongest enrichment of about 6-fold. MiR-423-5p showed the strongest enrichment in the Ago2-ip, in comparison to the total cellular profile, by more than 6- fold in SUDH-EBV (0.134 vs. 0.936) and about 8 fold (0.188 vs. 1.639), in SUDHL5. In addition, miR-423 about 1.75 fold downregulated in Ago2-IP in SUDHL5-EBV, compared to SUDHL5. By performing Ago2-IP-NB, using again 200 ng of extracted RNA from Ago2-IP fraction, we found an enrichment of miR-363-3p in the Ago2-IP of SUDHL5-EBV. After stripping and reprobing the membrane with miR423-5p, we observed depletion of mir423-5p in Ago2-IP of SUDHL5, compared to SUDHL5-EBV. These results were also in line with our NGS and RT-qPCR data.
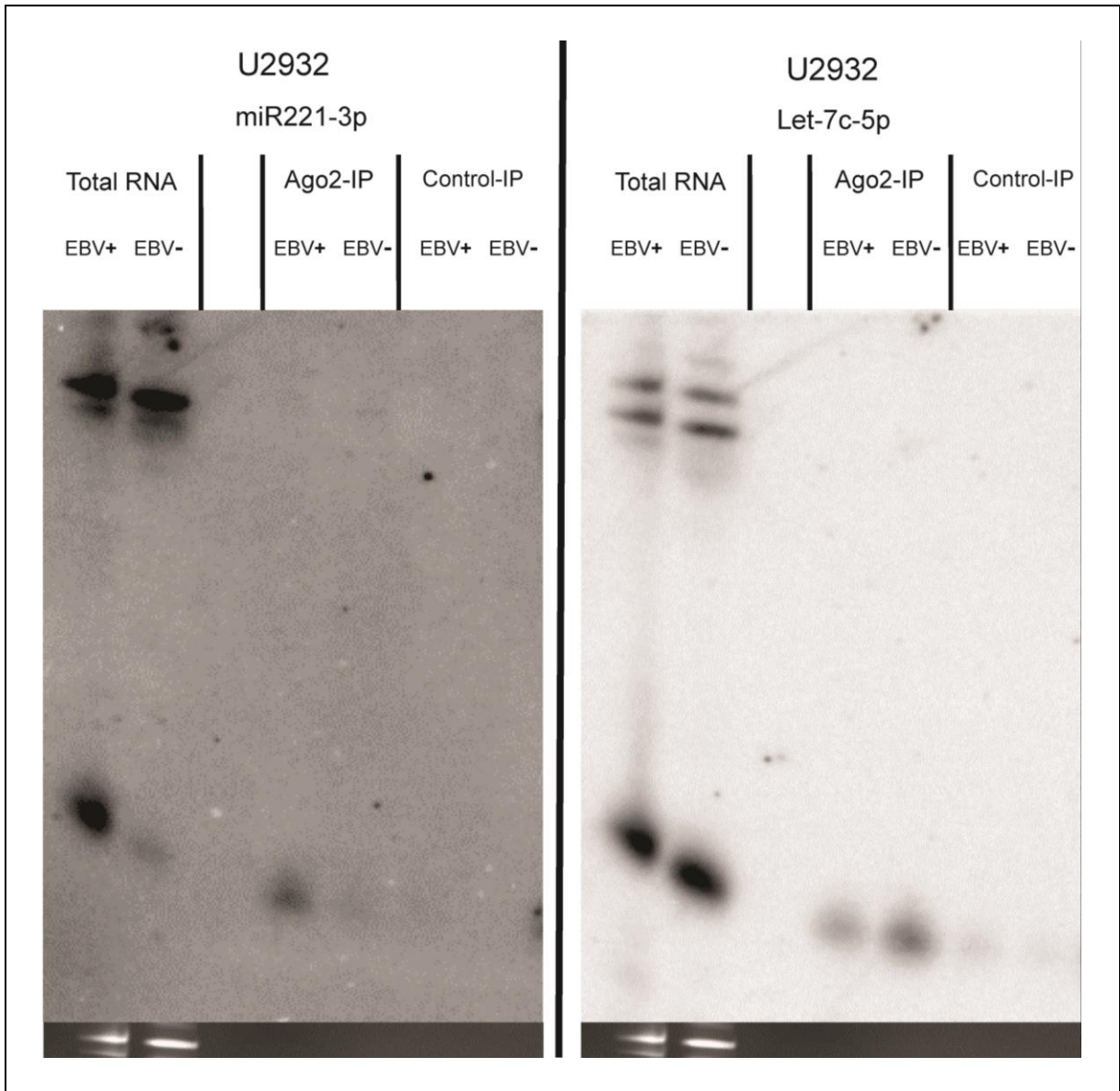
Figure 16: Validation of Ago2-IP-Seq by northern blotting.
Total RNA isolated from U2932-EBV and U2932 total cellular and Ago2-IP cell lines. (20 µg per lane from total cellular RNA and 200 ng per lane from Ago2-IP) were applied to 12.5% urea gel and assayed by NB using the indicated probes. First miR-221-3p probe were used and then the membrane was probed with let-7c-5p (after stripping the membrane to remove the primary signal).The EtBr loading control is shown under the blot. Due to the low amount of RNA loaded in Ago2-IP fraction (200 ng), no signals were detected in EtBr of Ago2-IPs and Control-IPs.
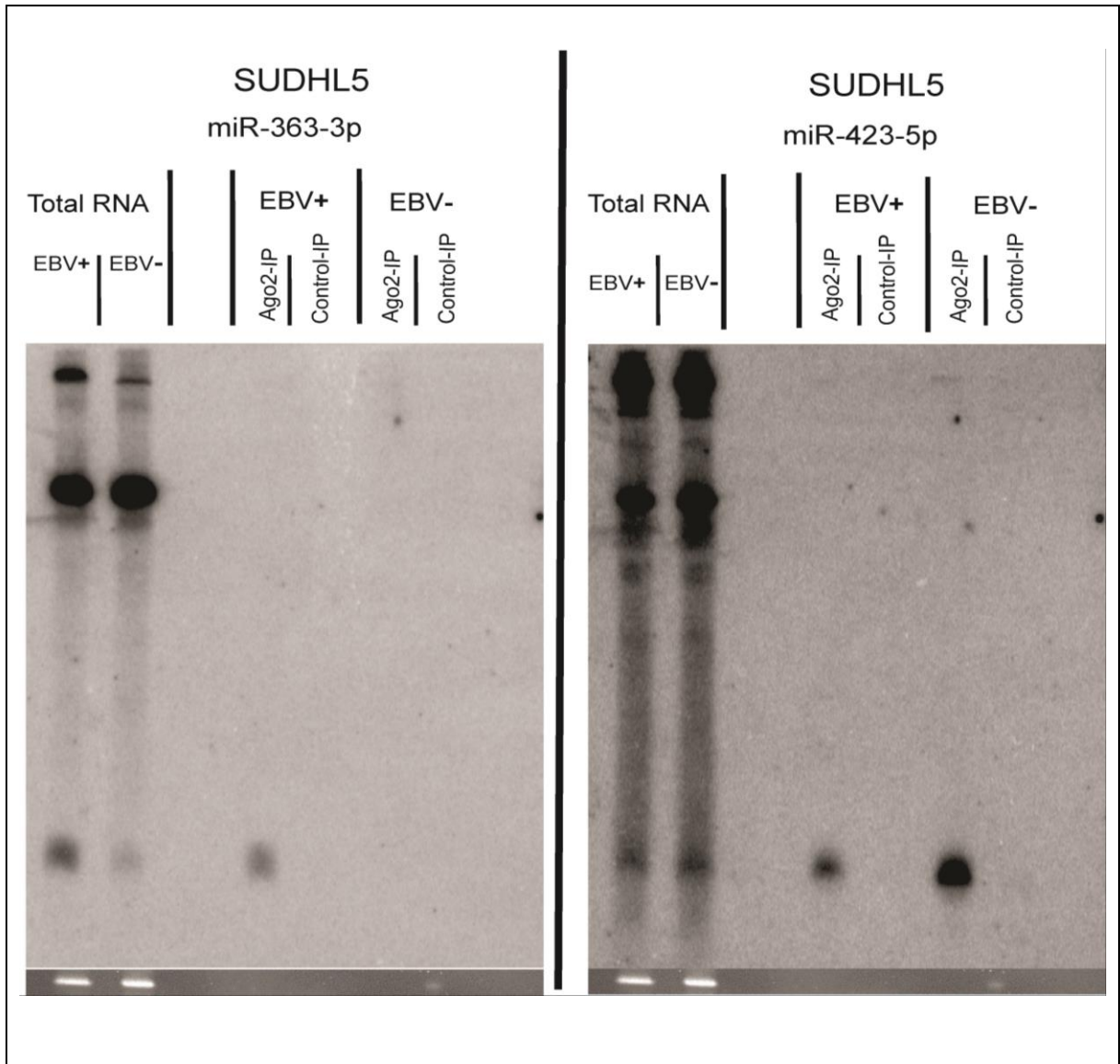
Figure 17: Validation of Ago2-IP-Seq by northern blotting.
Total RNA isolated from SUDHL5-EBV and SUDHL5 total cellular and Ago2-IP cell lines. (20 µg per lane from total cellular RNA and 200 ng per lane from Ago2-IP) were applied to 12.5% urea gel and assayed by NB using the indicated probes. First miR-363-3p probe were used and then the membrane was probed with miR-423-5p (after stripping the membrane to remove the primary signal).The EtBr loading control is shown under the blot. Due to the low amount of RNA loaded in Ago2-IP fraction (200 ng), no signals were detected in EtBr of Ago2-IPs and Control-IPs.

4 Discussion

Non-Hodgkin lymphoma (NHL) is the fifth most common type of malignancy globally. Of these, diffuse large B-cell lymphoma (DLBCL) is the most common form of NHL (BRADSHAW et al., 2016; SKRABEK et al., 2013). DLBCL is a heterogeneous group of disease in regard to pathology and clinical and genetic characteristics. The heterogeneity arises due to dysregulation of different transcription factors such as B-cell lymphoma 6 (BCL-6) at different stages of B-cell development (GATTO, BRINK, 2010; IQBAL et al., 2009; IQBAL et al., 2015). DLBCL is categorized into two common types: Activated B-cell like (ABC) and Germinal Center B-cell like (GCB), based on gene expression profiling (GEP) (ALIZADEH et al., 2000). Due to difficulties in the characterization and differentiation of GCB- from ABC-DLBCL, many investigators attempt to identify a miRNA or a set of miRNAs to use as potential diagnostic differentiation biomarkers (ALIZADEH et al., 2000; IQBAL et al., 2015; JORGENSEN et al., 2015; ROSENWALD et al., 2002).

Ago2-IP, followed by miRNA sequencing, is becoming an advanced tool to determine the miRNA profile of a given tumor and to investigate functionally active miRNA, as it has been shown recently by the Cullen group that simply the level of a miRNA in the total cellular lysate is not a clear indication of its biological function but rather the loading of the Ago-complex (FLORES et al., 2014).

For this reason, this study was carried out to compare by ultra-deep sequencing the miRNAs bound to Ago2 with the overall miRNA present in two sets of DLBCL cell lines with and without EBV-conversion. The first cell line was U2932, which has a gene expression profile (GEP) similar to ABC-DLBCL (AMINI et al., 2002) and the second cell line was SUDHL5, which has a GEP similar to GCB-DLBCL. We investigated enriched or depleted miRNAs in the Ago2- associated complex as compared to their total cellular miRNA profile. We also validated our results by RT-qPCR and northern blot (NB) for a selected set of up or downregulated miRNAs that were deregulated in the total cellular RNA and in the Ago2-IP.

The total miRNA profiling of the four cell lines yielded between 713-851 different miRNAs while the number of miRNAs in the Ago2-IP yielded 1102-1372 different miRNAs. Further, the number of sequencing reads increased dramatically, by almost ten times, in the Ago2-IP fraction in the four cell lines, as compared to miRNAs detected in the total cellular profiles. In addition, the number of detected miRNAs in the Ago2-IP fraction was significantly increased, by more than 35% in all four cell lines, as compared to the total cellular miRNA profile. The increase in the number of reads and detected miRNAs in Ago2-IP fraction is a clear indication of enrichment and specificity of our Ago2-IP. In addition, we observed miRNAs expressed at low abundance that were not detectable in the total miRNAs profiles. This approach might therefore be applied as a very promising tool in the discovery of new miRNAs. Most importantly, the Ago-associated miRNAs might be considered as the potentially relevant miRNAs to serve as biomarkers for diagnosis and for the determination of potential mRNA targets.

As it had been suggested that functional miRNAs should be present above 0.1% of the total reads, a 0.1% cut-off was applied in all cell lines for the selection of functionally relevant miRNAs (FLORES et al., 2014; MULLOKANDOV et al., 2012). The application of this cut-off left only 59-62 out of more than about 713-851 miRNAs that were present overall in the four lines, but the application of this cut-off also left only between 50-57 miRNAs in the Ago2-profile. The miRNAs that were left, however, were present at different ratios in both U2932 and U2932-EBV as well as SUDHL5 and SUDHL5-EBV. The miRNAs above the 0.1% cut-off did nevertheless represent over 95% of all miRNAs in the four cell lines.

In the U2932-EBV cells, the EBV-encoded miRNAs represent 1.3% of the total and 1.6% of all Ago2-bound miRNAs. In this line, EBV was in latency I or II as only EBNA1 and LMP1 but not significant amounts of EBNA2 were detectable. Here, ebv-miR-BART10-3p with 0.43% of the total had the highest relative expression of the EBV-miRNAs, but was not among top 20 miRNA in U2932-EBV. In contrast, ebv-miR-BART8-5p accounted for 0.4% of Ago2-associated viral miRNAs. In SUDHL5-EBV, however, which has the characteristic of EBV-latency type III (high EBNA2, EBNA1,

LMP1), EBV miRNAs represented about 23.4% of total cellular profile, and an enrichment to about 28.2% of viral miRNAs was observed in the Ago2-IP profile. Here, ebv-miR-BHRF1-1, -BART-10-3p and BART8-5p were the most abundant viral miRNAs in total miRNA profile with frequencies of 5.9%, 3.2%, 2.9%, respectively. BHRF1-1 and BART8-5p with 7.0% and 4.1%, respectively, were also among the most abundant miRNAs in Ago2 profile in SUDHL5-EBV. This suggests that under type III EBV latency, for example, in EBV-associated PTLD, EBV miRNAs might functionally displace a significant amount of human cellular miRNAs from the Ago2-complex. In addition, the viral infection had dysregulated the human cellular miRNA expression. Alternatively, it might be possible that miRNAs in type III latency are more efficiently processed. The changes in the cellular miRNA profile in EBV latency type III, compared to type I, were previously reported by Flemington and coworkers (CAMERON et al., 2008a). We have also observed elevated expression of miR-21-5p, miR-27a-3p and miR-146b-5p in SUDHL5-EBV vs. SUDHL5 cells, which is consistent with their data.

The Venn diagrams shown in Figures 18 depict the miRNAs that are not present or exclusively in the Ago2-complexes in the four cell lines. We note that miRNAs miR-1260a/b were not present in the Ago2-complex in U2932, SUDHL5 and SUDHL5-EBV and were strongly depleted from Ago2 in U2932-EBV. Likewise, miR-486-5p was below the 0.1% cut-off in the Ago2-complex in U2932, U2932-EBV, SUDHL5-EBV except in SUDHL5.Surprisingly, the number of cellular miRNAs excluded from the Ago2-complex in U2932-EBV and SUDHL5-EBV did not differ significantly as we had expected that the large amount of EBV-miRNAs associated with Ago2 in SUDHL5-EBV (almost 30%) would lead to a stronger loss of cell miRNAs as compared to U2932-EBV where the viral miRNAs accounted for only 1.6% of the Ago2-bound miRNAs above the 0.1% cut-off. In SUDHL5, miRNAs miR-4485-3p, -4792, and -4532 were only present in the total profile, and miR-4485-3p was not Ago2-bound in SUDHL5-EBV. We assume that these sequences, although listed in miRBASE, are not real miRNAs but probably breakdown products of other non-coding RNAs. For instance, probing the RNA of the U2932 and SUDHL5 cell line did not yield a detectable signal for this sequence at the position where miRNAs migrate in a

Northern blot. Again, miR-1260a/b and -98-5p were not present in both cells, leaving miR-1246 to be excluded from Ago2 in SUDHL5, while miR-486-5p, 20a-5p, -210-3p, -15a-5p and -181a-3p were excluded from Ago2 in SUDHL5-EBV. Likewise, miR-4792, not present in the SUDHL5- Ago2, was also not Ago2-bound in the U2932/U2392-EBV pair. Here, miR-486-5p and miR-301a-3P were Ago2-excluded in both lines while U2932-EBV also had no significant amounts of let7b-3p, -miR-17-3p, -18a-5p, -21-3p, 193-3p, 222-3p, and miR-1246, the latter also being excluded in the SUDHL5-Ago2 complex (Figure 18). It may thus be assumed that the EBV-conversion results in a loss of some more miRNAs from the Ago2-complex and that the presence of EBV under latency III conditions might result in an overall reduction of cell miRNAs associated with the Ago2-complex. The displacement of miRNAs under type III latency is somewhat more prominent than type I latency, and the presence of the virus nevertheless changes the overall expression of certain cellular miRNAs. This question needs further attention in additional experiments beyond the scope of this thesis.
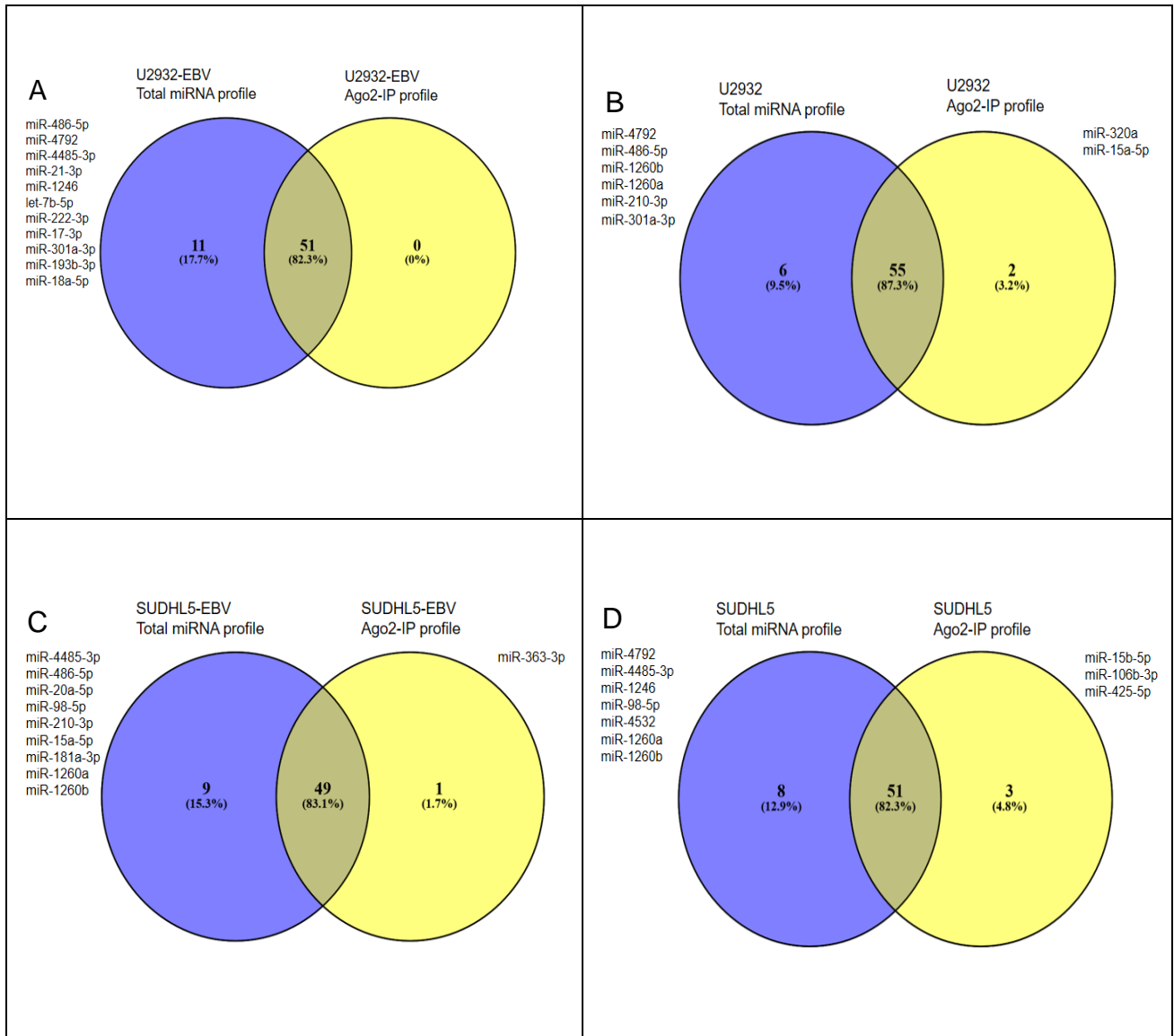
Figure 18: Venn diagrams: showing the miRNAs found exclusively either in the total RNA or the Ago2-profiling of the U2932, SUDHL5 and their EBV infected counterparts. (A) Total miRNA profile vs. Ago2-profile of U2932-EBV, (B) Total miRNA profile vs. Ago2-profile of U2932 (C) Total miRNA profile vs. Ago2-profile of SUDHL5-EBV, (D) Total miRNA profile vs. Ago2-profile of SUDHL5.

MiR-21-5p was the most abundant miRNA in the total and in the Ago2 miRNA profile of SUDHL5-EBV cells. It has been shown that EBNA2 induces miR-21 expression, due to post-transcriptional mechanisms and in EBV latency type III (CAMERON et al., 2008a; ROSATO et al., 2012). Upregulation of mir-21 has been reported in different type of cancers, such as colorectal (ASANGANI et al., 2008), sinonasal

(KOVARIKOVA et al., 2017), glioblastoma (CHAN et al., 2005) and breast cancer (IORIO et al., 2005).

Microarray or NGS assay may over- or underestimate the quantification of small RNAs, due to different designing platforms (LESHKOWITZ et al., 2013). For example, in microarray biases may arise due to primer and/or array design or in the sample preparation, differences in labeling, hybridization strength and cross-hybridization (LESHKOWITZ et al., 2013). NGS biases could be a consequence of sample preparation, such as adapter ligation, cDNA synthesis and PCR (HAFNER et al., 2011; LESHKOWITZ et al., 2013; LINSEN et al., 2009; TIAN et al., 2010).

Using microarray to compare the miRNA profiles of U2932-EBV versus U2932, we found that only 14 were miRNAs significantly down-regulated in total cellular profile of U2932-EBV while 169 human miRNAs were down-regulated in the Ago2-IP.

In the comparison of U2932-EBV vs. U2932 in total cellular profile only miR-222 was upregulated more than 2 fold in both microarray and NGS results. In the Ago2-IP of U2932-EBV vs. U2932 in Ago2-IP profile, only miR-27a, miR-339 and miR-30c were downregulated more than 2 fold in both microarray and NGS results. By relating these findings with EBV infection it could be concluded that a large number of human miRNAs were dislocated in the Ago2-IP profile. In sequencing miRNA expression is defined as a relative copy number of sequence reads for a miRNA of interest; such a quantification can be applied to analyse the enrichment or depletion of a given miRNA, whereas such a quantification cannot be applied to microarray data where quantification is based on the relative expression value. For this purpose, NGS results were used for further analysis as we could not apply our microarray results to compare the enrichment or depletion of specific miRNA in the Ago2-complex. In addition, only after sequencing it was possible to apply the aforementioned 0.1% cut-off to filter out presumably non-functional miRNAs in our analysis (MULLOKANDOV et al., 2012).

For selected miRNAs, we carried out northern blotting (NB) in addition to the confirmation of the NGS data by RT-qPCR. We could confirm the up-or down-regulation of various miRNAs by this assay which has the advantage of the absence

of biochemical manipulations during sample preparation. We could confirm not only the changes in total miRNA expression but also a few miRNAs from the Ago2-IP. As we had no loading or internal control, we choose to analyze miRNAs that were up- or down-regulated. We reasoned that if we saw up-regulation of a miRNA in a given sample, then we should conversely observe down-regulation of another miRNA in the same sample. This was indeed the case. For this reason, we re-assayed the same membrane with consecutive probes and could indeed show up- and down-regulation of miRNAs on the same membrane (Figure 16 and Figure 17) additionally confirming some of the initial sequencing data. For instance, we could confirm the dramatic enrichment of miR-363 into to Ago2-complex of SUDHL5-EBV cells.

Based on read counts, we detected miR-146a-5p was enriched in Ago2-IP and induced in EBV positive cell lines, congruent with previous reports that miR-146a-5p was induced by LMP1 (CAMERON et al., 2008b). MiR-146b-5p is up-regulated in EBV positive DLBCL lymphoma (DE ANDRADE et al., 2014). Low expression of MiR-146b-5p, a tumor suppressor, has been reported to be associated with poor prognosis, in DLBCL and gliomas cancer (LIU et al., 2015b; WU et al., 2014). In our data, the miR-146b was down-regulated in U2932-EBV (type 1 latency) as compare to U2932, while the miR-146b-5p was upregulated over two-fold in SUDHL5-EBV as compared to SUDHL5, while this miRNA was depleted over two-fold in total and Ago2-IP complex in U2932-EBV. Another tumor suppressor, miR-148a-3p/-5p was found to be down-regulated in U2932-EBV vs. U2932, while being up-regulated in SUDHL5-EBV vs. SUDHL5 (YU et al., 2016) .

Further, we found a very strong enrichment of the oncogenic miR-363-3p (SUN et al., 2013) in SUDHL5-EBV. The miR-106-363 cluster has close homology with the miR-17-92 cluster (LANDAIS et al., 2007). The miR-17-92 cluster (miR-17, miR-18a, miR-19a, miR-20a, miR-19b-1, and miR-92-1) is located in 13q31.3 (DIOSDADO et al., 2009). It has been reported that the miR-17-92 cluster undergoes amplification and overexpression in lymphoma tumors, such as DLBCL, chronic lymphocytic leukemia (CLL), Burkitt's lymphoma (BL) and mantle cell lymphoma (MCL) (DAL BO et al., 2015; DIOSDADO et al., 2009; OTA et al., 2004; TAGAWA, SETO, 2005; VOLINIA et al.,

2006). From the miR-17-92 cluster, miR-92a-3p showed the strongest expression in U2932 cells and was the fourth highly expressed miRNA in the Ago2 profile of SUDHL5 and SUDHL5-EBV.

In SUDHL5, SUDHL5-EBV and also U2932-EBV, miR-423-5p and -3p were the most strongly RISC enriched miRNAs, and still the 2nd and 4th enriched in U2932, pointing at an important role for miR-423 in DLBCL tumorigenesis. miRNA-423-5p has been shown to be down-regulated in the plasma of colorectal cancer (CRC) patients (FANG et al., 2015) . However miR-423 is up-regulated in glioblastoma and it has been shown that overexpression of miR-423-5p induces proliferation, angiogenesis, and invasion in the glioblastoma cell lines U87 and U251 cells (LI et al., 2017). MiR-inhibitor of growth family proteins 4 (*ING4)* is a direct target of 423-5p (LI et al., 2017). It has also been shown that in EBV infected cell lines, the EBNA3C protein perturbs the interaction between *p53* and *ING4/5* in EBV infected cell lines, resulting in attenuation of *p53*, apoptosis and induction of cell proliferation (SAHA et al., 2011).

We observed an almost complete loss of miR-1260a and miR1260b, in the Ago2-IP profile, in all cell lines used in this study. MiR-1260a and miR1260b has an oncogenic potential (XU et al., 2015) . MiR-1260a and miR1260b have been shown to be part of transfer RNAs (tRNAs) group3 (tRF-3). tRF-3 are generated by Dicer and the RNase Z nuclease from 3′ ends of tRNA (LEE et al., 2009; VENKATESH et al., 2016). It was shown that tRF-3s family members are associated with AGO1, 3, and 4, in HEK293 cells, but not with Ago2. This might explain the failure to detect 1260a/b in the Ago2-IP (KUMAR et al., 2014) .

MiR-486-5p is downregulated in lung cancer (WANG et al., 2014). In our experiments, miR-486-5p was above 0.1% cut-off level of total known miRNA reads in total cellular profile and upregulated in U2932-EBV and SUDHL5-EBV as compare to the uninfected cells. Intriguingly miR-486-5p was strongly lost in Ago2-complex with less than 0.03% abundance in all cell lines except SUDHL5, and downregulated in SUDHL-EBV and U2932-EBV compared to uninfected counterparts. We infer from these results that the Ago2-IP profile gives a better picture about the tumor suppressor

activity of miR-486-5p. As already pointed out above, we have noticed the absence of miR-4792, miR-4485-3p and miR-4532 in the Ago2-complexes when compared to the total cellular miRNA profiles. No proper signal was detected by using NB. These miRNAs might be part of transfer RNAs, associated with other types of Ago protein, or could be degraded tRNA products and are therefore most likely not bona fide miRNAs. The function of the aforementioned potential miRNAs should be investigated in more detail. Mir-221-3p and miR-155-5p were induced in U2932-EBV as compared to U2932. These results were consistent with those of Lawrie and co-workers (LAWRIE et al., 2007). However, miR-221-3p was not detected in neither of SUDHL5-EBV or SUDHL5 cell line.

MiR-142-3p was found to be downregulated in the Ago2 profile of U2932-EBV and SUDHL5-EBV cells. In contrast, in the total cellular profile of U2932-EBV cell line, miR-142-3p was upregulated. Overall, the depletion of miR-142 in the Ago2 profile compared to the total cellular profile and down regulation of miR-142 in EBV-infected cells was a clear indication of miR-142 being a tumor suppressor in DLBCL. It has been shown that miR-142 is downregulated in many types of cancers and that low levels of mir-142 predict a poor outcome. In our group, we have shown that 20% of DLBCLs harbor mutations in miR-142 and that the mutations in the seed sequence confer loss of activity (KWANHIAN et al., 2012). Here, we propose that in addition to point mutations, the depletion of miR142 in the Ago2 complex supports the notion that loss of function or loss of Ago-bound miR-142 plays a role in DLBCL.

Taken together, we conclude that the human miRNA expression profile in the total cellular fraction is not always a real indicator of miRNA function and therefore functional activity. EBV, by encoding miRNAs, is displacing human miRNAs from the Ago complex and changes the balance of human miRNAs in the Ago complex. This change is dependent on the type of EBV latency or the origin of lymphoma, in our study ABC-DLBCL vs. GCB-DLBCL

5 Outlook

One question that arises from our data and the results from Cullen and co-workers is how the cell decides to sequester miRNAs into (a) functionally silent Ago-complex(es) or to enrich miRNAs of low abundance into active RISC complexes; in EBV transformed cells, the process of functional inactivation might be brought about by loading additional, virus-encoded miRNAs into the Ago-complexes. Conversely, the infected cell might sequester viral miRNAs that are deleterious for the cells into non-functional Ago-complexes thus activating otherwise non-functional miRNAs. We have found that ebv-miR-BART6 is highly present in the Ago2-complex of SUDHL5-EBV cells; this miRNA is known to target Dicer, an important enzyme in miRNA metabolism and function. It might be possible that reduced amounts of Dicer serve to inactivate cell miRNAs, for instance those that are necessary to indicate the innate immune response to the viral infection.

As miRNAs are more functional in the Ago complex than in the total cellular lysate, performing Ago2-IP followed by sequencing will give a better evaluation and understanding of highly functional miRNAs or, conversely, their loss of activity. This approach may improve our understanding the contribution of miRNAs in particular diseases or in developmental processes.

Further, the enrichment of miRNAs by the Ago-precipitation will be a promising tool in the near future for (1) the discovery of new miRNA due to the high number of reads generated by this procedure; (2) for the design and choice of antagomirs (short oligonucleotides complementary to miRNAs), based on highly abundant miRNA in the Ago2-complex; (3) choosing miRNAs as biomarkers to differentiate ABC-DLBCL from GCB-DLBCL, using the Ago-bound miRNA profiles.

6 References

1.   Alizadeh AA, Eisen MB, Davis RE, Ma C, Lossos IS, Rosenwald A, Boldrick JC, Sabet H, Tran T, Yu X, Powell JI, Yang L, Marti GE, Moore T, Hudson J, Jr., Lu L, Lewis DB, Tibshirani R, Sherlock G, Chan WC, Greiner TC, Weisenburger DD, Armitage JO, Warnke R, Levy R, Wilson W, Grever MR, Byrd JC, Botstein D, Brown PO, Staudt LM (2000) Distinct types of diffuse large B-cell lymphoma identified by gene expression profiling. Nature 403:503-511
2.   Allegra D, Bilan V, Garding A, Dohner H, Stilgenbauer S, Kuchenbauer F, Mertens D, Zucknick M (2014) Defective DROSHA processing contributes to downregulation of MiR-15/-16 in chronic lymphocytic leukemia. Leukemia 28:98-107
3.   Ambros V, Bartel B, Bartel DP, Burge CB, Carrington JC, Chen X, Dreyfuss G, Eddy SR, Griffiths-Jones S, Marshall M, Matzke M, Ruvkun G, Tuschl T (2003) A uniform system for microRNA annotation. Rna 9:277-279
4.   Ambros V (2004) The functions of animal microRNAs. Nature 431:350-355
5.   Amini RM, Berglund M, Rosenquist R, Von Heideman A, Lagercrantz S, Thunberg U, Bergh J, Sundstrom C, Glimelius B, Enblad G (2002) A novel B-cell line (U-2932) established from a patient with diffuse large B-cell lymphoma following Hodgkin lymphoma. Leuk Lymphoma 43:2179-2189
6.   Asangani IA, Rasheed SA, Nikolova DA, Leupold JH, Colburn NH, Post S, Allgayer H (2008) MicroRNA-21 (miR-21) post-transcriptionally downregulates tumor suppressor Pdcd4 and stimulates invasion, intravasation and metastasis in colorectal cancer. Oncogene 27:2128-2136
7.   Bartel DP (2004) MicroRNAs: genomics, biogenesis, mechanism, and function. Cell 116:281-297
8.   Barth S, Pfuhl T, Mamiani A, Ehses C, Roemer K, Kremmer E, Jaker C, Hock J, Meister G, Grasser FA (2008) Epstein-Barr virus-encoded microRNA miR-BART2 down-regulates the viral DNA polymerase BALF5. Nucleic Acids Res 36:666-675
9.   Basso K, Dalla-Favera R (2015) Germinal centres and B cell lymphomagenesis. Nat Rev Immunol 15:172-184
10.   Béguelin W, Popovic R, Teater M, Jiang Y, Bunting KL, Rosen M, Shen H, Yang SN, Wang L, Ezponda T, Martinez-Garcia E, Zhang H, Zhang Y, Verma SK, McCabe MT, Ott HM, Van Aller GS, Kruger RG, Liu Y, McHugh CF, Scott DW, Chung YR, Kelleher N, Shaknovich R, Creasy CL, Gascoyne RD, Wong K-K, Cerchietti LC, Levine RL, Abdel-Wahab O, Licht JD, Elemento O, Melnick AM (2013) EZH2 is required for germinal center formation and somatic EZH2 mutations promote lymphoid transformation. Cancer cell 23:677-692
11.   Bhende PM, Dickerson SJ, Sun X, Feng WH, Kenney SC (2007) X-box-binding protein 1 activates lytic Epstein-Barr virus gene expression in combination with protein kinase D. J Virol 81:7363-7370
12.   Boccellato F, Anastasiadou E, Rosato P, Kempkes B, Frati L, Faggioni A, Trivedi P (2007) EBNA2 interferes with the germinal center phenotype by downregulating BCL6 and TCL1 in non-Hodgkin's lymphoma cells. J Virol 81:2274-2282
13.   Bohnsack MT, Czaplinski K, Gorlich D (2004) Exportin 5 is a RanGTP-dependent dsRNA-binding protein that mediates nuclear export of pre-miRNAs. Rna 10:185-191
14.   Bradshaw G, Sutherland HG, Haupt LM, Griffiths LR (2016) Dysregulated MicroRNA Expression Profiles and Potential Cellular, Circulating and Polymorphic Biomarkers in Non-Hodgkin Lymphoma. Genes 7:130

15. Cai L, Ye Y, Jiang Q, Chen Y, Lyu X, Li J, Wang S, Liu T, Cai H, Yao K, Li JL, Li X (2015) Epstein-Barr virus-encoded microRNA BART1 induces tumour metastasis by regulating PTEN-dependent pathways in nasopharyngeal carcinoma. Nat Commun 6:7353

16. Calin GA, Dumitru CD, Shimizu M, Bichi R, Zupo S, Noch E, Aldler H, Rattan S, Keating M, Rai K, Rassenti L, Kipps T, Negrini M, Bullrich F, Croce CM (2002) Frequent deletions and down-regulation of micro- RNA genes miR15 and miR16 at 13q14 in chronic lymphocytic leukemia. Proc Natl Acad Sci U S A 99:15524-15529

17. Cameron JE, Fewell C, Yin Q, McBride J, Wang X, Lin Z, Flemington EK (2008a) Epstein-Barr virus growth/latency III program alters cellular microRNA expression. Virology 382:257-266

18. Cameron JE, Yin Q, Fewell C, Lacey M, McBride J, Wang X, Lin Z, Schaefer BC, Flemington EK (2008b) Epstein-Barr Virus Latent Membrane Protein 1 Induces Cellular MicroRNA miR-146a, a Modulator of Lymphocyte Signaling Pathways. Journal of Virology 82:1946-1958

19. Campo E, Swerdlow SH, Harris NL, Pileri S, Stein H, Jaffe ES (2011) The 2008 WHO classification of lymphoid neoplasms and beyond: evolving concepts and practical applications. Blood 117:5019-5032

20. Chan JA, Krichevsky AM, Kosik KS (2005) MicroRNA-21 is an antiapoptotic factor in human glioblastoma cells. Cancer Res 65:6029-6033

21. Copie-Bergman C, Plonquet A, Alonso MA, Boulland ML, Marquet J, Divine M, Moller P, Leroy K, Gaulard P (2002) MAL expression in lymphoid cells: further evidence for MAL as a distinct molecular marker of primary mediastinal large B-cell lymphomas. Mod Pathol 15:1172-1180

22. Countryman J, Miller G (1985) Activation of expression of latent Epstein-Barr herpesvirus after gene transfer with a small cloned subfragment of heterogeneous viral DNA. Proceedings of the National Academy of Sciences of the United States of America 82:4085-4089

23. Cullen BR (2004) Transcription and processing of human microRNA precursors. Mol Cell 16:861-865

24. Cummin T, Johnson P (2016) Lymphoma: turning biology into cures. Clin Med (Lond) 16:s125-s129

25. Dal Bo M, Bomben R, Hernández L, Gattei V (2015) The MYC/miR-17-92 axis in lymphoproliferative disorders: A common pathway with therapeutic potential. Oncotarget 6:19381-19392

26. de Andrade TA, Evangelista AF, Campos AHF, Poles WA, Borges NM, Camillo CMC, Soares FA, Vassallo J, Paes RP, Zerbini MC, Scapulatempo C, Alves AC, Young KH, Colleoni GWB (2014) A microRNA signature profile in EBV(+) diffuse large B-cell lymphoma of the elderly. Oncotarget 5:11813-11826

27. De Craene B, Berx G (2013) Regulatory networks defining EMT during cancer initiation and progression. Nat Rev Cancer 13:97-110

28. de Martel C, Ferlay J, Franceschi S, Vignat J, Bray F, Forman D, Plummer M (2012) Global burden of cancers attributable to infections in 2008: a review and synthetic analysis. Lancet Oncol 13:607-615

29. Delecluse HJ, Feederle R, O'Sullivan B, Taniere P (2007) Epstein Barr virus-associated tumours: an update for the attention of the working pathologist. J Clin Pathol 60:1358-1364

30. Dembla M, Wahl S, Katiyar R, Schmitz F (2014) ArfGAP3 is a component of the photoreceptor synaptic ribbon complex and forms an NAD(H)-regulated, redox-sensitive complex with RIBEYE that is important for endocytosis. J Neurosci 34:5245-5260

31. Diosdado B, van de Wiel MA, Terhaar Sive Droste JS, Mongera S, Postma C, Meijerink WJ, Carvalho B, Meijer GA (2009) MiR-17-92 cluster is associated with 13q gain and c-myc

expression during colorectal adenoma to adenocarcinoma progression. Br J Cancer 101:707-714

32. Dolken L, Malterer G, Erhard F, Kothe S, Friedel CC, Suffert G, Marcinowski L, Motsch N, Barth S, Beitzinger M, Lieber D, Bailer SM, Hoffmann R, Ruzsics Z, Kremmer E, Pfeffer S, Zimmer R, Koszinowski UH, Grasser F, Meister G, Haas J (2010) Systematic analysis of viral and cellular microRNA targets in cells latently infected with human gamma-herpesviruses by RISC immunoprecipitation assay. Cell Host Microbe 7:324-334

33. Dölken L, Malterer G, Erhard F, Kothe S, Friedel CC, Suffert G, Marcinowski L, Motsch N, Barth S, Beitzinger M, Lieber D, Bailer SM, Hoffmann R, Ruzsics Z, Kremmer E, Pfeffer S, Zimmer R, Koszinowski UH, Grässer F, Meister G, Haas J (2010) Systematic Analysis of Viral and Cellular MicroRNA Targets in Cells Latently Infected with Human γ-Herpesviruses by RISC Immunoprecipitation Assay. Cell Host & Microbe 7:324-334

34. Dunleavy K, Grant C, Wilson WH (2013) Using biologic predictive factors to direct therapy of diffuse large B-cell lymphoma. Therapeutic Advances in Hematology 4:43-57

35. Elkayam E, Kuhn C-D, Tocilj A, Haase AD, Greene EM, Hannon GJ, Joshua-Tor L (2012) The Structure of Human Argonaute-2 in Complex with miR-20a. Cell 150:100-110

36. Epstein MA, Achong BG, Barr YM (1964) VIRUS PARTICLES IN CULTURED LYMPHOBLASTS FROM BURKITT'S LYMPHOMA. Lancet 1:702-703

37. Fang Z, Tang J, Bai Y, Lin H, You H, Jin H, Lin L, You P, Li J, Dai Z, Liang X, Su Y, Hu Q, Wang F, Zhang Z-Y (2015) Plasma levels of microRNA-24, microRNA-320a, and microRNA-423-5p are potential biomarkers for colorectal carcinoma. Journal of Experimental & Clinical Cancer Research : CR 34:86

38. Fehlmann T, Meese E, Keller A (2017) Exploring ncRNAs in Alzheimer's disease by miRMaster. Oncotarget 8:3771-3772

39. Flores O, Kennedy EM, Skalsky RL, Cullen BR (2014) Differential RISC association of endogenous human microRNAs predicts their inhibitory potential. Nucleic Acids Res 42:4629-4639

40. Gatto D, Brink R (2010) The germinal center reaction. J Allergy Clin Immunol 126:898-907; quiz 908-899

41. Gross H, Barth S, Palermo RD, Mamiani A, Hennard C, Zimber-Strobl U, West MJ, Kremmer E, Grasser FA (2010) Asymmetric Arginine dimethylation of Epstein-Barr virus nuclear antigen 2 promotes DNA targeting. Virology 397:299-310

42. Grundhoff A, Sullivan CS, Ganem D (2006) A combined computational and microarray-based approach identifies novel microRNAs encoded by human gamma-herpesviruses. Rna 12:733-750

43. Ha M, Kim VN (2014) Regulation of microRNA biogenesis. Nat Rev Mol Cell Biol 15:509-524

44. Hafner M, Renwick N, Brown M, Mihailovic A, Holoch D, Lin C, Pena JT, Nusbaum JD, Morozov P, Ludwig J, Ojo T, Luo S, Schroth G, Tuschl T (2011) RNA-ligase-dependent biases in miRNA representation in deep-sequenced small RNA cDNA libraries. Rna 17:1697-1712

45. Hans CP, Weisenburger DD, Greiner TC, Gascoyne RD, Delabie J, Ott G, Muller-Hermelink HK, Campo E, Braziel RM, Jaffe ES, Pan Z, Farinha P, Smith LM, Falini B, Banham AH, Rosenwald A, Staudt LM, Connors JM, Armitage JO, Chan WC (2004) Confirmation of the molecular classification of diffuse large B-cell lymphoma by immunohistochemistry using a tissue microarray. Blood 103:275-282

46. Healy JA, Dave SS (2015) The Role of EBV in the Pathogenesis of Diffuse Large B Cell Lymphoma. Curr Top Microbiol Immunol 390:315-337

47.	Hsu C-Y, Yi Y-H, Chang K-P, Chang Y-S, Chen S-J, Chen H-C (2014) The Epstein-Barr Virus-Encoded MicroRNA MiR-BART9 Promotes Tumor Metastasis by Targeting E-Cadherin in Nasopharyngeal Carcinoma. PLOS Pathogens 10:e1003974

48.	Iizasa H, Wulff B-E, Alla NR, Maragkakis M, Megraw M, Hatzigeorgiou A, Iwakiri D, Takada K, Wiedmer A, Showe L, Lieberman P, Nishikura K (2010) Editing of Epstein-Barr Virus-encoded BART6 MicroRNAs Controls Their Dicer Targeting and Consequently Affects Viral Latency. Journal of Biological Chemistry 285:33358-33370

49.	Imig J, Motsch N, Zhu JY, Barth S, Okoniewski M, Reineke T, Tinguely M, Faggioni A, Trivedi P, Meister G, Renner C, Grasser FA (2011) microRNA profiling in Epstein-Barr virus-associated B-cell lymphoma. Nucleic Acids Res 39:1880-1893

50.	Intlekofer AM, Younes A (2014) Precision therapy for lymphoma--current state and future directions. Nat Rev Clin Oncol 11:585-596

51.	Iorio MV, Ferracin M, Liu CG, Veronese A, Spizzo R, Sabbioni S, Magri E, Pedriali M, Fabbri M, Campiglio M, Menard S, Palazzo JP, Rosenberg A, Musiani P, Volinia S, Nenci I, Calin GA, Querzoli P, Negrini M, Croce CM (2005) MicroRNA gene expression deregulation in human breast cancer. Cancer Res 65:7065-7070

52.	Iqbal J, Liu Z, Deffenbacher K, Chan WC (2009) Gene expression profiling in lymphoma diagnosis and management. Best Pract Res Clin Haematol 22:191-210

53.	Iqbal J, Shen Y, Huang X, Liu Y, Wake L, Liu C, Deffenbacher K, Lachel CM, Wang C, Rohr J, Guo S, Smith LM, Wright G, Bhagavathi S, Dybkaer K, Fu K, Greiner TC, Vose JM, Jaffe E, Rimsza L, Rosenwald A, Ott G, Delabie J, Campo E, Braziel RM, Cook JR, Tubbs RR, Armitage JO, Weisenburger DD, Staudt LM, Gascoyne RD, McKeithan TW, Chan WC (2015) Global microRNA expression profiling uncovers molecular markers for classification and prognosis in aggressive B-cell lymphoma. Blood 125:1137-1145

54.	Jorgensen LK, Poulsen MO, Laursen MB, Marques SC, Johnsen HE, Bogsted M, Dybkaer K (2015) MicroRNAs as novel biomarkers in diffuse large B-cell lymphoma--a systematic review. Dan Med J 62

55.	Kanda T, Miyata M, Kano M, Kondo S, Yoshizaki T, Iizasa H (2015) Clustered microRNAs of the Epstein-Barr virus cooperatively downregulate an epithelial cell-specific metastasis suppressor. J Virol 89:2684-2697

56.	Khan G, Hashim MJ (2014) Global burden of deaths from Epstein-Barr virus attributable malignancies 1990-2010. Infect Agent Cancer 9:38

57.	Kieff E, Rickinson A (2007) Epstein-Barr Virus and Its Replication, Vol 2 (Philadelphia, PA., Lippincott Williams & Wilkins,).

58.	Kim VN (2005) MicroRNA biogenesis: coordinated cropping and dicing. Nat Rev Mol Cell Biol 6:376-385

59.	Kim VN, Han J, Siomi MC (2009) Biogenesis of small RNAs in animals. Nat Rev Mol Cell Biol 10:126-139

60.	Koganti S, de la Paz A, Freeman AF, Bhaduri-McIntosh S (2014) B lymphocytes from patients with a hypomorphic mutation in STAT3 resist Epstein-Barr virus-driven cell proliferation. J Virol 88:516-524

61.	Kovarikova H, Bubancova I, Laco J, Sieglova K, Vosmikova H, Vosmik M, Dundr P, Nemejcova K, Michalek J, Palicka V, Chmelarova M (2017) Deregulation of selected microRNAs in sinonasal carcinoma: Value of miR-21 as prognostic biomarker in sinonasal squamous cell carcinoma. Head Neck

62.	Kozomara A, Griffiths-Jones S (2014) miRBase: annotating high confidence microRNAs using deep sequencing data. Nucleic Acids Research 42:D68-D73

63.   Krichevsky AM, Gabriely G (2009) miR-21: a small multi-faceted RNA. J Cell Mol Med 13:39-53

64.   Kumar P, Anaya J, Mudunuri SB, Dutta A (2014) Meta-analysis of tRNA derived RNA fragments reveals that they are evolutionarily conserved and associate with AGO proteins to recognize specific RNA targets. BMC Biology 12:78

65.   Kurosu T, Fukuda T, Miki T, Miura O (2003) BCL6 overexpression prevents increase in reactive oxygen species and inhibits apoptosis induced by chemotherapeutic reagents in B-cell lymphoma cells. Oncogene 22:4459-4468

66.   Kwanhian W, Lenze D, Alles J, Motsch N, Barth S, Doll C, Imig J, Hummel M, Tinguely M, Trivedi P, Lulitanond V, Meister G, Renner C, Grasser FA (2012) MicroRNA-142 is mutated in about 20% of diffuse large B-cell lymphoma. Cancer Med 1:141-155

67.   Laichalk LL, Thorley-Lawson DA (2005) Terminal Differentiation into Plasma Cells Initiates the Replicative Cycle of Epstein-Barr Virus In Vivo. Journal of Virology 79:1296-1307

68.   Landais S, Landry S, Legault P, Rassart E (2007) Oncogenic potential of the miR-106-363 cluster and its implication in human T-cell leukemia. Cancer Res 67:5699-5707

69.   Langmead B, Trapnell C, Pop M, Salzberg SL (2009) Ultrafast and memory-efficient alignment of short DNA sequences to the human genome. Genome Biology 10:R25-R25

70.   Lawrie CH, Soneji S, Marafioti T, Cooper CD, Palazzo S, Paterson JC, Cattan H, Enver T, Mager R, Boultwood J, Wainscoat JS, Hatton CS (2007) MicroRNA expression distinguishes between germinal center B cell-like and activated B cell-like subtypes of diffuse large B cell lymphoma. Int J Cancer 121:1156-1161

71.   Lee KT, Tan JK, Lam AK, Gan SY (2016) MicroRNAs serving as potential biomarkers and therapeutic targets in nasopharyngeal carcinoma: A critical review. Crit Rev Oncol Hematol 103:1-9

72.   Lee RC, Feinbaum RL, Ambros V (1993) The C. elegans heterochronic gene lin-4 encodes small RNAs with antisense complementarity to lin-14. Cell 75:843-854

73.   Lee YS, Shibata Y, Malhotra A, Dutta A (2009) A novel class of small RNAs: tRNA-derived RNA fragments (tRFs). Genes Dev 23:2639-2649

74.   Lenz G, Wright GW, Emre NCT, Kohlhammer H, Dave SS, Davis RE, Carty S, Lam LT, Shaffer AL, Xiao W, Powell J, Rosenwald A, Ott G, Muller-Hermelink HK, Gascoyne RD, Connors JM, Campo E, Jaffe ES, Delabie J, Smeland EB, Rimsza LM, Fisher RI, Weisenburger DD, Chan WC, Staudt LM (2008) Molecular subtypes of diffuse large B-cell lymphoma arise by distinct genetic pathways. Proceedings of the National Academy of Sciences of the United States of America 105:13520-13525

75.   Leshkowitz D, Horn-Saban S, Parmet Y, Feldmesser E (2013) Differences in microRNA detection levels are technology and sequence dependent. Rna 19:527-538

76.   Leung AK, Young AG, Bhutkar A, Zheng GX, Bosson AD, Nielsen CB, Sharp PA (2011) Genome-wide identification of Ago2 binding sites from mouse embryonic stem cells with and without mature microRNAs. Nat Struct Mol Biol 18:237-244

77.   Li S, Zeng A, Hu Q, Yan W, Liu Y, You Y (2017) miR-423-5p contributes to a malignant phenotype and temozolomide chemoresistance in glioblastomas. Neuro Oncol 19:55-65

78.   Lieberman PM (2015) Chromatin Structure of Epstein-Barr Virus Latent Episomes. Curr Top Microbiol Immunol 390:71-102

79.   Lin S, Gregory RI (2015) MicroRNA biogenesis pathways in cancer. Nat Rev Cancer 15:321-333

80.   Linsen SE, de Wit E, Janssens G, Heater S, Chapman L, Parkin RK, Fritz B, Wyman SK, de Bruijn E, Voest EE, Kuersten S, Tewari M, Cuppen E (2009) Limitations and possibilities of small RNA digital gene expression profiling. Nat Methods 6:474-476

81. Liu G, Sun Y, Ji P, Li X, Cogdell D, Yang D, Parker Kerrigan BC, Shmulevich I, Chen K, Sood AK, Xue F, Zhang W (2014) MiR-506 suppresses proliferation and induces senescence by directly targeting the CDK4/6-FOXM1 axis in ovarian cancer. J Pathol 233:308-318

82. Liu G, Yang D, Rupaimoole R, Pecot CV, Sun Y, Mangala LS, Li X, Ji P, Cogdell D, Hu L, Wang Y, Rodriguez-Aguayo C, Lopez-Berestein G, Shmulevich I, De Cecco L, Chen K, Mezzanzanica D, Xue F, Sood AK, Zhang W (2015a) Augmentation of response to chemotherapy by microRNA-506 through regulation of RAD51 in serous ovarian cancers. J Natl Cancer Inst 107

83. Liu J, Carmell MA, Rivas FV, Marsden CG, Thomson JM, Song JJ, Hammond SM, Joshua-Tor L, Hannon GJ (2004) Argonaute2 is the catalytic engine of mammalian RNAi. Science 305:1437-1441

84. Liu J, Xu J, Li H, Sun C, Yu L, Li Y, Shi C, Zhou X, Bian X, Ping Y, Wen Y, Zhao S, Xu H, Ren L, An T, Wang Q, Yu S (2015b) miR-146b-5p functions as a tumor suppressor by targeting TRAF6 and predicts the prognosis of human gliomas. Oncotarget 6:29129-29142

85. Liu XS, Fan BY, Pan WL, Li C, Levin AM, Wang X, Zhang RL, Zervos TM, Hu J, Zhang XM, Chopp M, Zhang ZG (2016) Identification of miRNomes associated with adult neurogenesis after stroke using Argonaute 2-based RNA sequencing. RNA Biol:1-12

86. Lo AK, To KF, Lo KW, Lung RW, Hui JW, Liao G, Hayward SD (2007) Modulation of LMP1 protein expression by EBV-encoded microRNAs. Proc Natl Acad Sci U S A 104:16164-16169

87. Ludwig N, Kim YJ, Mueller SC, Backes C, Werner TV, Galata V, Sartorius E, Bohle RM, Keller A, Meese E (2015) Posttranscriptional deregulation of signaling pathways in meningioma subtypes by differential expression of miRNAs. Neuro Oncol 17:1250-1260

88. Lund E, Guttinger S, Calado A, Dahlberg JE, Kutay U (2004) Nuclear export of microRNA precursors. Science 303:95-98

89. Lung RW, Tong JH, Sung YM, Leung PS, Ng DC, Chau SL, Chan AW, Ng EK, Lo KW, To KF (2009) Modulation of LMP2A expression by a newly identified Epstein-Barr virus-encoded microRNA miR-BART22. Neoplasia 11:1174-1184

90. Martello G, Rosato A, Ferrari F, Manfrin A, Cordenonsi M, Dupont S, Enzo E, Guzzardo V, Rondina M, Spruce T, Parenti AR, Daidone MG, Bicciato S, Piccolo S (2010) A MicroRNA targeting dicer for metastasis control. Cell 141:1195-1207

91. Matsui M, Li L, Janowski BA, Corey DR (2015) Reduced Expression of Argonaute 1, Argonaute 2, and TRBP Changes Levels and Intracellular Distribution of RNAi Factors. Scientific Reports 5:12855

92. Meister G (2013) Argonaute proteins: functional insights and emerging roles. Nat Rev Genet 14:447-459

93. Melo SA, Moutinho C, Ropero S, Calin GA, Rossi S, Spizzo R, Fernandez AF, Davalos V, Villanueva A, Montoya G, Yamamoto H, Schwartz S, Jr., Esteller M (2010) A genetic defect in exportin-5 traps precursor microRNAs in the nucleus of cancer cells. Cancer Cell 18:303-315

94. Mendell JT (2008) miRiad roles for the miR-17-92 cluster in development and disease. Cell 133:217-222

95. Miyashita EM, Yang B, Lam KM, Crawford DH, Thorley-Lawson DA (1995) A novel form of Epstein-Barr virus latency in normal B cells in vivo. Cell 80:593-601

96. Miyazaki K (2016) Treatment of Diffuse Large B-Cell Lymphoma. J Clin Exp Hematop 56:79-88

97. Mugnaini EN, Ghosh N (2016) Lymphoma. Prim Care 43:661-675

98. Mullokandov G, Baccarini A, Ruzo A, Jayaprakash AD, Tung N, Israelow B, Evans MJ, Sachidanandam R, Brown BD (2012) High-throughput assessment of microRNA activity and function using microRNA sensor and decoy libraries. Nat Methods 9:840-846

99.   Ota A, Tagawa H, Karnan S, Tsuzuki S, Karpas A, Kira S, Yoshida Y, Seto M (2004) Identification and characterization of a novel gene, C13orf25, as a target for 13q31-q32 amplification in malignant lymphoma. Cancer Res 64:3087-3095

100.   Parekh S, Prive G, Melnick A (2008) Therapeutic targeting of the BCL6 oncogene for diffuse large B-cell lymphomas. Leuk Lymphoma 49:874-882

101.   Parker JS, Roe SM, Barford D (2005) Structural insights into mRNA recognition from a PIWI domain-siRNA guide complex. Nature 434:663-666

102.   Pasquinelli AE, Reinhart BJ, Slack F, Martindale MQ, Kuroda MI, Maller B, Hayward DC, Ball EE, Degnan B, Muller P, Spring J, Srinivasan A, Fishman M, Finnerty J, Corbo J, Levine M, Leahy P, Davidson E, Ruvkun G (2000) Conservation of the sequence and temporal expression of let-7 heterochronic regulatory RNA. Nature 408:86-89

103.   Pekarsky Y, Croce CM (2015) Role of miR-15/16 in CLL. Cell Death and Differentiation 22:6-11

104.   Pfeffer S, Zavolan M, Grasser FA, Chien M, Russo JJ, Ju J, John B, Enright AJ, Marks D, Sander C, Tuschl T (2004) Identification of virus-encoded microRNAs. Science 304:734-736

105.   Reinhart BJ, Slack FJ, Basson M, Pasquinelli AE, Bettinger JC, Rougvie AE, Horvitz HR, Ruvkun G (2000) The 21-nucleotide let-7 RNA regulates developmental timing in Caenorhabditis elegans. Nature 403:901-906

106.   Rosato P, Anastasiadou E, Garg N, Lenze D, Boccellato F, Vincenti S, Severa M, Coccia EM, Bigi R, Cirone M, Ferretti E, Campese AF, Hummel M, Frati L, Presutti C, Faggioni A, Trivedi P (2012) Differential regulation of miR-21 and miR-146a by Epstein-Barr virus-encoded EBNA2. Leukemia 26:2343-2352

107.   Roschewski M, Staudt LM, Wilson WH (2014) Diffuse large B-cell lymphoma[mdash]treatment approaches in the molecular era. Nat Rev Clin Oncol 11:12-23

108.   Rosenwald A, Wright G, Chan WC, Connors JM, Campo E, Fisher RI, Gascoyne RD, Muller-Hermelink HK, Smeland EB, Giltnane JM, Hurt EM, Zhao H, Averett L, Yang L, Wilson WH, Jaffe ES, Simon R, Klausner RD, Powell J, Duffey PL, Longo DL, Greiner TC, Weisenburger DD, Sanger WG, Dave BJ, Lynch JC, Vose J, Armitage JO, Montserrat E, Lopez-Guillermo A, Grogan TM, Miller TP, LeBlanc M, Ott G, Kvaloy S, Delabie J, Holte H, Krajci P, Stokke T, Staudt LM (2002) The use of molecular profiling to predict survival after chemotherapy for diffuse large-B-cell lymphoma. N Engl J Med 346:1937-1947

109.   Rupaimoole R, Ivan C, Yang D, Gharpure KM, Wu SY, Pecot CV, Previs RA, Nagaraja AS, Armaiz-Pena GN, McGuire M, Pradeep S, Mangala LS, Rodriguez-Aguayo C, Huang L, Bar-Eli M, Zhang W, Lopez-Berestein G, Calin GA, Sood AK (2016) Hypoxia-upregulated microRNA-630 targets Dicer, leading to increased tumor progression. Oncogene 35:4312-4320

110.   Rupaimoole R, Slack FJ (2017) MicroRNA therapeutics: towards a new era for the management of cancer and other diseases. Nat Rev Drug Discov 16:203-222

111.   Saha A, Bamidele A, Murakami M, Robertson ES (2011) EBNA3C attenuates the function of p53 through interaction with inhibitor of growth family proteins 4 and 5. J Virol 85:2079-2088

112.   Sample J, Young L, Martin B, Chatman T, Kieff E, Rickinson A, Kieff E (1990) Epstein-Barr virus types 1 and 2 differ in their EBNA-3A, EBNA-3B, and EBNA-3C genes. J Virol 64:4084-4092

113.   Sasaki T, Shiohama A, Minoshima S, Shimizu N (2003) Identification of eight members of the Argonaute family in the human genome. Genomics 82:323-330

114.   Schirle NT, MacRae IJ (2012) The crystal structure of human Argonaute2. Science 336:1037-1040

115.   Scott DW, Wright GW, Williams PM, Lih C-J, Walsh W, Jaffe ES, Rosenwald A, Campo E, Chan WC, Connors JM, Smeland EB, Mottok A, Braziel RM, Ott G, Delabie J, Tubbs RR, Cook JR,

Weisenburger DD, Greiner TC, Glinsmann-Gibson BJ, Fu K, Staudt LM, Gascoyne RD, Rimsza LM (2014) Determining cell-of-origin subtypes of diffuse large B-cell lymphoma using gene expression in formalin-fixed paraffin-embedded tissue. Blood 123:1214-1217

116. Shankland KR, Armitage JO, Hancock BW (2012) Non-Hodgkin lymphoma. Lancet 380:848-857

117. Shen J, Xia W, Khotskaya YB, Huo L, Nakanishi K, Lim SO, Du Y, Wang Y, Chang WC, Chen CH, Hsu JL, Wu Y, Lam YC, James BP, Liu X, Liu CG, Patel DJ, Hung MC (2013) EGFR modulates microRNA maturation in response to hypoxia through phosphorylation of AGO2. Nature 497:383-387

118. Skrabek P, Turner D, Seftel M (2013) Epidemiology of non-Hodgkin lymphoma. Transfus Apher Sci 49:133-138

119. Sun Q, Zhang J, Cao W, Wang X, Xu Q, Yan M, Wu X, Chen W (2013) Dysregulated miR-363 affects head and neck cancer invasion and metastasis by targeting podoplanin. Int J Biochem Cell Biol 45:513-520

120. Swerdlow SH, Campo E, Pileri SA, Harris NL, Stein H, Siebert R, Advani R, Ghielmini M, Salles GA, Zelenetz AD, Jaffe ES (2016) The 2016 revision of the World Health Organization classification of lymphoid neoplasms. Blood 127:2375-2390

121. Tagawa H, Seto M (2005) A microRNA cluster as a target of genomic amplification in malignant lymphoma. Leukemia 19:2013-2016

122. Tashiro H, Brenner MK (2017) Immunotherapy against cancer-related viruses. Cell Res 27:59-73

123. Thorley-Lawson DA (2001) Epstein-Barr virus: exploiting the immune system. Nat Rev Immunol 1:75-82

124. Tian G, Yin X, Luo H, Xu X, Bolund L, Zhang X, Gan SQ, Li N (2010) Sequencing bias: comparison of different protocols of microRNA library construction. BMC Biotechnol 10:64

125. Tokumaru S, Suzuki M, Yamada H, Nagino M, Takahashi T (2008) let-7 regulates Dicer expression and constitutes a negative feedback loop. Carcinogenesis 29:2073-2077

126. Tomita N, Takasaki H, Fujisawa S, Miyashita K, Ogusa E, Kishimoto K, Matsuura S, Sakai R, Koharazawa H, Yamamoto W, Fujimaki K, Fujita H, Ishii Y, Taguchi J, Kuwabara H, Motomura S, Ishigatsubo Y (2013) Standard R-CHOP therapy in follicular lymphoma and diffuse large B-cell lymphoma. J Clin Exp Hematop 53:121-125

127. Venkatesh T, Suresh PS, Tsutsumi R (2016) tRFs: miRNAs in disguise. Gene 579:133-138

128. Victora GD, Nussenzweig MC (2012) Germinal centers. Annu Rev Immunol 30:429-457

129. Volinia S, Calin GA, Liu CG, Ambs S, Cimmino A, Petrocca F, Visone R, Iorio M, Roldo C, Ferracin M, Prueitt RL, Yanaihara N, Lanza G, Scarpa A, Vecchione A, Negrini M, Harris CC, Croce CM (2006) A microRNA expression signature of human solid tumors defines cancer gene targets. Proc Natl Acad Sci U S A 103:2257-2261

130. Wang J, Tian X, Han R, Zhang X, Wang X, Shen H, Xue L, Liu Y, Yan X, Shen J, Mannoor K, Deepak J, Donahue JM, Stass SA, Xing L, Jiang F (2014) Downregulation of miR-486-5p contributes to tumor progression and metastasis by targeting protumorigenic ARHGAP5 in lung cancer. Oncogene 33:1181-1189

131. Wilson WH, Young RM, Schmitz R, Yang Y, Pittaluga S, Wright G, Lih CJ, Williams PM, Shaffer AL, Gerecitano J, de Vos S, Goy A, Kenkre VP, Barr PM, Blum KA, Shustov A, Advani R, Fowler NH, Vose JM, Elstrom RL, Habermann TM, Barrientos JC, McGreivy J, Fardis M, Chang BY, Clow F, Munneke B, Moussa D, Beaupre DM, Staudt LM (2015) Targeting B cell receptor signaling with ibrutinib in diffuse large B cell lymphoma. Nat Med 21:922-926

132.   Wu PY, Zhang XD, Zhu J, Guo XY, Wang JF (2014) Low expression of microRNA-146b-5p and microRNA-320d predicts poor outcome of large B-cell lymphoma treated with cyclophosphamide, doxorubicin, vincristine, and prednisone. Hum Pathol 45:1664-1673

133.   Xu L, Li L, Li J, Li H, Shen Q, Ping J, Ma Z, Zhong J, Dai L (2015) Overexpression of miR-1260b in Non-small Cell Lung Cancer is Associated with Lymph Node Metastasis. Aging Dis 6:478-485

134.   Ye Z, Jin H, Qian Q (2015) Argonaute 2: A Novel Rising Star in Cancer Research. J Cancer 6:877-882

135.   Young LS, Yap LF, Murray PG (2016) Epstein-Barr virus: more than 50 years old and still providing surprises. Nat Rev Cancer 16:789-802

136.   Yu B, Lv X, Su L, Li J, Yu Y, Gu Q, Yan M, Zhu Z, Liu B (2016) MiR-148a Functions as a Tumor Suppressor by Targeting CCK-BR via Inactivating STAT3 and Akt in Human Gastric Cancer. PLoS One 11:e0158961

137.   Yu X, Li Z (2015) New insights into MicroRNAs involves in drug resistance in diffuse large B cell lymphoma. American Journal of Translational Research 7:2536-2542

138.   Zhai L, Wang L, Teng F, Zhou L, Zhang W, Xiao J, Liu Y, Deng W (2016) Argonaute and Argonaute-Bound Small RNAs in Stem Cells. Int J Mol Sci 17:208

139.   Zhang J, Grubor V, Love CL, Banerjee A, Richards KL, Mieczkowski PA, Dunphy C, Choi W, Au WY, Srivastava G, Lugar PL, Rizzieri DA, Lagoo AS, Bernal-Mizrachi L, Mann KP, Flowers C, Naresh K, Evens A, Gordon LI, Czader M, Gill JI, Hsi ED, Liu Q, Fan A, Walsh K, Jima D, Smith LL, Johnson AJ, Byrd JC, Luftig MA, Ni T, Zhu J, Chadburn A, Levy S, Dunson D, Dave SS (2013) Genetic heterogeneity of diffuse large B-cell lymphoma. Proc Natl Acad Sci U S A 110:1398-1403

7 Appendices

Table A1. Highly expressed miRNAs in U2932 and SUDHL5 and their EBV positive counterparts in "Total" profile at 0.1% cut-off.

% of total cellular miRNA pool							
U2932				**SUDHL5**			
miRNA	**EBV Positive**	**miRNA**	**EBV Negative**	**miRNA**	**EBV Positive**	**miRNA**	**EBV Negative**
miR-92a-3p	16.783	miR-92a-3p	17.205	miR-21-5p	14.164	miR-142-5p	28.391
miR-191-5p	9.169	miR-191-5p	11.556	miR-142-5p	6.891	miR-21-5p	10.992
miR-181a-5p	7.785	miR-148a-3p	8.417	miR-BHRF1-1	5.971	miR-181a-5p	5.613
miR-146a-5p	5.849	miR-181a-5p	7.073	miR-148a-3p	5.807	miR-26a-5p	5.057
miR-148a-3p	5.704	let-7a-5p	4.559	miR-191-5p	4.947	miR-191-5p	4.122
miR-142-5p	5.213	miR-26a-5p	4.159	miR-181a-5p	3.619	miR-16-5p	3.588
miR-16-5p	3.929	miR-142-5p	3.854	miR-16-5p	3.321	miR-30d-5p	3.031
let-7f-5p	3.555	let-7f-5p	3.787	miR-BART10-3p	3.254	miR-92a-3p	3.013
let-7a-5p	3.472	miR-146a-5p	3.380	miR-22-3p	3.158	let-7a-5p	2.848
miR-30d-5p	3.379	miR-16-5p	3.123	miR-30d-5p	3.060	miR-22-3p	2.781
miR-26a-5p	2.887	miR-30d-5p	2.736	miR-BART8-5p	2.975	let-7f-5p	2.746
miR-21-5p	2.551	miR-182-5p	2.566	let-7a-5p	2.587	miR-148a-3p	2.681
miR-27b-3p	1.753	miR-30e-5p	1.728	let-7f-5p	2.587	miR-142-3p	2.657
miR-19b-3p	1.744	miR-20a-5p	1.666	miR-26a-5p	2.549	miR-30e-5p	1.960
miR-182-5p	1.609	miR-27b-3p	1.625	miR-92a-3p	2.364	miR-28-3p	1.466
miR-155-5p	1.339	miR-192-5p	1.623	miR-30e-5p	1.862	miR-4792	1.349
miR-192-5p	1.300	miR-21-5p	1.331	miR-182-5p	1.550	miR-21-3p	1.106
miR-20a-5p	1.157	let-7g-5p	1.322	miR-BART7-5p	1.367	miR-192-5p	0.881
miR-30e-5p	1.139	miR-186-5p	1.048	miR-BART19-5p	1.267	let-7g-5p	0.776
miR-186-5p	0.879	miR-22-3p	0.860	miR-146b-5p	1.188	miR-4485-3p	0.709
let-7g-5p	0.858	miR-17-5p	0.778	miR-BART11-3p	1.130	miR-25-3p	0.680
miR-103a-3p	0.808	miR-378a-3p	0.685	miR-BART6-3p	1.098	miR-27b-3p	0.659
miR-378a-3p	0.803	miR-103a-3p	0.675	miR-BART22	0.935	miR-378a-3p	0.624
miR-17-5p	0.728	miR-19b-3p	0.664	miR-28-3p	0.877	miR-186-5p	0.598
let-7i-5p	0.530	miR-26b-5p	0.577	miR-192-5p	0.849	miR-146a-5p	0.477
miR-22-3p	0.490	miR-98-5p	0.566	miR-21-3p	0.841	miR-26b-5p	0.456
miR-142-3p	0.437	miR-25-3p	0.556	miR-146a-5p	0.799	miR-182-5p	0.419
miR-BART10-3p	0.436	miR-28-3p	0.508	let-7g-5p	0.664	miR-151a-5p	0.379

miR-101-3p	0.429	miR-155-5p	0.503	miR-378a-3p	0.650	miR-30b-5p	0.378
miR-486-5p	0.425	miR-101-3p	0.474	miR-BHRF1-3	0.644	miR-103a-3p	0.370
miR-25-3p	0.409	miR-30c-5p	0.422	miR-27b-3p	0.564	miR-146b-5p	0.367
miR-98-5p	0.399	miR-142-3p	0.399	miR-26b-5p	0.520	miR-1246	0.339
miR-93-5p	0.386	miR-4792	0.384	miR-4485-3p	0.517	miR-20a-5p	0.334
miR-9-5p	0.385	miR-93-5p	0.369	miR-BART17-5p	0.511	miR-101-3p	0.307
miR-30b-5p	0.377	let-7i-5p	0.340	miR-BART13-5p	0.494	miR-486-5p	0.302
miR-28-3p	0.338	miR-425-5p	0.333	miR-25-3p	0.485	miR-19b-3p	0.293
miR-425-5p	0.338	miR-30b-5p	0.319	miR-142-3p	0.468	miR-30c-5p	0.291
miR-181b-5p	0.334	miR-423-3p	0.313	miR-103a-3p	0.424	miR-93-5p	0.289
miR-26b-5p	0.332	miR-29a-3p	0.289	miR-486-5p	0.403	let-7i-5p	0.283
miR-29a-3p	0.324	miR-181b-5p	0.280	miR-BART18-3p	0.401	miR-28-5p	0.277
miR-BART8-5p	0.296	let-7c-5p	0.245	miR-186-5p	0.394	miR-423-3p	0.254
miR-4792	0.287	miR-9-5p	0.240	miR-BART19-3p	0.354	miR-98-5p	0.229
miR-19a-3p	0.276	miR-148a-5p	0.223	miR-30c-5p	0.343	miR-17-5p	0.213
miR-4485-3p	0.276	miR-486-5p	0.199	miR-30b-5p	0.332	miR-181a-3p	0.197
miR-15a-5p	0.255	miR-183-5p	0.198	miR-BART7-3p	0.323	miR-423-5p	0.188
miR-423-3p	0.233	miR-423-5p	0.195	miR-101-3p	0.304	miR-151a-3p	0.184
miR-30c-5p	0.224	let-7d-5p	0.187	miR-20a-5p	0.302	miR-29a-3p	0.184
miR-423-5p	0.217	let-7b-5p	0.181	miR-BART9-5p	0.300	miR-181b-5p	0.172
miR-221-3p	0.210	miR-27a-3p	0.177	miR-BART2-5p	0.290	miR-210-3p	0.168
miR-148a-5p	0.206	miR-769-5p	0.170	miR-BART6-5p	0.288	miR-155-5p	0.163
miR-21-3p	0.202	miR-146b-5p	0.163	miR-BART8-3p	0.287	miR-15a-5p	0.154
miR-BART6-3p	0.197	miR-339-3p	0.142	miR-BHRF1-2-3p	0.287	let-7d-5p	0.153
let-7d-5p	0.176	miR-1260b	0.127	miR-BART17-3p	0.274	miR-140-3p	0.143
miR-107	0.167	miR-1260a	0.126	miR-98-5p	0.260	miR-4532	0.138
miR-BART11-3p	0.158	miR-92b-3p	0.125	miR-93-5p	0.257	miR-769-5p	0.138
miR-769-5p	0.156	miR-140-3p	0.122	miR-BART14-3p	0.252	miR-941	0.120
miR-1246	0.151	miR-19a-3p	0.113	miR-151a-5p	0.249	miR-1260a	0.117
let-7b-5p	0.142	miR-210-3p	0.108	miR-155-5p	0.219	miR-1260b	0.117
miR-130b-3p	0.132	miR-15b-5p	0.108	let-7i-5p	0.200	miR-148a-5p	0.103
miR-BART22	0.128	miR-107	0.106	miR-17-5p	0.195		
miR-140-3p	0.124	miR-301a-3p	0.102	miR-19b-3p	0.193		
miR-222-3p	0.122			miR-148a-5p	0.184		
miR-183-5p	0.121			miR-151a-3p	0.183		
miR-BART7-5p	0.114			miR-423-3p	0.175		

miR-17-3p	0.111		miR-10a-5p	0.155	
miR-301a-3p	0.110		miR-27a-3p	0.153	
miR-193b-3p	0.104		miR-BART3-5p	0.153	
miR-18a-5p	0.103		miR-28-5p	0.137	
			miR-BART1-3p	0.137	
			miR-423-5p	0.134	
			miR-BART1-5p	0.131	
			miR-210-3p	0.129	
			miR-BART16	0.125	
			miR-BART5-5p	0.120	
			let-7d-5p	0.118	
			miR-29a-3p	0.116	
			miR-15a-5p	0.110	
			miR-425-5p	0.108	
			miR-181a-3p	0.108	
			miR-941	0.107	
			miR-1260a	0.107	
			miR-1260b	0.107	
			miR-181b-5p	0.102	
			miR-140-3p	0.100	

Table A2. Highly expressed miRNAs in U2932 and SUDHL5 and their EBV positive counterparts in "Ago2-IP" profile at 0.1% cut-off.

% of Ago2-IP miRNA pool							
U2932				**SUDHL5**			
miRNA	EBV Positive	miRNA	EBV Negative	miRNA	EBV Positive	miRNA	EBV Negative
miR-92a-3p	26.551	miR-92a-3p	23.235	miR-21-5p	16.151	miR-21-5p	14.373
miR-181a-5p	10.446	miR-181a-5p	9.224	miR-BHRF1-1	7.030	miR-142-5p	13.376
miR-146a-5p	10.051	miR-148a-3p	7.232	miR-92a-3p	4.881	miR-181a-5p	8.794
miR-191-5p	5.372	miR-146a-5p	7.106	miR-148a-3p	4.216	miR-92a-3p	7.077
miR-16-5p	4.615	miR-191-5p	6.580	miR-BART8-5p	4.154	miR-26a-5p	6.298
miR-148a-3p	4.096	miR-26a-5p	4.317	miR-181a-5p	4.149	miR-16-5p	5.130
miR-30d-5p	3.184	miR-16-5p	3.565	miR-22-3p	3.862	miR-22-3p	4.762
miR-26a-5p	3.124	miR-182-5p	3.089	miR-142-5p	3.435	miR-191-5p	3.399
let-7f-5p	2.665	miR-30d-5p	3.074	miR-16-5p	3.231	let-7f-5p	3.294
miR-21-5p	2.581	let-7f-5p	2.949	miR-BART6-3p	3.143	miR-28-3p	3.260
miR-142-5p	2.074	let-7a-5p	2.257	miR-191-5p	2.883	miR-30d-5p	3.027
miR-182-5p	1.966	miR-21-5p	1.956	miR-30d-5p	2.617	miR-148a-3p	2.644
miR-27b-3p	1.916	miR-142-5p	1.939	let-7f-5p	2.566	miR-423-5p	1.639
miR-155-5p	1.311	miR-27b-3p	1.707	miR-BART10-3p	2.498	miR-30e-5p	1.612
let-7a-5p	1.153	miR-30e-5p	1.502	miR-26a-5p	2.210	miR-142-3p	1.501
miR-192-5p	1.080	miR-192-5p	1.470	miR-BART11-3p	1.950	let-7a-5p	1.437
miR-186-5p	0.865	miR-22-3p	1.289	miR-BART19-5p	1.889	miR-146a-5p	1.258
miR-30e-5p	0.804	miR-186-5p	1.275	miR-182-5p	1.827	miR-192-5p	1.018
miR-378a-3p	0.790	miR-378a-3p	0.852	miR-28-3p	1.728	miR-186-5p	0.944
miR-22-3p	0.756	miR-19b-3p	0.750	miR-BART7-5p	1.677	miR-27b-3p	0.892
miR-423-5p	0.738	miR-155-5p	0.730	miR-146a-5p	1.381	miR-25-3p	0.879
let-7i-5p	0.588	miR-28-3p	0.695	miR-30e-5p	1.280	miR-423-3p	0.785
miR-103a-3p	0.566	miR-25-3p	0.678	let-7a-5p	1.060	miR-378a-3p	0.767
miR-423-3p	0.516	miR-103a-3p	0.598	miR-146b-5p	0.988	miR-182-5p	0.667
miR-19b-3p	0.505	let-7g-5p	0.595	miR-BART22	0.951	let-7i-5p	0.662
miR-181b-5p	0.504	miR-425-5p	0.544	miR-423-5p	0.936	miR-151a-5p	0.625
miR-425-5p	0.484	miR-20a-5p	0.540	miR-BART17-5p	0.844	miR-21-3p	0.594
let-7g-5p	0.475	miR-17-5p	0.513	miR-192-5p	0.743	miR-28-5p	0.515
miR-17-5p	0.469	let-7i-5p	0.478	miR-378a-3p	0.733	let-7g-5p	0.493
miR-28-3p	0.454	miR-93-5p	0.459	miR-BART13-5p	0.725	miR-146b-5p	0.472
miR-93-5p	0.446	miR-423-5p	0.442	miR-BHRF1-3	0.659	miR-181b-5p	0.383
miR-BART8-5p	0.425	miR-423-3p	0.429	miR-27b-3p	0.605	miR-93-5p	0.368
miR-25-3p	0.373	miR-101-3p	0.398	miR-25-3p	0.565	miR-103a-3p	0.360
miR-20a-5p	0.355	miR-181b-5p	0.368	miR-21-3p	0.561	miR-155-5p	0.310

miRNA	Value	miRNA	Value	miRNA	Value	miRNA	Value
miR-BART11-3p	0.339	miR-29a-3p	0.343	miR-423-3p	0.496	miR-26b-5p	0.305
miR-BART6-3p	0.318	miR-26b-5p	0.318	miR-186-5p	0.443	miR-101-3p	0.245
miR-9-5p	0.286	miR-30c-5p	0.291	let-7i-5p	0.377	miR-30c-5p	0.245
miR-15a-5p	0.276	miR-98-5p	0.231	miR-103a-3p	0.364	miR-19b-3p	0.242
miR-29a-3p	0.263	miR-142-3p	0.228	let-7g-5p	0.349	miR-151a-3p	0.224
miR-BART10-3p	0.243	miR-183-5p	0.214	miR-BART18-3p	0.338	miR-29a-3p	0.204
miR-101-3p	0.240	miR-9-5p	0.200	miR-155-5p	0.338	miR-15a-5p	0.187
miR-BART19-5p	0.189	miR-146b-5p	0.191	miR-BHRF1-2-3p	0.326	miR-140-3p	0.182
miR-26b-5p	0.183	miR-148a-5p	0.185	miR-151a-5p	0.304	miR-425-5p	0.179
miR-142-3p	0.172	miR-30b-5p	0.183	miR-BART6-5p	0.287	let-7d-5p	0.175
miR-130b-3p	0.145	let-7d-5p	0.159	miR-26b-5p	0.261	miR-17-5p	0.170
let-7d-5p	0.144	miR-92b-3p	0.152	miR-93-5p	0.255	miR-106b-3p	0.159
miR-148a-5p	0.144	miR-769-5p	0.152	miR-BART14-3p	0.253	miR-30b-5p	0.153
miR-30c-5p	0.139	miR-320a	0.151	miR-101-3p	0.244	miR-181a-3p	0.145
miR-BART7-5p	0.136	miR-339-3p	0.149	miR-BART2-5p	0.235	miR-210-3p	0.138
miR-107	0.135	miR-140-3p	0.148	miR-30c-5p	0.235	miR-941	0.138
miR-98-5p	0.134	miR-27a-3p	0.143	miR-BART8-3p	0.221	miR-15b-5p	0.132
miR-30b-5p	0.129	miR-19a-3p	0.134	miR-142-3p	0.219	miR-769-5p	0.126
miR-183-5p	0.117	miR-15b-5p	0.132	miR-BART7-3p	0.201	miR-486-5p	0.124
miR-221-3p	0.114	let-7b-5p	0.119	miR-BART9-5p	0.201	miR-20a-5p	0.118
miR-19a-3p	0.114	let-7c-5p	0.115	miR-181b-5p	0.191		
miR-769-5p	0.107	miR-15a-5p	0.109	miR-10a-5p	0.189		
miR-140-3p	0.103	miR-107	0.107	miR-28-5p	0.189		
				miR-151a-3p	0.186		
				miR-BART16	0.185		
				miR-BART3-5p	0.176		
				miR-BART19-3p	0.175		
				miR-19b-3p	0.144		
				miR-425-5p	0.143		
				miR-30b-5p	0.133		
				miR-27a-3p	0.130		
				miR-148a-5p	0.126		
				miR-140-3p	0.116		
				miR-BART17-3p	0.115		
				miR-941	0.113		
				miR-17-5p	0.109		
				miR-29a-3p	0.107		
				miR-363-3p	0.105		
				let-7d-5p	0.104		

Table A3. List of miRNAs enriched or depleted from the "Ago2-IP"as compared to the "Total" profile in U2932-EBV and U2932 at 0.1% cut-off.

U2932-EBV				U2932			
miRNA	% of total miRNA pool	% of RISC assoc. pool	RISC enriched	miRNA	% of total miRNA pool	% of RISC assoc. pool	RISC enriched
miR-423-5p	0.217	0.738	3.407	miR-320a	0.064	0.151	2.345
miR-423-3p	0.233	0.516	2.22	miR-423-5p	0.195	0.442	2.267
miR-146a-5p	5.849	10.051	1.718	miR-146a-5p	3.38	7.106	2.103
miR-92a-3p	16.783	26.551	1.582	miR-425-5p	0.333	0.544	1.635
miR-22-3p	0.49	0.756	1.542	miR-22-3p	0.86	1.289	1.498
miR-181b-5p	0.334	0.504	1.512	miR-21-5p	1.331	1.956	1.469
miR-425-5p	0.338	0.484	1.434	miR-155-5p	0.503	0.73	1.452
miR-181a-5p	7.785	10.446	1.342	let-7i-5p	0.34	0.478	1.407
miR-28-3p	0.338	0.454	1.342	miR-423-3p	0.313	0.429	1.369
miR-182-5p	1.609	1.966	1.222	miR-28-3p	0.508	0.695	1.367
miR-16-5p	3.929	4.615	1.175	miR-92a-3p	17.205	23.235	1.35
miR-93-5p	0.386	0.446	1.156	miR-181b-5p	0.28	0.368	1.317
let-7i-5p	0.53	0.588	1.109	miR-181a-5p	7.073	9.224	1.304
miR-130b-3p	0.132	0.145	1.093	miR-93-5p	0.369	0.459	1.245
miR-27b-3p	1.753	1.916	1.093	miR-378a-3p	0.685	0.852	1.244
miR-15a-5p	0.255	0.276	1.083	miR-15b-5p	0.108	0.132	1.221
miR-26a-5p	2.887	3.124	1.082	miR-25-3p	0.556	0.678	1.218
miR-21-5p	2.551	2.581	1.012	miR-186-5p	1.048	1.275	1.217
miR-186-5p	0.879	0.865	0.984	miR-92b-3p	0.125	0.152	1.214
miR-378a-3p	0.803	0.79	0.984	miR-140-3p	0.122	0.148	1.209
miR-155-5p	1.339	1.311	0.979	miR-182-5p	2.566	3.089	1.204
miR-183-5p	0.121	0.117	0.968	miR-19a-3p	0.113	0.134	1.192
miR-30d-5p	3.379	3.184	0.942	miR-15a-5p	0.091	0.109	1.189
miR-25-3p	0.409	0.373	0.912	miR-29a-3p	0.289	0.343	1.186
miR-192-5p	1.3	1.08	0.831	miR-146b-5p	0.163	0.191	1.172
miR-140-3p	0.124	0.103	0.826	miR-16-5p	3.123	3.565	1.142
let-7d-5p	0.176	0.144	0.818	miR-19b-3p	0.664	0.75	1.13
miR-29a-3p	0.324	0.263	0.811	miR-30d-5p	2.736	3.074	1.124
miR-107	0.167	0.135	0.811	miR-183-5p	0.198	0.214	1.079
miR-17-3p	0.111	0.088	0.791	miR-27b-3p	1.625	1.707	1.051
let-7f-5p	3.555	2.665	0.75	miR-339-3p	0.142	0.149	1.05
miR-9-5p	0.385	0.286	0.743	miR-26a-5p	4.159	4.317	1.038
miR-148a-3p	5.704	4.096	0.718	miR-107	0.106	0.107	1.012
miR-30e-5p	1.139	0.804	0.706	miR-192-5p	1.623	1.47	0.906
miR-103a-3p	0.808	0.566	0.7	miR-769-5p	0.17	0.152	0.894
miR-148a-5p	0.206	0.144	0.699	miR-103a-3p	0.675	0.598	0.885
miR-769-5p	0.156	0.107	0.689	miR-30e-5p	1.728	1.502	0.869
miR-222-3p	0.122	0.08	0.651	miR-148a-3p	8.417	7.232	0.859
miR-17-5p	0.728	0.469	0.645	let-7d-5p	0.187	0.159	0.85

miR				miR			
miR-30c-5p	0.224	0.139	0.624	miR-101-3p	0.474	0.398	0.839
miR-301a-3p	0.11	0.068	0.619	miR-9-5p	0.24	0.2	0.833
miR-191-5p	9.169	5.372	0.586	miR-148a-5p	0.223	0.185	0.831
miR-101-3p	0.429	0.24	0.559	miR-27a-3p	0.177	0.143	0.809
let-7g-5p	0.858	0.475	0.553	let-7f-5p	3.787	2.949	0.779
miR-26b-5p	0.332	0.183	0.552	miR-301a-3p	0.102	0.079	0.774
miR-221-3p	0.21	0.114	0.544	miR-210-3p	0.108	0.082	0.758
miR-193b-3p	0.104	0.048	0.462	miR-30c-5p	0.422	0.291	0.688
let-7b-5p	0.142	0.064	0.453	miR-17-5p	0.778	0.513	0.659
miR-21-3p	0.202	0.084	0.413	let-7b-5p	0.181	0.119	0.657
miR-19a-3p	0.276	0.114	0.413	miR-30b-5p	0.319	0.183	0.574
miR-142-5p	5.213	2.074	0.398	miR-142-3p	0.399	0.228	0.572
miR-142-3p	0.437	0.172	0.394	miR-191-5p	11.556	6.58	0.569
miR-30b-5p	0.377	0.129	0.343	miR-26b-5p	0.577	0.318	0.552
miR-18a-5p	0.103	0.035	0.342	miR-142-5p	3.854	1.939	0.503
miR-98-5p	0.399	0.134	0.336	let-7a-5p	4.559	2.257	0.495
let-7a-5p	3.472	1.153	0.332	let-7c-5p	0.245	0.115	0.47
miR-20a-5p	1.157	0.355	0.307	let-7g-5p	1.322	0.595	0.45
miR-19b-3p	1.744	0.505	0.29	miR-98-5p	0.566	0.231	0.408
miR-486-5p	0.425	0.033	0.077	miR-20a-5p	1.666	0.54	0.324
miR-4485-3p	0.276	0.004	0.013	miR-486-5p	0.199	0.03	0.15
miR-1246	0.151	0.001	0.003	miR-4792	0.384	0.003	0.008
miR-4792	0.287	0.001	0.003	miR-1260b	0.127	0.0005	0.004
				miR-1260a	0.126	0.0004	0.003

Table A4. List of miRNAs enriched or depleted from the "Ago2-IP"as compared to the "Total" profile in SUDHL5-EBV and SUDHL5 at 0.1% cut-off

	SUDHL5-EBV				SUDHL5		
miRNA	% of total miRNA pool	% of RISC assoc. pool	RISC enriched	miRNA	% of total miRNA pool	% of RISC assoc. pool	RISC enriched
miR-423-5p	0.134	0.936	6.989	miR-423-5p	0.188	1.639	8.721
miR-423-3p	0.175	0.496	2.834	miR-423-3p	0.254	0.785	3.087
miR-92a-3p	2.364	4.881	2.064	miR-146a-5p	0.477	1.258	2.636
miR-28-3p	0.877	1.728	1.972	miR-92a-3p	3.013	7.077	2.349
let-7i-5p	0.2	0.377	1.886	let-7i-5p	0.283	0.662	2.337
miR-181b-5p	0.102	0.191	1.873	miR-181b-5p	0.172	0.383	2.225
miR-146a-5p	0.799	1.381	1.729	miR-28-3p	1.466	3.26	2.224
miR-155-5p	0.219	0.338	1.547	miR-106b-3p	0.082	0.159	1.932
miR-28-5p	0.137	0.189	1.381	miR-155-5p	0.163	0.31	1.901
miR-425-5p	0.108	0.143	1.323	miR-425-5p	0.095	0.179	1.879
miR-22-3p	3.158	3.862	1.223	miR-28-5p	0.277	0.515	1.861
miR-151a-5p	0.249	0.304	1.221	miR-22-3p	2.781	4.762	1.712
miR-10a-5p	0.155	0.189	1.219	miR-151a-5p	0.379	0.625	1.651
miR-363-3p	0.089	0.105	1.179	miR-182-5p	0.419	0.667	1.592
miR-182-5p	1.55	1.827	1.179	miR-186-5p	0.598	0.944	1.579
miR-25-3p	0.485	0.565	1.165	miR-181a-5p	5.613	8.794	1.567
miR-140-3p	0.1	0.116	1.152	miR-16-5p	3.588	5.13	1.43
miR-181a-5p	3.619	4.149	1.146	miR-27b-3p	0.659	0.892	1.354
miR-21-5p	14.164	16.151	1.14	miR-15b-5p	0.099	0.132	1.328
miR-378a-3p	0.65	0.733	1.128	miR-21-5p	10.992	14.373	1.308
miR-186-5p	0.394	0.443	1.124	miR-25-3p	0.68	0.879	1.293
miR-27b-3p	0.564	0.605	1.073	miR-146b-5p	0.367	0.472	1.284
miR-941	0.107	0.113	1.05	miR-93-5p	0.289	0.368	1.272
miR-151a-3p	0.183	0.186	1.012	miR-140-3p	0.143	0.182	1.271
miR-93-5p	0.257	0.255	0.992	miR-26a-5p	5.057	6.298	1.245
let-7f-5p	2.587	2.566	0.992	miR-378a-3p	0.624	0.767	1.228
miR-16-5p	3.321	3.231	0.973	miR-151a-3p	0.184	0.224	1.218
miR-29a-3p	0.116	0.107	0.92	miR-15a-5p	0.154	0.187	1.214
let-7d-5p	0.118	0.104	0.881	let-7f-5p	2.746	3.294	1.2
miR-192-5p	0.849	0.743	0.875	miR-192-5p	0.881	1.018	1.155
miR-26a-5p	2.549	2.21	0.867	miR-941	0.12	0.138	1.148
miR-103a-3p	0.424	0.364	0.858	let-7d-5p	0.153	0.175	1.143
miR-30d-5p	3.06	2.617	0.855	miR-29a-3p	0.184	0.204	1.107
miR-15a-5p	0.11	0.093	0.852	miR-30d-5p	3.031	3.027	0.999
miR-27a-3p	0.153	0.13	0.848	miR-148a-3p	2.681	2.644	0.986
miR-146b-5p	1.188	0.988	0.832	miR-103a-3p	0.37	0.36	0.973
miR-101-3p	0.304	0.244	0.803	miR-769-5p	0.138	0.126	0.917
miR-19b-3p	0.193	0.144	0.746	miR-30c-5p	0.291	0.245	0.841

miRNA			
miR-148a-3p	5.807	4.216	0.726
miR-181a-3p	0.108	0.077	0.711
miR-210-3p	0.129	0.089	0.691
miR-30e-5p	1.862	1.28	0.687
miR-148a-5p	0.184	0.126	0.684
miR-30c-5p	0.343	0.235	0.684
miR-21-3p	0.841	0.561	0.667
miR-191-5p	4.947	2.883	0.583
miR-17-5p	0.195	0.109	0.558
let-7g-5p	0.664	0.349	0.526
miR-26b-5p	0.52	0.261	0.502
miR-142-5p	6.891	3.435	0.498
miR-142-3p	0.468	0.219	0.468
let-7a-5p	2.587	1.06	0.41
miR-30b-5p	0.332	0.133	0.4
miR-98-5p	0.26	0.077	0.295
miR-20a-5p	0.302	0.084	0.278
miR-486-5p	0.403	0.036	0.089
miR-4485-3p	0.517	0.004	0.009
miR-1260b	0.107	0.0003	0.003
miR-1260a	0.107	0.0002	0.002

miRNA			
miR-148a-5p	0.103	0.085	0.831
miR-19b-3p	0.293	0.242	0.826
miR-191-5p	4.122	3.399	0.825
miR-30e-5p	1.96	1.612	0.822
miR-210-3p	0.168	0.138	0.822
miR-101-3p	0.307	0.245	0.798
miR-17-5p	0.213	0.17	0.798
miR-181a-3p	0.197	0.145	0.736
miR-26b-5p	0.456	0.305	0.669
let-7g-5p	0.776	0.493	0.635
miR-142-3p	2.657	1.501	0.565
miR-21-3p	1.106	0.594	0.537
let-7a-5p	2.848	1.437	0.505
miR-142-5p	28.391	13.376	0.471
miR-486-5p	0.302	0.124	0.409
miR-30b-5p	0.378	0.153	0.405
miR-20a-5p	0.334	0.118	0.352
miR-98-5p	0.229	0.081	0.351
miR-4485-3p	0.709	0.009	0.013
miR-1246	0.339	0.001	0.002
miR-1260b	0.117	0.00012	0.001
miR-4792	1.349	0.001	0.001
miR-1260a	0.117	0.00009	0.001
miR-4532	0.138	0.00004	0.0003

Table A5. Comparison of miRNA profiles in EBV + vs. EBV - in "Total" profile in U2932 and SUDHL5 cell lines at 0.1% cut-off.

	U2932 total				SUDHL5 total		
miRNA	EBV Positive	EBV Negative	Ratio EBV +/ EBV-	miRNA	EBV Positive	EBV Negative	Ratio EBV +/EBV -
miR-4485-3p	0.276	0.062	4.432	miR-182-5p	1.55	0.419	3.699
miR-221-3p	0.21	0.056	3.767	miR-146b-5p	1.188	0.367	3.235
miR-222-3p	0.122	0.037	3.332	miR-10a-5p	0.155	0.061	2.561
miR-193b-3p	0.104	0.034	3.087	miR-148a-3p	5.807	2.681	2.166
miR-18a-5p	0.103	0.035	2.985	miR-148a-5p	0.184	0.103	1.793
miR-1246	0.151	0.051	2.976	miR-146a-5p	0.799	0.477	1.674
miR-15a-5p	0.255	0.091	2.787	miR-27a-3p	0.153	0.097	1.579
miR-155-5p	1.339	0.503	2.663	miR-155-5p	0.219	0.163	1.341
miR-19b-3p	1.744	0.664	2.626	miR-486-5p	0.403	0.302	1.335
miR-19a-3p	0.276	0.113	2.454	miR-21-5p	14.164	10.992	1.289
miR-486-5p	0.425	0.199	2.138	miR-191-5p	4.947	4.122	1.2
miR-21-3p	0.202	0.098	2.07	miR-30c-5p	0.343	0.291	1.178
miR-21-5p	2.551	1.331	1.916	miR-103a-3p	0.424	0.37	1.145
miR-130b-3p	0.132	0.076	1.737	miR-26b-5p	0.52	0.456	1.14
miR-146a-5p	5.849	3.38	1.731	miR-22-3p	3.158	2.781	1.136
miR-9-5p	0.385	0.24	1.603	miR-98-5p	0.26	0.229	1.134
miR-107	0.167	0.106	1.58	miR-425-5p	0.108	0.095	1.132
let-7i-5p	0.53	0.34	1.561	miR-378a-3p	0.65	0.624	1.04
miR-142-5p	5.213	3.854	1.352	miR-30d-5p	3.06	3.031	1.01
miR-17-3p	0.111	0.083	1.348	miR-151a-3p	0.183	0.184	0.997
miR-16-5p	3.929	3.123	1.258	miR-101-3p	0.304	0.307	0.99
miR-30d-5p	3.379	2.736	1.235	miR-192-5p	0.849	0.881	0.963
miR-103a-3p	0.808	0.675	1.197	miR-30e-5p	1.862	1.96	0.95
miR-181b-5p	0.334	0.28	1.193	let-7f-5p	2.587	2.746	0.942
miR-30b-5p	0.377	0.319	1.183	miR-16-5p	3.321	3.588	0.926
miR-378a-3p	0.803	0.685	1.172	miR-17-5p	0.195	0.213	0.916
miR-29a-3p	0.324	0.289	1.121	miR-1260a	0.107	0.117	0.915
miR-423-5p	0.217	0.195	1.112	miR-1260b	0.107	0.117	0.914
miR-181a-5p	7.785	7.073	1.101	let-7a-5p	2.587	2.848	0.908
miR-142-3p	0.437	0.399	1.096	miR-20a-5p	0.302	0.334	0.905
miR-27b-3p	1.753	1.625	1.079	miR-941	0.107	0.12	0.893
miR-301a-3p	0.11	0.102	1.078	miR-93-5p	0.257	0.289	0.891
miR-93-5p	0.386	0.369	1.046	miR-30b-5p	0.332	0.378	0.877
miR-425-5p	0.338	0.333	1.014	miR-27b-3p	0.564	0.659	0.857
miR-140-3p	0.124	0.122	1.014	let-7g-5p	0.664	0.776	0.856
miR-92a-3p	16.783	17.205	0.975	miR-92a-3p	2.364	3.013	0.785
let-7d-5p	0.176	0.187	0.943	let-7d-5p	0.118	0.153	0.77
let-7f-5p	3.555	3.787	0.939	miR-210-3p	0.129	0.168	0.77
miR-17-5p	0.728	0.778	0.935	miR-21-3p	0.841	1.106	0.76
miR-148a-5p	0.206	0.223	0.923	miR-4485-3p	0.517	0.709	0.729
miR-769-5p	0.156	0.17	0.918	miR-15a-5p	0.11	0.154	0.713

miR-101-3p	0.429	0.474	0.904	miR-25-3p	0.485	0.68	0.713
miR-15b-5p	0.091	0.108	0.842	miR-423-5p	0.134	0.188	0.713
miR-186-5p	0.879	1.048	0.838	miR-769-5p	0.098	0.138	0.708
miR-192-5p	1.3	1.623	0.801	let-7i-5p	0.2	0.283	0.707
miR-191-5p	9.169	11.556	0.793	miR-140-3p	0.1	0.143	0.7
let-7b-5p	0.142	0.181	0.786	miR-423-3p	0.175	0.254	0.688
let-7a-5p	3.472	4.559	0.762	miR-186-5p	0.394	0.598	0.659
miR-4792	0.287	0.384	0.748	miR-19b-3p	0.193	0.293	0.658
miR-423-3p	0.233	0.313	0.743	miR-151a-5p	0.249	0.379	0.658
miR-25-3p	0.409	0.556	0.735	miR-181a-5p	3.619	5.613	0.645
miR-98-5p	0.399	0.566	0.704	miR-29a-3p	0.116	0.184	0.633
miR-20a-5p	1.157	1.666	0.694	miR-28-3p	0.877	1.466	0.598
miR-26a-5p	2.887	4.159	0.694	miR-181b-5p	0.102	0.172	0.592
miR-148a-3p	5.704	8.417	0.678	miR-181a-3p	0.108	0.197	0.547
miR-28-3p	0.338	0.508	0.665	miR-26a-5p	2.549	5.057	0.504
miR-30e-5p	1.139	1.728	0.659	miR-28-5p	0.137	0.277	0.494
let-7g-5p	0.858	1.322	0.649	miR-4532	0.054	0.138	0.392
miR-182-5p	1.609	2.566	0.627	miR-142-5p	6.891	28.391	0.243
miR-183-5p	0.121	0.198	0.61	miR-1246	0.069	0.339	0.205
miR-26b-5p	0.332	0.577	0.576	miR-142-3p	0.468	2.657	0.176
miR-22-3p	0.49	0.86	0.57	miR-4792	0.095	1.349	0.07
miR-210-3p	0.058	0.108	0.537				
miR-30c-5p	0.224	0.422	0.53				
miR-1260b	0.062	0.127	0.488				
miR-1260a	0.061	0.126	0.486				
miR-339-3p	0.064	0.142	0.454				
miR-146b-5p	0.073	0.163	0.448				
miR-92b-3p	0.049	0.125	0.389				
miR-27a-3p	0.032	0.177	0.179				
let-7c-5p	0.024	0.245	0.097				

Table A6. Comparison of miRNA profiles in EBV+ vs. EBV- in "Ago2-IP" profile in U2932 and SUDHL5 cell lines at 0.1% cut-off.

	U2932 Ago2-IP				SUDHL5 Ago2-IP		
miRNA	EBV Positive	EBV Negative	Ratio EBV +/ EBV-	miRNA	EBV Positive	EBV Negative	Ratio EBV +/ EBV-
miR-15a-5p	0.276	0.109	2.539	**miR-363-3p**	0.105	0.017	6.046
miR-221-3p	0.114	0.045	2.538	miR-182-5p	1.827	0.667	2.739
miR-155-5p	1.311	0.730	1.795	miR-146b-5p	0.988	0.472	2.095
miR-130b-3p	0.145	0.082	1.759	miR-10a-5p	0.189	0.097	1.956
miR-423-5p	0.738	0.442	1.671	miR-148a-3p	4.216	2.644	1.595
miR-9-5p	0.286	0.200	1.430	miR-148a-5p	0.126	0.085	1.476
miR-146a-5p	10.051	7.106	1.414	miR-27a-3p	0.130	0.097	1.336
miR-181b-5p	0.504	0.368	1.369	miR-21-5p	16.151	14.373	1.124
miR-21-5p	2.581	1.956	1.320	miR-146a-5p	1.381	1.258	1.098
miR-16-5p	4.615	3.565	1.294	miR-155-5p	0.338	0.310	1.091
miR-107	0.135	0.107	1.266	miR-103a-3p	0.364	0.360	1.009
let-7i-5p	0.588	0.478	1.231	miR-101-3p	0.244	0.245	0.997
miR-423-3p	0.516	0.429	1.205	miR-30c-5p	0.235	0.245	0.958
miR-92a-3p	26.551	23.235	1.143	miR-378a-3p	0.733	0.767	0.956
miR-181a-5p	10.446	9.224	1.132	miR-21-3p	0.561	0.594	0.944
miR-27b-3p	1.916	1.707	1.122	miR-30b-5p	0.133	0.153	0.868
miR-142-5p	2.074	1.939	1.070	miR-30d-5p	2.617	3.027	0.865
miR-30d-5p	3.184	3.074	1.036	miR-26b-5p	0.261	0.305	0.856
miR-93-5p	0.446	0.459	0.972	miR-191-5p	2.883	3.399	0.848
miR-103a-3p	0.566	0.598	0.947	miR-151a-3p	0.186	0.224	0.828
miR-378a-3p	0.790	0.852	0.927	miR-941	0.113	0.138	0.817
miR-17-5p	0.469	0.513	0.916	miR-22-3p	3.862	4.762	0.811
let-7d-5p	0.144	0.159	0.908	miR-425-5p	0.143	0.179	0.797
let-7f-5p	2.665	2.949	0.904	miR-30e-5p	1.280	1.612	0.794
miR-425-5p	0.484	0.544	0.890	let-7f-5p	2.566	3.294	0.779
miR-19a-3p	0.114	0.134	0.850	let-7a-5p	1.060	1.437	0.738
miR-191-5p	5.372	6.580	0.816	miR-192-5p	0.743	1.018	0.730
let-7g-5p	0.475	0.595	0.798	miR-20a-5p	0.084	0.118	0.713
miR-148a-5p	0.144	0.185	0.777	let-7g-5p	0.349	0.493	0.709
miR-29a-3p	0.263	0.343	0.767	miR-93-5p	0.255	0.368	0.695
miR-142-3p	0.172	0.228	0.753	miR-92a-3p	4.881	7.077	0.690
miR-192-5p	1.080	1.470	0.735	miR-27b-3p	0.605	0.892	0.679
miR-26a-5p	3.124	4.317	0.724	miR-210-3p	0.089	0.138	0.648
miR-769-5p	0.107	0.152	0.708	miR-25-3p	0.565	0.879	0.643
miR-30b-5p	0.129	0.183	0.707	miR-17-5p	0.109	0.170	0.640
miR-140-3p	0.103	0.148	0.693	miR-140-3p	0.116	0.182	0.635
miR-186-5p	0.865	1.275	0.678	miR-423-3p	0.496	0.785	0.632
miR-19b-3p	0.505	0.750	0.673	miR-16-5p	3.231	5.130	0.630
miR-15b-5p	0.088	0.132	0.672	miR-15b-5p	0.081	0.132	0.612
miR-20a-5p	0.355	0.540	0.657	miR-19b-3p	0.144	0.242	0.595
miR-28-3p	0.454	0.695	0.653	let-7d-5p	0.104	0.175	0.594

miR-182-5p	1.966	3.089	0.636	miR-769-5p	0.073	0.126	0.579
miR-92b-3p	0.096	0.152	0.631	**miR-423-5p**	0.936	1.639	0.571
miR-101-3p	0.240	0.398	0.602	let-7i-5p	0.377	0.662	0.570
miR-22-3p	0.756	1.289	0.586	miR-106b-3p	0.085	0.159	0.532
miR-98-5p	0.134	0.231	0.580	miR-28-3p	1.728	3.260	0.530
miR-26b-5p	0.183	0.318	0.576	miR-181a-3p	0.077	0.145	0.529
miR-320a	0.086	0.151	0.572	miR-29a-3p	0.107	0.204	0.526
miR-148a-3p	4.096	7.232	0.566	miR-15a-5p	0.093	0.187	0.501
miR-25-3p	0.373	0.678	0.550	miR-181b-5p	0.191	0.383	0.498
miR-183-5p	0.117	0.214	0.547	miR-151a-5p	0.304	0.625	0.486
let-7b-5p	0.064	0.119	0.542	miR-181a-5p	4.149	8.794	0.472
miR-339-3p	0.080	0.149	0.536	miR-186-5p	0.443	0.944	0.469
miR-30e-5p	0.804	1.502	0.535	miR-28-5p	0.189	0.515	0.366
let-7a-5p	1.153	2.257	0.511	miR-26a-5p	2.210	6.298	0.351
miR-30c-5p	0.139	0.291	0.480	miR-486-5p	0.036	0.124	0.292
miR-146b-5p	0.090	0.191	0.468	miR-142-5p	3.435	13.376	0.257
miR-27a-3p	0.031	0.143	0.215	miR-142-3p	0.219	1.501	0.146
let-7c-5p	0.013	0.115	0.116				

Table A7.
Abundance of EBV miRNAs in total- and Ago2-miRNA profiles in U2932-EBV and SUDHL5-EBV infected cell line.

U2932-EBV				SUDHL5-EBV			
miRNA	**Total**	**miRNA**	**Ago**	**miRNA**	**Total**	**miRNA**	**Ago2**
	rel. expr. %		rel. expr. %		rel. expr. %		rel. expr. %
BART10-3p	0.4365	BART8-5p	0.42474	BHRF1-1	5.971	BHRF1-1	7.0296
BART8-5p	0.2964	BART11-3p	0.33851	BART10-3p	3.2542	BART8-5p	4.1537
BART6-3p	0.1967	BART6-3p	0.31849	BART8-5p	2.9754	BART6-3p	3.1426
BART11-3p	0.1582	BART10-3p	0.24271	BART7-5p	1.3665	BART10-3p	2.4979
BART22	0.1281	BART19-5p	0.18918	BART19-5p	1.2667	BART11-3p	1.9503
BART7-5p	0.1138	BART7-5p	0.13593	BART11-3p	1.1298	BART19-5p	1.889
BART19-5p	0.0922	BART22	0.09825	BART6-3p	1.0978	BART7-5p	1.6766
BHRF1-1	0.0871	BHRF1-1	0.08756	BART22	0.9351	BART22	0.9512
BART7-3p	0.0829	BART17-5p	0.07884	BHRF1-3	0.6435	BART17-5p	0.8444
BART18-3p	0.0701	BART18-3p	0.05162	BART17-5p	0.5107	BART13-5p	0.7252
BART17-5p	0.0589	BART13-5p	0.04266	BART13-5p	0.4936	BHRF1-3	0.6585
BART16	0.0538	BART16	0.03831	BART18-3p	0.4007	BART18-3p	0.3384
BART8-3p	0.0409	BART2-5p	0.03258	BART19-3p	0.3536	BHRF1-2-3p	0.3256
BART9-5p	0.0408	BART7-3p	0.03072	BART7-3p	0.3231	BART6-5p	0.2869
BART2-5p	0.0403	BART6-5p	0.03005	BART9-5p	0.3	BART14-3p	0.2532
BART13-5p	0.0394	BART14-3p	0.02783	BART2-5p	0.2895	BART2-5p	0.2351
BART14-3p	0.0342	BART8-3p	0.02579	BART6-5p	0.2882	BART8-3p	0.2212
BART6-5p	0.034	BART9-5p	0.02475	BART8-3p	0.2875	BART7-3p	0.2011
BART5-5p	0.0307	BART3-5p	0.02096	BHRF1-2-3p	0.2872	BART9-5p	0.2006
BART3-5p	0.0276	BART9-3p	0.0136	BART17-3p	0.2741	BART16	0.1845
BART1-3p	0.0255	BART11-5p	0.01217	BART14-3p	0.2516	BART3-5p	0.1761
BART17-3p	0.0224	BART17-3p	0.01134	BART3-5p	0.153	BART19-3p	0.1746
BART1-5p	0.0208	BART19-3p	0.00716	BART1-3p	0.1365	BART17-3p	0.1147
BART19-3p	0.0187	BART3-3p	0.00692	BART1-5p	0.131	BART9-3p	0.0764
BART3-3p	0.0147	BART1-5p	0.00685	BART16	0.1251	BART1-5p	0.0749
BART11-5p	0.0123	BHRF1-2-3p	0.00683	BART5-5p	0.1204	BART4-5p	0.0705
BART4-5p	0.0115	BHRF1-3	0.0068	BART11-5p	0.082	BART11-5p	0.0664
BART9-3p	0.0115	BART1-3p	0.00633	BART4-5p	0.0626	BART1-3p	0.0437
BHRF1-3	0.0096	BART4-5p	0.00563	BART9-3p	0.0622	BART18-5p	0.0392
BART18-5p	0.009	BART18-5p	0.00473	BART18-5p	0.0605	BART5-5p	0.0339
BART13-3p	0.0068	BART5-5p	0.00323	BART3-3p	0.0581	BART3-3p	0.0192
BHRF1-2-3p	0.0066	BART4-3p	0.002	BART13-3p	0.0287	BART13-3p	0.0136
BART21-3p	0.0064	BART15	0.00131	BART21-3p	0.0276	BART12	0.0134
BART4-3p	0.0029	BART12	0.00099	BART15	0.0145	BART21-5p	0.0116
BART15	0.0026	BART13-3p	0.00091	BART21-5p	0.0145	BART20-3p	0.011
BART12	0.0017	BART21-5p	0.00087	BART14-5p	0.0145	BART15	0.0107
BART21-5p	0.0014	BART21-3p	0.00075	BART12	0.0142	BART14-5p	0.0099
BART20-3p	0.0011	BART14-5p	0.00068	BART20-3p	0.0123	BART21-3p	0.0059
BART10-5p	0.0007	BART20-3p	0.00059	BHRF1-2-5p	0.009	BART4-3p	0.0054

BART14-5p	0.0005	BART10-5p	0.00017	BART4-3p	0.0075	BHRF1-2-5p	0.0045
BART5-3p	0.0002	BART2-3p	0.00015	BART10-5p	0.0038	BART10-5p	0.0021
BHRF1-2-5p	0.0002	BART20-5p	0.00006	BART20-5p	0.0028	BART2-3p	0.0014
BART2-3p	0.0001	BHRF1-2-5p	0.00005	BART5-3p	0.0014	BART20-5p	0.0008
BART20-5p	0.0001	BART5-3p	0.00004	BART2-3p	0.0013	BART5-3p	0.0004

Table A8.
List of EBV-miRNAs enriched or depleted from the "Ago2-IP"as compared to the
"Total" profile in U2932-EBV and SUDHL5-EBV

U2932-EBV				SUDHL5-EBV			
EBV miRNA	% Total miRNA pool	% RISC assoc. pool	RISC enriched fold change	EBV miRNA	% Total miRNA pool	% RISC assoc. pool	RISC enriched fold change
miR-BART11-3p	0.158	0.339	2.140	miR-BART6-3p	1.098	3.143	2.863
miR-BART19-5p	0.092	0.189	2.053	miR-BART11-3p	1.130	1.950	1.726
miR-BART6-3p	0.197	0.318	1.619	miR-BART17-5p	0.511	0.844	1.653
miR-BART8-5p	0.296	0.425	1.433	miR-BART19-5p	1.267	1.889	1.491
miR-BART7-5p	0.114	0.136	1.194	miR-BART16	0.125	0.185	1.476
miR-BART22	0.128	0.098	0.767	miR-BART13-5p	0.494	0.725	1.469
miR-BART10-3p	0.436	0.243	0.556	miR-BART8-5p	2.975	4.154	1.396
				miR-BART7-5p	1.367	1.677	1.227
				miR-BHRF1-1	5.971	7.030	1.177
				miR-BART3-5p	0.153	0.176	1.151
				miR-BHRF1-2-3p	0.287	0.326	1.133
				miR-BHRF1-3	0.644	0.659	1.023
				miR-BART22	0.935	0.951	1.017
				miR-BART14-3p	0.252	0.253	1.006
				miR-BART6-5p	0.288	0.287	0.995
				miR-BART18-3p	0.401	0.338	0.845
				miR-BART2-5p	0.290	0.235	0.812
				miR-BART8-3p	0.287	0.221	0.769
				miR-BART10-3p	3.254	2.498	0.768
				miR-BART9-5p	0.300	0.201	0.669
				miR-BART7-3p	0.323	0.201	0.623
				miR-BART1-5p	0.131	0.075	0.572
				miR-BART19-3p	0.354	0.175	0.494
				miR-BART17-3p	0.274	0.115	0.418
				miR-BART1-3p	0.137	0.044	0.320
				miR-BART5-5p	0.120	0.034	0.281

Table A9. Up and down regulated miRNAs in "Ago2-IP"U2932-EBV vs. U2932 measured by microarray

miR-551b	8.85	miR-339-3p	-2.23	miR-7	-2.71	miR-574-3p	-3.89
miR-137	6.89	miR-139-5p	-2.23	miR-3654	-2.71	miR-30e*	-3.92
miR-363	6.53	miR-1286	-2.24	miR-365	-2.73	miR-1207-3p	-3.92
miR-494	6.37	miR-499-5p	-2.25	miR-192*	-2.73	miR-505*	-3.96
miR-449a	5.08	miR-627	-2.25	miR-3656	-2.73	miR-128	-3.98
miR-130a	4.77	miR-188-3p	-2.26	miR-32	-2.74	miR-532-3p	-3.99
miR-630	3.48	miR-500a	-2.27	miR-548b-3p	-2.76	miR-590-5p	-4.00
miR-3651	2.87	miR-181a-2*	-2.28	miR-577	-2.77	miR-342-3p	-4.01
miR-10a	2.75	miR-625*	-2.28	miR-629	-2.78	miR-25*	-4.01
miR-718	2.67	miR-188-5p	-2.30	miR-140-3p	-2.78	miR-4306	-4.13
miR-1268	2.20	miR-1301	-2.30	miR-378*	-2.79	miR-501-3p	-4.19
miR-450a	2.16	miR-331-5p	-2.31	miR-374a	-2.80	miR-3194	-4.42
miR-4299	2.14	miR-103-2*	-2.34	miR-660	-2.80	miR-500a*	-4.45
miR-3659	2.10	let-7d*	-2.35	miR-193a-5p	-2.83	miR-421	-4.45
miR-15a	2.08	miR-132	-2.35	miR-1307	-2.84	miR-185	-4.56
miR-4317	-2.00	miR-425*	-2.36	miR-454*	-2.88	miR-374c	-4.62
miR-30c-1*	-2.00	miR-155*	-2.37	miR-502-5p	-2.89	miR-7-1*	-4.79
miR-1973	-2.01	miR-331-3p	-2.37	miR-92a-1*	-2.93	miR-140-5p	-4.80
miR-1280	-2.01	miR-642b	-2.38	miR-129-5p	-2.93	miR-769-3p	-4.81
miR-192	-2.02	miR-19a*	-2.39	miR-106b*	-2.96	miR-589*	-4.82
miR-19b-1*	-2.02	miR-95	-2.40	miR-152	-2.97	miR-191	-4.88
miR-200b	-2.02	miR-29c*	-2.40	miR-23a	-2.99	miR-944	-5.07
miR-3198	-2.03	miR-361-3p	-2.41	miR-362-5p	-3.09	miR-362-3p	-5.07
miR-16-2*	-2.03	miR-30d*	-2.42	miR-570	-3.11	miR-129*	-5.19
miR-22*	-2.04	miR-18a*	-2.44	miR-769-5p	-3.16	miR-550a*	-5.22
miR-628-3p	-2.04	miR-125a-3p	-2.44	miR-148b	-3.16	miR-21*	-5.39
miR-148b*	-2.05	miR-1908	-2.44	miR-27a	-3.17	miR-1270	-5.40
miR-3195	-2.05	miR-22	-2.47	miR-422a	-3.19	miR-582-5p	-5.40
miR-181d	-2.06	miR-423-3p	-2.47	miR-24	-3.22	miR-1303	-5.43
miR-25	-2.09	miR-183	-2.50	miR-548b-5p	-3.24	miR-4291	-5.43

miR-4284	-2.09	miR-24-1*	-2.50	miR-186	-3.26	miR-502-3p	-5.46
miR-491-5p	-2.12	miR-624	-2.53	miR-342-5p	-3.31	miR-4286	-5.64
miR-874	-2.13	miR-215	-2.53	miR-15b*	-3.32	miR-148a*	-5.69
miR-330-3p	-2.17	miR-548e	-2.55	miR-181a*	-3.33	miR-199b-5p	-5.85
miR-597	-2.18	miR-193b*	-2.56	miR-744	-3.40	miR-1180	-6.19
miR-30b*	-2.19	miR-182	-2.57	miR-374b	-3.50	miR-193a-3p	-6.25
miR-3934	-2.19	miR-598	-2.58	miR-3074	-3.50	miR-126	-6.44
miR-1224-5p	-2.19	miR-182*	-2.63	miR-505	-3.53	miR-624*	-6.45
miR-30a	-2.19	miR-193b	-2.63	miR-766	-3.53	miR-345	-6.48
miR-1285	-2.19	miR-378	-2.63	miR-197	-3.54	miR-1260	-7.17
miR-548c-5p	-2.20	miR-628-5p	-2.64	miR-296-5p	-3.58	miR-1260b	-7.32
miR-4323	-2.21	miR-29b-1*	-2.65	miR-652	-3.58	miR-1274b	-8.48
miR-183*	-2.21	miR-3150b	-2.66	miR-93*	-3.65	miR-720	-10.62
miR-429	-2.22	miR-532-5p	-2.68	miR-1255a	-3.70	miR-340*	-12.56
miR-339-5p	-2.22	miR-625	-2.69	miR-28-5p	-3.71	miR-1274a	-12.75
miR-550a	-2.23	miR-4327	-2.70	miR-199a-3p	-3.75	miR-340	-75.41

8   Abbreviations

Ago	Argonaute Protein
Ago2-RIP-seq	Ago2-based RNA immunoprecipitation (RIP)
APS	Ammonium persulfate
Bcl-2	B-cell CLL/lymphoma 2
BHRF1	Bam HI fragment H rightward open reading frame 1
DNA	Deoxyribonucleic acid
dNTP	Desoxyribonucleosidtriphosphate
EDTA	Ethylenediaminetetraacetic acid
FCS	Fetal Calf Serum
CACNG8	Calcium Voltage-Gated Channel Auxiliary Subunit Gamma 8
H_2O_2	Hydrogen Peroxide
HCL	Hydrogen Chloride
KCl	Potassium Chloride
kDa	Kilo Dalton
M	Molar
mA	Milliampere
mg	Milligram
$MgCl_2$	Magnesium Chloride
min	Minute
ml	Milliliter
mRNA	Messenger RNA
Na_2HPO_4	Sodium Hydrogen Phosphate
NaOH	Sodium Hydroxide
NTP	Nucleoside Triphosphate
PBS	Phosphate Buffered Saline
RISC	RNA Induced Silencing Complex
RNA	Ribonucleic Acid
RPM	Rotations Per Minute

RPMI-1640	Roswell Park Memorial Instiute-1640
SDS	Sodium Dodecyl Sulphate
SDS-PAGE	Sodium Dodecyl Sulphate- Polyacrylamide Gel Electrophoresis
sec	Second
SSC	Saline Sodium Citrate
TAE	Tris base, acetic acid, EDTA
TBE	Tris base, boric acid, EDTA
TE	Tris base, EDTA
TEMED	N,N,N',N'-tetramethylethane-1,2-diamine
TNRC6A	Trinucleotide repeat containing 6 A
V	Volt
W	Watt
µL	Microliter
µg	Microgram

9 List of figures

10 List of tables

11 Acknowledgements

Contributions

Collaborations and interdisciplinary team work are prerequisite to Investigate scientific questions. I would like to acknowledge the following persons how contributed at various stages of experimentation and in obtaining results for my PhD Project: